UNIVERSITY OF CALIFORNIA, SAN DIEGO

Proteasome Inhibitor Biosynthesis and Self-Resistance in the Marine Actinobacterium *Salinispora tropica*

A dissertation in partial satisfaction of the requirements for the degree
Doctor of Philosophy

in

Marine Biology

by

Andrew John Kale

Committee in charge:

Bradley S. Moore, Chair
Pieter Dorrestein
William Gerwick
Paul Jensen
Joseph Noel

2012

The Dissertation of Andrew John Kale is approved, and it is acceptable in quality and form for publication on microfilm and electronically.

Chair

University of California, San Diego

2012

DEDICATION

To my parent, Robert and Judith, for their perpetual love and support. I could not have made it this far without you.

To Stephanie, for being so incredibly loving, supportive, and understanding.

TABLE OF CONTENTS

LIST OF ABBREVIATIONS

0912	ONX 0912
0914	ONX 0914
5AHQ	5-amino-8-hydroxyquinole
5-ClR	5-chloro-5-deoxy-D-ribose
5-ClRI	5-chloro-5-deoxy-D-ribonic acid
5-ClRL	5-chloro-5-deoxy-D-ribono-γ-lactone
5fl	5-fluorouacil
A	Adenylation domain
ACN	Acetonitrile
ACP	Acyl carrier protein
ALLN	Ac-Leu-Leu-Nle-al
amc	7-amino-4-methylcoumarin
apra	Apramycin
AT	Acyl transferase domain
BLAST	Basic local alignment search tool
ble	Bleomycin
C	Condensation domain
chl	Chloroquine
cis	Cisplatin
C-L	Caspase-like
C-MT	C-methyl transferase
CoA	Coenzyme A

CT-L	Chymotrypsin-like
cyc	Cyclosporin A
daun	Daunoribicin
DEPT	Distortionless enhancement of polarization transfer
DH	Dehydrogenase domain
DMF	Dimethylformamide
DMSO	Dimethyl sulfoxide
DNA	Deoxy-ribonucleic acid
dox	Doxorubicin
E. coli	*Escherichia coli*
EDTA	Ethylenediaminetetraacetic acid
epox	Epoxomicin
ER	Enoyl reductase domain
eto	Etoposide
FAD(H)	Flavin adenine dinucleotide
FDA	Food and Drug Administration
fld	fludarabine
FPLC	Fast protein liquid chromatography
Fs	*Frankia* sp. ACN14a
gef	Gefitnib
gel	Geldanamycin
hct	Hydrocortisone
het	Heterozygous

hom	Homozygous
HPLC	High performance liquid chromatography
Hs	*Homo sapiens*
Kan	Kanamycin
KR	Ketoreductase domain
KS	Ketosynthase domain
lact	lactacystin
LB	Luria-Bertani
LC-MS	Liquid chromatography-mass spectroscopy
LPAAT	Lysophosphatidic acid acyl-transferase
Ma	*Micromonospora aurantiaca* ATCC 27029
MCL	Mantle cell lymphoma
MDR	Medium-chain dehydrogenase reductase
mel	Melphalan
MeOH	Methanol
mit	Mitoxantrone
MM	Multiple myeloma
mpr	Methylprednisolone
mtx	Methotrexate
N-MT	N-methyl transferase
$NAD^+(H)$	Nicotinamide adenine dinucleotide
NI	Not inhibitory
Ni-NTA	Nickel-nitraloacetic acid

NLVS	4-hydroxy-5-iodo-3-nitrophenylacetyl-Leu-Leu-Leu-vinylsulfone
NMR	Nuclear magnetic resonance
NRPS	Non-ribosomal peptide synthetase
ORF	Open reading frame
PAGE	Polyacrylamide gel electrophoresis
PCP	Peptidyl carrier protein
PCR	Polymerase chain reaction
PDB	Protein Data Bank
Pgp	P-glycoprotein
PI	Proteasome inhibitor
PKS	Polyketide synthase
ppm	parts per million
PUP	Prokaryotic ubiquitin-like protien
Re	*Rhodococcus erythropolis* PR4
RFU	Relative fluorescence units
RNA	Ribonucleic acid
sal	Salinosporamide
SAM	S-adenosyl-L-methionine
SAMP	Small archaeal modifying protein
Sc	*Saccharomyces cerevisiae*
SDR	Short-chain dehydrogenase reductase
SDS	Sodium dodecyl sulfate
St	*Salinispora tropica* CNB-440

Stc	*Streptomyces coelicolor* A3(2)
sts	Stauroporine
Suc	Succinate/succinyl
sulf	Sulfasalazine
TB	Terrific broth
TE	Thioesterase
TE	Thioesterase domain
T-L	Trypsin-like
Ub	Ubiquitin/Ubiquitinated
vinc	Vincristine
vind	Vindesine
Z	Carboxybenzyl group
ZL_3VS	Z-Leu-Leu-Leu-vinylsulfone

LIST OF FIGURES

LIST OF TABLES

LIST OF SCHEMES

ACKNOWLEDGEMENTS

I would like to sincerely thank everyone who has contributed to my education and development as a scientist over the years. I would like to specifically acknowledge the following people:

I would like to acknowledge Professor Bradley S. Moore for the opportunity to work in his lab for the past five years. I consider myself fortunate to have been advised by someone who not only pushes me to succeed as a scientist but also to enjoy life outside of the lab. Thank you for providing guidance when needed but also giving me the freedom to take charge of my projects. I especially appreciate your prompt assistance with paper revisions and submissions. I additionally would like to thank you for sending me to scientific conferences located in exotic worldwide destinations. Lastly, I thank you for the delicious homemade meringues that you prepared for my birthday.

I would also like to acknowledge all of the members of the Moore lab, both past and present, for their support and friendship over the past five years. In particular, I would like to thank former postdocs Ryan McGlinchey, Markus Nett, Tobias Gulder, Alexandra Roberts, and Alessandra Eustáquio for guiding my development as a laboratory scientist in the areas of protein biochemistry, analytical and organic chemistry, molecular biology, and microbiology. The Moore group has been like a family to me and it will be difficult to move on.

I would like to thank my committee members, Paul Jensen, Bill Gerwick, Joe Noel, and Pieter Dorrestein for their advice and support. I have had the privilege of collaborating with each of their groups during my graduate work. In particular, I thank

Joe Noel who allowed me to briefly work in his lab in an attempt to crystalize one of my proteins.

Additionally I would like to thank the support and training of former scientific mentors, Prof. Diane Larson and Prof. Laura Ranum from the University of Minnesota, Dr. Gabriela Chakarova and Dr. Bill Doering at Oxonica, Inc., and high school science teachers Jon Erickson, Joe Helm, and John Iverson.

Chapter 1 and Chapter 4, in part, were submitted as Uncovering the Molecular Mechanisms of Proteasome Inhibitor Resistance (2012). Kale, Andrew J. and Moore, Bradley S., Journal of Medicinal Chemistry. The dissertation author was the primary author of this submission.

Chapter 2, in part, is a reprint of the material as it appears in Characterization of 5-Chloro-5-Deoxy-D-Ribose-1-Dehydrogenase in Chloroethylmalonyl-Coenzyme A Biosynthesis: Substrate and Reaction Profiling (2010). Kale, Andrew J.; McGlinchey, Ryan P.; and Moore, Bradley S., Journal of Biological Chemistry, volume 285, 33710-33717. The dissertation author was the primary investigator and author of this paper.

Chapter 3, in part, is a reprint of the material as it appears in Bacterial Self-resistance to the Natural Proteasome Inhibitor Salinosporamide A (2011). Kale, Andrew J.; McGlinchey, Ryan P.; Lechner, Anna; and Moore, Bradley S., ACS Chemical Biology, volume 6, 1257-1267. The dissertation author was the primary investigator and author of this paper.

VITA

2007-2012 **Doctor of Philosophy,** Marine Biology, Scripps Institution of Oceanography, University of California, San Diego

2001-2005 **Bachelor of Science,** Biology, *summa cum laude*, University of Minnesota, Twin Cities

PUBLICATIONS

Pereira, A. R., **Kale, A. J.**, Fenley, A. T., Byrum, T., Debonsi, H. M., Gilson, M. K, Valeriote, F. A., Moore, B. S., Gerwick, W. H. (2012) The carmaphycins: new proteasome inhibitors exhibiting an α,β-epoxyketone warhead from a marine cyanobacterium, *ChemBioChem.* 16, 810-817.

Chen, C.-H., Wang, B.-L., **Kale, A. J.**, Moore, B. S., Wang, R.-W., Qing, F.-L. (2012) Coupling of sterically hindered aldehyde with fluorinated synthons: stereoselective synthesis of fluorinated analogues of salinosporamide A, *J. Fluorine Chem.* 136, 12-19.

Kale, A. J., McGlinchey, R. P., Lechner, A., and Moore, B. S. (2011) Bacterial self-resistance to the natural proteasome inhibitor salinosporamide A, *ACS Chem. Biol.* 6, 1257-1264.

Kale, A. J., McGlinchey, R. P., and Moore, B. S. (2010) Characterization of 5-chloro-5-deoxy-D-ribose 1-dehydrogenase in chloroethylmalonyl coenzyme A biosynthesis. Substrate and reaction profiling, *J. Biol. Chem.* 285, 33710-33717.

Nett, M., Guider, T. A. M., **Kale, A. J.**, Hughes, C. C., and Moore, B. S. (2009) Function-oriented biosynthesis of β-lactone proteasome inhibitors in *Salinispora tropica*, *J. Med. Chem.* 52, 6163-6167.

Eustáquio, A. S., McGlinchey, R. P., Liu, Y., Hazzard, C., Beer, L. L., Florova, G., Alhamadsheh, M. M., Lechner, A., **Kale**, **A. J.**, Kobayashi, Y., Reynolds, K. A., and Moore, B. S. (2009) Biosynthesis of the salinosporamide A polyketide synthase substrate chloroethylmalonyl-coenzyme A from S-adenosyl-L-methionine, *Proc. Natl. Acad. Sci. U. S. A.* 106, 12295-12300.

PRESENTATIONS

2011 **A. J. Kale**, R. P. McGlinchey, A. Lechner, and B. S. Moore. "Biochemical characterization of bacterial self-resistance to the natural proteasome inhibitor salinosporamide A." Society for Industrial Microbiology Annual Meeting, New Orleans, LA.

2010 **A. J. Kale**, R. P. McGlinchey, and B. S. Moore. "Real-time visualization of the transformation of 5-chloro-5-deoxy-D-ribose in chloroethylmalonyl-CoA biosynthesis." Trends in Enzymology 2010, Ascona, Switzerland.

2009 **A. J. Kale**, M. Nett., T. A. M. Gulder, C. C. Hughes, and B. S. Moore. "Generation of salinosporamide analogs for altered 20S proteasome binding affinity." San Diego Ubiquitination symposium, San Diego, CA.

2008 **A. J. Kale**, Y. Liu, R. P. McGlinchey, and B. S. Moore. "Enzymatic oxidation of 5-chlororibose in the biosynthesis of salinosporamide A." Society for Industrial Microbiology Annual Meeting, San Diego, CA.

FELLOWSHIPS AND AWARDS

2011 Outstanding Student Poster Presentation - Natural Products, Society for Industrial Microbiology Annual Meeting

2010 Life Science Professional Development Scholarship for the Medicinal Chemistry Intensive Program, UCSD Extension

2009 National Science Foundation Graduate Research Fellowship Program, Honorable Mention

2007 Director's Fellowship, Scripps Institution of Oceanography, University of California, San Diego

2001 AAL/Thrivent Financial Scholarship

2001 University of Minnesota Presidential Scholarship

RESEARCH EXPERIENCE

2003 **Undergraduate Laboratory Assistant,** University of Minnesota – Twin Cities, Prof. Laura Ranum.

2004-2005 **Undergraduate Research Project,** University of Minnesota – Twin Cities, Prof. Diane Larson.

PROFESSIONAL EXPERIENCE

2006-2007 **Process Development Associate,** Oxonica, Inc., Mountain View, CA.

ACADEMIC TEACHING EXPERIENCE

2011 **Graduate Teaching Assistant,** Metabolic Biochemistry, University of California, San Diego, Dr. Aaron Coleman.

2004-2005 **Undergraduate Teaching Assistant,** Human Anatomy and Physiology, University of Minnesota, Twin Cities, Prof. Murray Jensen

ABSTRACT OF THE DISSERTATION

Proteasome Inhibitor Biosynthesis and Self-Resistance in the Marine Actinobacterium *Salinispora tropica*

by

Andrew John Kale

Doctor of Philosophy in Marine Biology

University of California, San Diego, 2012

Professor Bradley S. Moore, Chair

Proteasome inhibitors (PIs) have recently emerged as a therapeutic strategy in cancer chemotherapy with the FDA approval of bortezomib. The marine actinobacterium *Salinispora tropica,* discovered in sediments off the Bahamas, produces a potent natural product PI, salinosporamide A (NPI-0052 or marizomib), which is now in clinical trials for the treatment of multiple myeloma. A chlorine atom,

incorporated via the novel polyketide synthase extender unit chloroethylmalonyl-CoA, confers highly potent and irreversible inhibition of the eukaryotic 20S proteasome. Herein I report the *in vitro* characterization of one enzyme, the short-chain dehydrogenase/reductase SalM, responsible for the oxidation of 5-chloro-5-deoxy-D-ribose to 5-chloro-5-deoxy-D-ribono-γ-lactone en route to chloroethylmalonyl-CoA. Using heterologously produced SalM, a sensitive, real-time ^{13}C NMR assay was developed to monitor transient product formation followed by spontaneous lactone hydrolysis. SalM was determined to have an atypical divalent cation dependence (Mg^{2+}, Mn^{2+} or Ca^{2+}) and to oxidize tetrose or pentose furanoses with hydroxy stereochemistry equivalent to that of D-ribose, making it the first reported stereospecific non-phosphorylated ribose-1-dehydrogenase. Additionally, I explored the question of PI self-resistance in *S. tropica* as actinobacteria possess 20S proteasome machinery. A secondary catalytic β-subunit (SalI) encoded adjacent to the salinosporamide biosynthetic gene cluster was characterized by heterologous expression and *in vitro* assaying of the α/SalI complex. An altered proteolytic specificity and 30-fold resistance toward salinosporamide A inhibition was demonstrated for the α/SalI complex relative to the housekeeping α/β_1 complex. Sequence comparison of these two β-subunits revealed two mutations, M45F and A49V, which likely conferred resistance. Mutational analysis demonstrated that the A49V mutation of SalI is partially responsible for resistance which correlates to identical mutations observed in bortezomib resistant human cancer cell lines. The α/SalI complex was also cross-resistant to bortezomib and to salinosporamide analogs, suggesting that S1 binding pocket mutation leads to

resistance against all proteasome β-subunit inhibitors. As bortezomib therapy is plagued by intrinsic and acquired resistance, it is critical to determine if salinosporamide A will suffer the same fate. My analysis suggests that bortezomib resistant cancer cell lines are likely cross-resistant to salinosporamide A. Moreover, these results suggest that self-resistance to natural PIs may predict clinical outcomes.

Chapter 1:

Introduction to Proteasome Inhibitor Discovery, Biosynthesis, and Resistance

1.1: Introduction

Life is a collection of controlled chemical reactions. Biochemical pathways such as glycolysis and fatty acid biosynthesis are virtually ubiquitous throughout all living organisms. These primary metabolic pathways are needed for basic growth and reproductive functions. However, many organisms possess specialized metabolic pathways to produce unique small molecules, called natural products or secondary metabolites, which likely confer an evolutionary advantage for ecological adaptation. While we often do not know the true ecological role of these compounds, it is believed that they function in self-defense, signaling, nutrient acquisition, and quorum sensing.[1,2] In spite of this, humans have developed other pharmacological uses for many natural products, such as the stimulant caffeine, the analgesic morphine, and the antibiotic penicillin.[3]

The constant need for new and improved medications has pushed chemists to search for novel compounds from natural sources. While most natural products chemists searched terrestrial environments, a small group of chemists began to explore the marine environment and a rich diversity of marine-derived, bioactive natural products has since been discovered.[4-6] Several marine natural products are, or have inspired, FDA approved drugs, including: the anti-cancer nucleotide analogs vidarabine and cytarabine which were inspired by marine sponge natural products; a peptide isolated from cone snails, zinconotide, used in the treatment of pain; and the antimitotic eribulin mesylate, a truncated analog of the sponge derived halichondrin B.[5] Additionally, many other marine natural products are currently in clinical trials.[5]

The terrestrial actinobacteria have been one of the most productive sources of natural product discovery.[7] Scripps Institution of Oceanography scientists Prof. William Fenical, Dr. Paul Jensen and colleagues reported the first marine obligate genus of actinobacteria, the *Salinispora,* from the sediments of the Bahamas.[8-10] Three *Salinispora* species, *S. tropica*, *S. arenicola,* and "*S. pacifica"* have been identified and collectively have yielded a treasure trove of bioactive natural products.[11-17] Most notably, the Fenical group described a family of compounds from *S. tropica* named the salinosporamides, and found them to be highly cytotoxic to HCT-116 human colon carcinoma cell lines and potent inhibitors of the eukaryotic 20S proteasome.[18,19] The chlorinated salinosporamide A was found to be the most potent family member *in vivo*, with low nM potency, and has since advanced to clinical trials for the treatment of hematological malignancies in humans.[20]

In eukaryotes, the regulated hydrolysis of cellular proteins is mediated by a ubiquitous macromolecular enzymatic complex, the 26S proteasome.[21] The proteasome acts as the central hub of cellular catabolism, mediating cellular processes such as cell cycle control, cell differentiation, immune response, amino acid recycling, and apoptosis; consequently, its disruption by genetic mutation or small molecule inhibitors has significant deleterious effects via multiple downstream pathways.[21] To underscore its universal role, inhibition of the proteasome has been explored in the treatment of diverse maladies such as cancer,[22-24] viruses,[22,23] stroke,[22] cardiovascular disease,[24] inflammation,[22] and transplant rejection.[25] To date, however, just one proteasome inhibitor (PI), bortezomib (Velcade®), has been FDA approved, where it is prescribed for the hematological malignancies multiple myeloma (MM), as front-line treatment,

and refractory mantle cell lymphoma (MCL).[26] Despite the successes of bortezomib therapy, many patients are intrinsically resistant to bortezomib and most patients that do respond eventually develop resistance.[27] Therefore the discovery and development of new proteasome inhibitors such as salinosporamide A is of the utmost importance.

1.2: The Eukaryotic Ubiquitin-26S Proteasome System

The 2.5 megadalton eukaryotic 26S proteasome is comprised of a 700 kDa 20S core particle and the 19S regulatory base and lid (Figure 1.1A).[28] The 20S core particle contains four heptameric rings stacked in a cylindrical $\alpha_7\beta_7\beta_7\alpha_7$ arrangement.[21] Each α and β-subunit per heptameric ring is unique, necessitating 14 genes for the 20S core alone. The α-subunits act as the exterior structural scaffold while the interior β-subunits catalyze proteolytic activity. Upon assembly, prosequences of the proteolytic β-subunits are autocatalytically removed yielding the N-terminal Thr1 residue, which serves as the nucleophile for proteolytic hydrolysis. Only three of the seven β-subunits in each heptameric ring are catalytically active; the *PSMB6* encoded β1-subunits possess caspase-like activity (C-L), the *PSMB7* encoded β2-subunits possess trypsin-like activity (T-L), and the *PSMB5* encoded β5-subunits possess chymotrypsin-like activity (CT-L). The designation of CT-L, T-L, and C-L activity refers to the character of the P1 residue, the amino acid side chain immediately to the N-terminal side of the point of proteolysis (Figure 1.2). This specificity is largely controlled by the S1 binding pocket, the cavity in which the P1 residue resides.[29] Mammals additionally possess γ-interferon

inducible β1i, β2i and β5i, which replace the constitutively expressed β1, β2 and β5, respectively.[21]

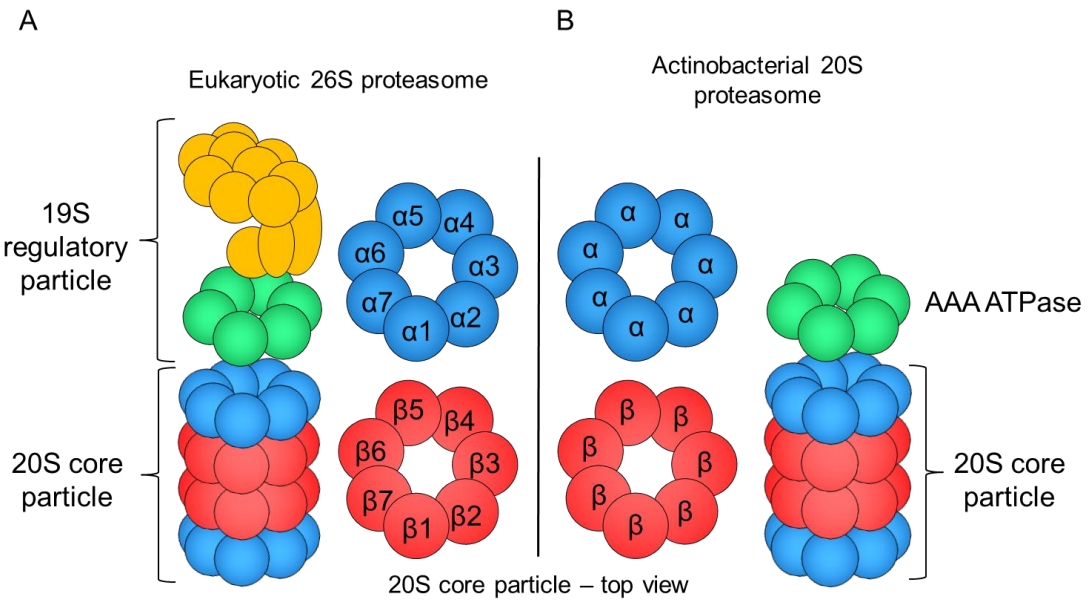

Figure 1.1. Structural architecture of the proteasome. (A) The eukaryotic 26S proteasome is comprised of the 20S core particle and 19S regulatory particle. Within the 20S core, seven distinct α (blue) and seven distinct β (red) subunits are used per heptameric ring. Only three β-subunits, β5, β2, and β1 are catalytically active. A heterohexemer of ATPases (green) and other regulatory proteins (yellow) form the 19S regulatory particle (B) The actinobacterial proteasome 20S core is typically comprised of a single α (blue) and single β (red) subunit. While no regulatory particle is known for the actinobacterial system, a homohexamer of ATPases (green) is believed to associate with the 20S core for substrate unfolding.

The 19S structure serves as the gate-keeper of the catalytic 20S core particle for the recognition and unfolding of polyubiquitinated substrates. Proteins destined for proteasome-mediated destruction in eukaryotic cells are covalently tagged with ubiquitin (Ub), a small protein modifier. Ub is transferred to Lys residues on the target

protein by a cascade of three enzymes, E1, E2, and E3 (Figure 1.3A). Ub bears a conserved C-terminal GG motif. The terminal glycine α-carboxylate group is first adenylated by E1 and then transferred to an E1 cysteine residue. The Ub-thioester is then transferred to an E2 cysteine. E2 transfers Ub to a target protein Lys, with the aide of E3 which recognizes the protein substrate, forming an isopeptide linkage. Ub may also be transferred to another Ub forming a poly-Ub chain, which signals the substrate protein for acceptance by the 19S regulatory cap and subsequent proteasomal degradation. The quantity and specificity of ubiquitinating enzymes increases from E1 to E3. Only two E1 isoforms are known in humans, while there are over 30 E2's and 300 E3's.[30] The ubiquitin-proteasome system has been well studied and extensively reviewed.[28,31]

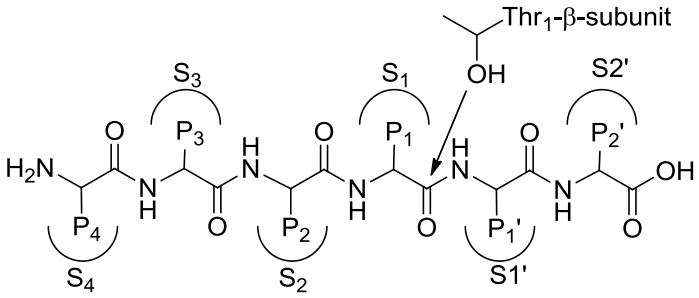

Figure 1.2. Proteasome substrate and binding pocket nomenclature. The amino acid directly to the N-terminal side of the point of proteolysis is termed the P1 residue. The P1 residue fits into the S1 binding pocket of the proteasome. Residue and pocket numbers increase toward the N-terminus. Residues and pockets on the C-terminal side of the point of hydrolysis are numbered P1´ and S1´ and numbering increases toward the C-terminus.

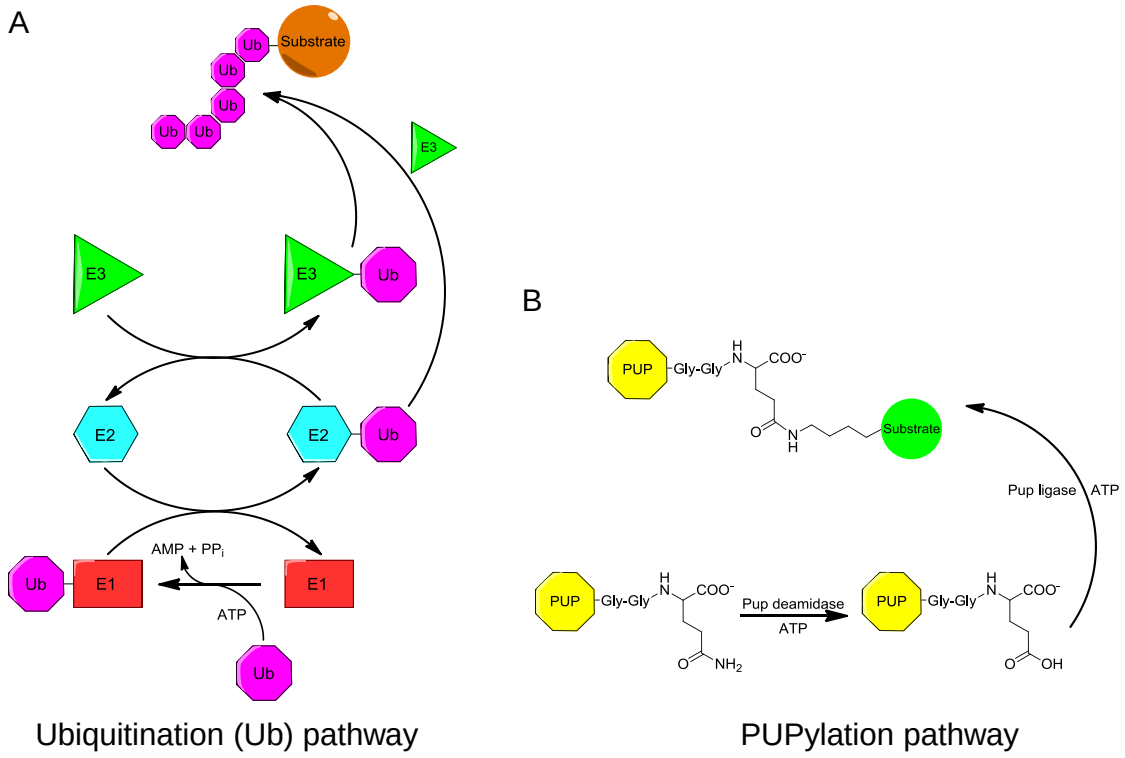

Figure 1.3. Covalent protein modification systems signaling for proteasomal destruction. (A) The Ubiquitin-proteasome system. Poly-ubiquitination of cellular proteins, catalyzed by the cascade of E1, E2 and E3 enzymes, assigns substrate proteins for 26S proteasomal degradation. (B) The PUPylation system in actinobacteria. The C-terminal Gln of PUP may first be deamidated by PUP deamidase (Dop), then covalently linked to a substrate Lys by PUP ligase (PafA).

1.3: Proteasomes in Prokaryotes

Archaea and the high GC-content Gram-positive actinobacteria also possess a simplified 20S proteasome.[29] Although eubacteria outside of the actinobacteria do not typically possess a proteasome, one Gram-negative bacterium of the phylum *Nitrospirae* was found to have proteasome encoding genes, likely from horizontal gene transfer with an actinobacteria.[32] Both archaea and actinobacteria possess 20S core particles in which the seven α and seven β-subunits are identical and therefore all

possess the same catalytic activity (Figure 1.1B). Occasionally a second copy of the α and/or β-subunit is also present, but the significance is not understood.[21,33] Prokaryotes lack the complex 19S regulatory lid complex. However, recent reports have illustrated that a hexameric ring of ATPases analogous to those in the eukaryotic 19S proteasome associate with the 20S core particle, likely with the role of substrate unfolding.[34] Proteasome inhibition or deletion of the archaeal proteasome related genes results in reduced growth rate, especially under stress conditions such as nitrogen limitation, low-salt stress, or thermal stress.[33] A complete abolishment of proteasome activity *in vivo* precludes cell viability. In contrast to eukaryotes, eubacterial proteasome function is not essential for survival, likely due to a redundancy of proteolytic machinery.[35]

The archaea and actinobacteria have distinct but analogous post-translational modification systems which target proteins for destruction. The archaea use small archaeal modifying proteins (SAMPs)[33] and the actinobacteria use a prokaryotic ubiquitin-like protein (PUP).[36] The discovery of PUP in 2008 shifted the prevailing theory on the role of the proteasome in actinobacteria from one of non-specific protein hydrolysis to an ordered system of protein degradation (Figure 1.3B).[37,38] Despite the analogous roles of the Ub and PUPylation systems, there are many striking differences. Unlike Ub, PUP is intrinsically disordered.[39,40] The C-terminal half of PUP binds to the AAA ATPase while the N-terminal half facilitates substrate unfolding.[34,41] Unlike the C-terminal di-glycine motif of ubiquitin, most actinobacteria encode a PUP protein ending in a C-terminal Gly-Gly-Gln motif (PUP-GGQ). Gln must first be deamidated by the ATP dependent PUP deamidase (also known as Dop, deamidase of PUP) enzyme

to form PUP-GGE.[42-44] This step is unnecessary in some actinobacteria, including *Salinispora tropica*, as the genome codes for PUP-GGE. The Glu γ-carboxylate group is then adenylated and covalently tethered to the ε-amino group of a Lys residue on the target protein by PUP ligase (or PafA, proteasome associating factor A).[44,45] Although deamidation of PUP-GGQ to PUP-GGE is unneeded in several actinobacteria, Dop is highly conserved. This conservation may be explained by a more recently described secondary function for Dop, dePUPylation, which may recycle PUP or rescue PUPylated protein.[46,47]

To elucidate which actinobacterial proteins are PUPylated for proteasomal dedgradation, His-tagged-PUP encoding genes have been incorporated into *Mycobacterium tuberculosis* and *Mycobacterium smegmatis*.[48-50] These studies have identified many proteins to be PUPylated, typically at a single Lys residue. No conserved sequence or structural motif has yet been identified at the PUPylation site. As opposed to Ub, poly-PUPylation has also not been observed. In *M. smegmatis* 41 proteins were identified as being PUPylated with 38 being homologous to proteins found in *M. tuberculosis.*[49] Most are involved in intermediary metabolism and cellular respiration pathways such as glycolysis and gluconeogenesis, lipid metabolism, and virulence, detoxification, and adaptation. Superoxide dismutase, involved in the removal of toxic superoxide radicals, was one of the first identified PUPylation substrates. Many of the PUPylated proteins were encoded from gene clusters, indicating pathway specific regulation. Further analysis of the *M. smegmatis* PUPylome revealed that several mycolic acid biosynthesis enzymes were PUPylated.[48] Fifty-five PUPylated

proteins were identified in *M. tuberculosis.*[50] PUPylated proteins such as isocitrate lyase, inositol-1-phosphate synthase, *Mtb* response regulator A, and phosphate response regulator P are linked to pathogenesis. Little is currently known about the regulation of the PUPylome. No PUPylation studies have been explored in prolific natural product producing organisms such as the *Streptomyces*. An attempt to reconstitute the PUPylation pathway in *E. coli*, which lacks the 20S proteasome and PUP machinery, by addition of PUP-GGE and PafA encoding genes resulted in the PUPylation of 51 *E. coli* proteins.[51] This provides evidence that no additional enzymes are needed for PUPylation.

1.4: Proteasome Inhibitors

1.4.1: Covalent Inhibitors.

Many small molecule inhibitors of 20S proteasome function, both synthetically prepared and naturally produced, have been discovered. The predominant structural theme of PIs is a short peptide-like substrate mimic with an electrophilic modification to covalently capture the N-terminal Thr1O$^{\gamma}$ of one or more of the catalytic β-subunits. Examples of electrophilic warheads include the reversibly inhibiting aldehydes and boronic acids, or the irreversibly inhibiting vinyl sulfones and epoxyketones. Potency and selectivity for each inhibitor is determined both by the nature of the electrophile and the interactions of the inhibitor with the active site binding pockets.[26,52] While the P1/S1 interaction is often considered the primary determinant of specificity, distal binding pockets may also influence substrate selectivity and inhibition potency.[52]

The peptide aldehydes were originally identified as inhibitors of serine and cysteine proteases. Calpain inhibitor I (**1**, Ac-Leu-Leu-Nle-al or ALLN) (Figure 1.4) and II were later found to inhibit proteasome activity as well. Another synthetic aldehyde, MG132 (**2**) has been extensively utilized as a probe of proteasome activity.[22,23] Aldehydes forms a reversible hemiacetal with Thr1O$^{\gamma}$ (Figure 1.5).[53,54] However, the reactive aldehyde results in oxidation and cross-reactivity, preventing the use of this class in therapy.[22,23] Leupeptin (**3**, *N*-acetyl-L-Leu-L-Leu-L-Arg-al), a naturally produced peptide aldehyde from various *Streptomycetes,*[55,56] bears a positively charged arginine P1 residue thereby preferentially inhibiting T-L activity[54,57] while fellutamide B (**4**), produced by the fungus *Penicillium fallutanum*, inhibits CT-L activity at low nM concentrations.[58]

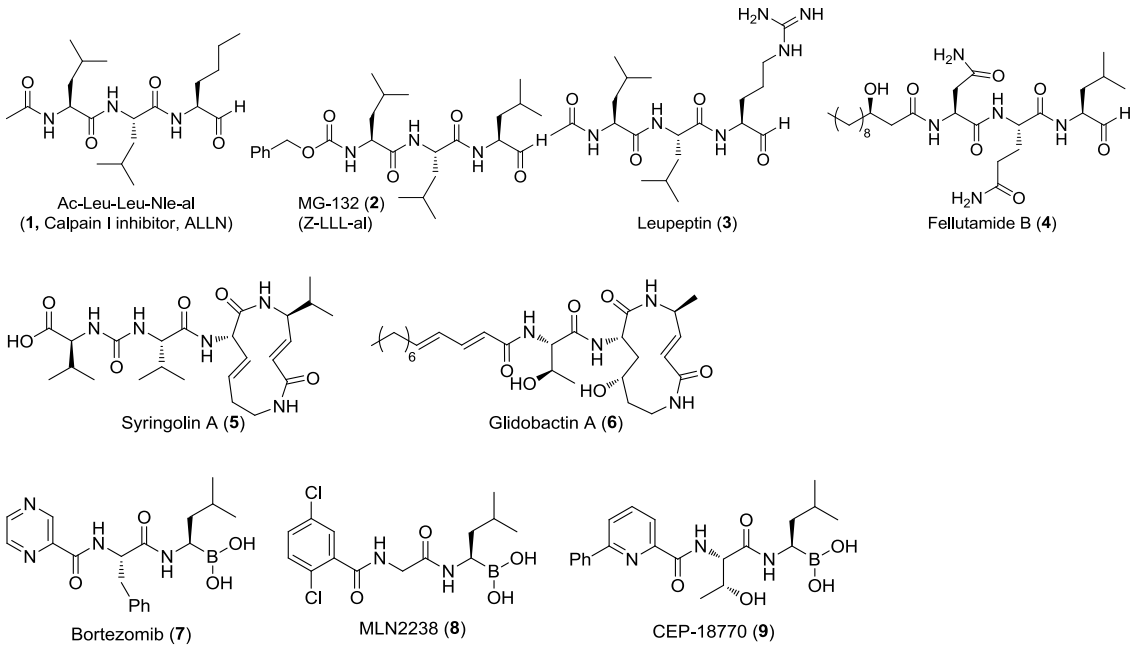

Figure 1.4. Structures of proteasome inhibitors discussed in Chapter 1.

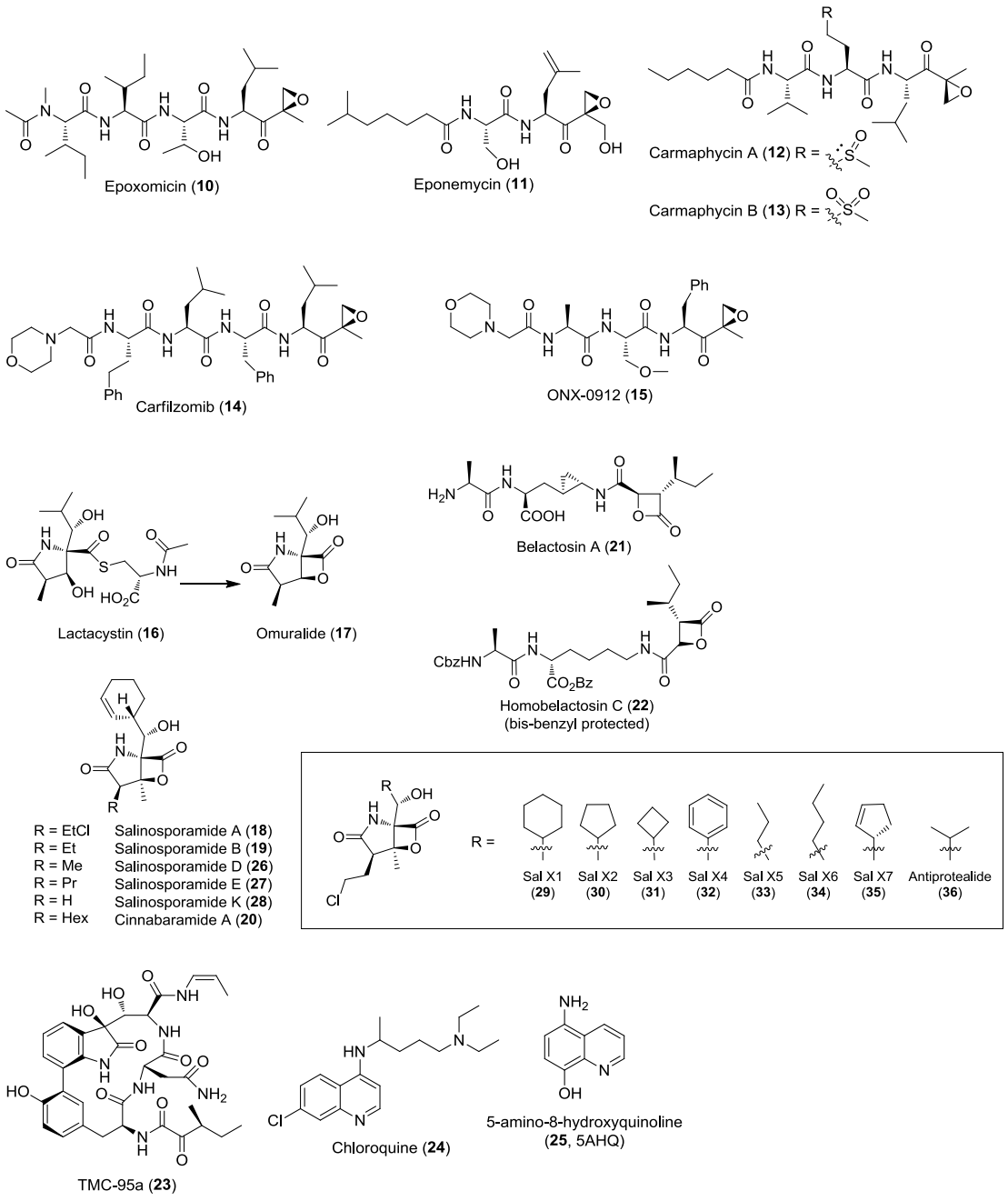

Figure 1.4. Structures of proteasome inhibitors discussed in Chapter 1, continued.

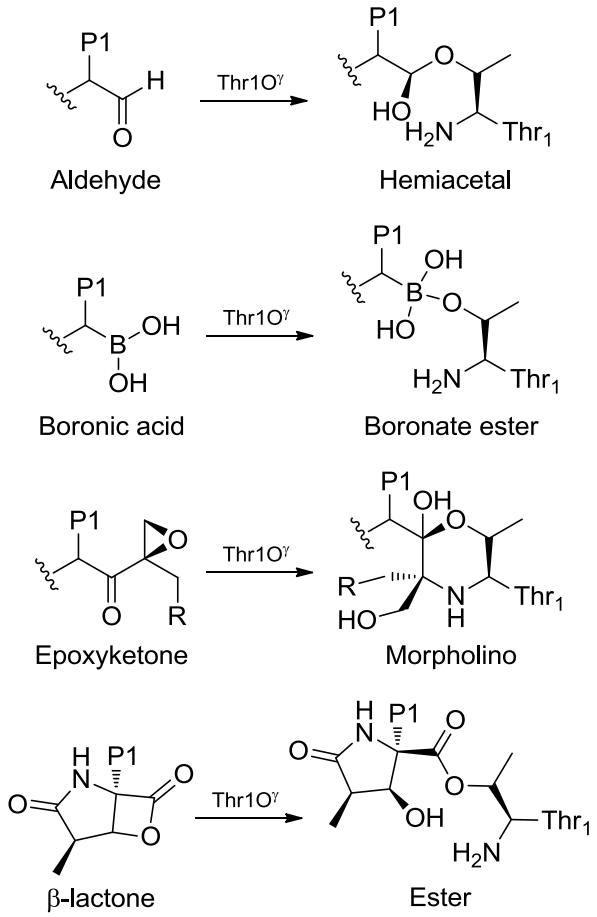

Figure 1.5. Covalent attachment mechanism for several classes of proteasome inhibitors to Thr1 of the proteasome β-subunit.

Michael-type electrophiles such as vinyl sulfones, vinyl esters, and vinyl amides result in an irreversible covalent linkage to Thr1O$^{\gamma}$. While less reactive than the peptide aldehydes, they also display cross-reactivity to other proteases.[22] Naturally produced examples include the syrbactins, which include syringolin A (**5**) isolated *Pseudomonas syringae* pv. *Syringae* and glidobactin A (**6**) isolated from a strain of *Polyangium brachysporum.*[59,60] Syringolin A binds to all three active β-subunits, while glidobactin A binds only to β2 and β5.[61]

The synthetic boronates are the most clinically successful class of PIs to date. Boronates act as an electron acceptor, forming reversible tetrahedral boronic esters with Thr1O$^{\gamma}$. The boronic acid analog of MG132, MG262 (Z-LLL-B(OH)$_2$), showed promising activity when it was shown to be 100-fold more potent than MG132.[62] Bortezomib (**7**, Velcade®) became the first and only PI approved by the FDA for treatment of MM in 2003 and MCL in 2006.[23] Bortezomib primarily inhibits the β5-subunit with low nM potency but also inhibits the β1-subunit to a lesser extent.[63] Despite its high potency, bortezomib possesses several drawbacks.[64] Side effects observed during bortezomib therapy include severe thrombocytopenia and peripheral neuropathy.[65] Bortezomib must also be dosed intravenously and is susceptible to innate and acquired resistance. Second generation PIs seek to improve upon one or more of these deleterious characteristics. Millennium Pharmaceuticals is developing the orally available prodrug MLN9708, which hydrolyzes *in vivo* to the active MLN2238 (**8**),[66] and Teva Pharmaceutical Industries (formerly Cephalon, Inc.) is developing the orally available CEP-18770 (**9**).[67,68] MLN9708 is currently in phase I for solid tumors and phase II for hematological malignancies.[69] CEP-18770 is more potent than bortezomib[68] and as of 2010 was in phase I clinical trials for solid tumors and non-Hodgkins lymphoma.[23,63]

The first highly potent and selective epoxyketone proteasome inhibitors were discovered from actinobacteria, epoxomicin (**10**) from actinomycete strain Q996-17[70] and eponemycin (**11**) from *Streptomyces hygroscopicus* No. P247-71.[71] Epoxyketones bind irreversibly to the β-subunit first by hemiacetal formation between Thr1O$^{\gamma}$ the PI

ketone, followed by attack of the epoxide by the N-terminus of the β-subunit resulting in a stable morpholino ring.[22] This intricate mechanism provides minimal cross-reactivity against other proteases such as trypsin, chymotrypsin, and cathepsin[72] as the mechanism is specific for hydrolases with N-terminal nucleophiles.[73] Epoxomicin irreversibly binds to all three active β-subunits, but most potently to the β5-subunit. Epoxyketone warhead PIs have also been isolated from the marine environment. The carmaphycins, isolated from the marine cyanobacteria *Symploca* sp., also possess the epoxyketone warhead and feature a unique methionine sulfoxide (carmaphycin A, (**12**)) or methionine sulfone (carmaphycin B, (**13**)) at the P2 position which may increase potency by hydrogen bonding within the S2 proteasome pocket.[74] Two synthetic epoxomicin derivatives, carfilzomib[75] (**14**) and the orally bioactive ONX-0912[76,77] (**15**, recently named Oprozomib and formerly PR-047), both developed by Onxy Pharmaceuticals, Inc., (formerly Proteolix, Inc.) are irreversible inhibitors of CT-L activity of the 20S proteasome. Carfilzomib is currently in phase III clinical trials for multiple myeloma, as a single agent or in synergy with lenalidomide and dexamethasone.[78] Phase 1b and II trials are also underway for solid tumors. A new drug application for carfilzomib was filed in the fall of 2011. ONX-0912 is currently in phase I clinical trials for multiple myeloma and solid tumors.[79]

Lactacystin (**16**), isolated from *Streptomyces* sp.,[80] was the first natural product identified as a proteasome inhibitor. Initially noted to induce neuritogenesis in murine neuroblastoma cell lines, it was shown to inhibit all three β-subunit but most potently the β5-subunit.[81] The natural product was found to act as a prodrug with spontaneous β-

lactone formation to *clasto*-lactacystin β-lactone (**17**),[82] also referred to as omuralide,[83] at pH 8. Salinosporamide A (**18**) and B (**19**) are structurally similar γ-lactam-β-lactone proteasome inhibitors isolated from the marine actinomycete *Salinispora tropica.*[14,18,19] Differing only in chlorination of the ethyl side chain extending from C-2 of the γ-lactam, salinosporamide A displays 1000-fold greater *in vivo* potency compared to salinosporamide B.[84] Crystallographic analysis of both compounds bound to the 20S proteasome of *Saccharomyces cerevisiae* revealed that while both β-lactones undergo attack to form esters, as for omuralide, salinosporamide A undergoes a secondary halide displacement to generate the stable cylic ether which blocks hydrolysis of the covalent Thr1 ester linkage (Figure 1.6).[85] Salinosporamide A (Marizomib or NPI-0052, Nereus Pharmaceuticals, Inc.) was undergoing several phase I clinical trials against solid and hematological malignancies as of 2010.[63] It is also the first clinical agent to be produced by saline fermentation.[20] One drawback of the β-lactone pharmacophore is its susceptibility to rapid hydrolysis at physiological pH as the resulting acid does not possess inhibitory activity.[86]

The cinnabaramides (**20**), isolated from *Streptomyces* sp. JS360, also bear a close resemblance to the salinosporamides, sharing the γ-lactam-β-lactone core, the non-proteinogenic cyclohexenylalanine P1 amino acid, and potent CT-L proteasome inhibition.[87] Belactosin A (**21**) and C were isolated from *Streptomyces* sp. UCK14 and reported to possess antiproliferative activity against HeLa S3 cells.[88] The mechanism of activity was later determined to be inhibition of CT-L activity of the 20S proteasome via Thr1 attack of the β-lactone.[89] Homobelactosin C (**22**), a synthetic belactosin

derivative, is significantly more potent with low nM *in vivo* inhibition of human colon cancer cells.[89] While homobelactosin C shares the mechanism of covalent attachment of Thr1 to the β-lactone, the aminocarbonyl binds to the S1' site and the majority of the molecule extends into the primed S pockets.[90]

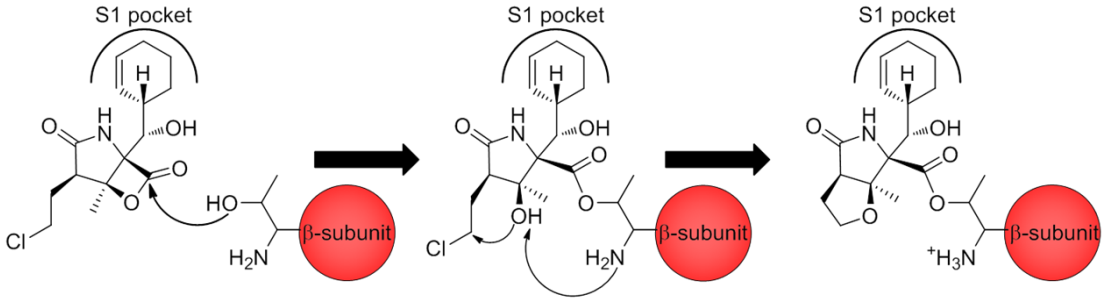

Figure 1.6. Mechanism of irreversible inhibition of the proteasome by salinosporamide A. As with other β-lactone inhibitors (Figure 1.5), binding is initiated by Thr1O$^{\gamma}$ attack of the β-lactone. However, subsequent displacement of chloride results in cyclic ether formation, creating a structural barrier against ester hydrolysis which renders the inhibitor irreversibly bound.

A total of six PIs mentioned above are either FDA approved or currently in clinical trials for the treatment of malignancies.[63,65] A comparison of these PIs is found in Table 1.1. All six PIs primarily target Thr1O$^{\gamma}$ of the β5-subunit. The development status of these PIs has recently been reviewed[63,65] and many thorough reviews of all known PI structures and catalytic mechanisms are currently available.[22,23,26,91]

Table 1.1. Properties of proteasome inhibitors explored for the treatment of malignancies. [a]NI – Not inhibitory, [b]Estimated from graph, [c]Inhibition of CT-L activity includes β5 and β5i subunits

Inhibitor	Electrophile	Developed by	P1 residue	Reversibility	Subunit target	Ref.
Bortezomib (**7**)	Boronate	Millennium Pharmaceuticals	Leucine	Reversible	IC50 (nM): β5 - 7.9, β2 - 590 β1 - 53	#64
MLN2238 (**8**)	Boronate	Millennium Pharmaceuticals	Leucine	Reversible	IC50 (nM): β5 - 3.4, β2 - 3500 β1 - 31	#66
CEP-18770 (**9**)	Boronate	Teva Pharmaceutical Industries	Leucine	Slowly reversible	IC50 (nM): β5 - 3.5 β2 - > 100 β1 – NI[a]	#67
Carfilzomib (1**4**)	Epoxyketone	Onyx Pharmaceuticals, Inc.	Leucine	Irreversible	Kinact/Ki (M-1 S-1): β5 - 33,000 β2 - < 100 β1 - < 100	#75
ONX 0912 (1**5**)	Epoxyketone	Onyx Pharmaceuticals, Inc.	Phenylalanine	Irreversible	IC50 (nM):[b,c] β5 - ~10 β2, β1 – NI @ 50	#77
Salinosporamide A (**18**)	β-lactone	Nereus Pharmaceuticals, Inc.	Hydroxy-cyclohexenyl-alanine	Irreversible	IC50 (nM): β5 - 3.5 β2 - 28 β1 - 430	#64

1.4.2: Non-covalent and Non-competitive Inhibitors.

Non-covalent inhibitors of the proteasome active sites have also been reported. The TMC-95 compounds were isolated from the fungi *Apiospora montangnei* Sacc. TC 1093.[92] These compounds competitively binds to all three β-subunits via non-covalent hydrogen bonding interactions at nanomolar concentrations.[93] TMC-95a (**23**) is selective for the proteasome as no inhibition has been observed for m-calpain, cathepsin L or trypsin.[92]

Several allosteric effectors of proteasome activity that bind away from the active sites have been recently been reported. PR-39 is a 39 amino acid peptide, originally isolated from pig intestines,[94] found to be a reversible, non-competitive inhibitor of the

α7 subunit of the 20S proteasome. It is believed to interfere with 26S assembly from 19S and 20S components.[95,96] The primary sequence is highly enriched in proline (P) and arginine (R) residues. Fragmentation analysis revealed that only the first eleven N-terminal amino acids (PR-11) are required for activity.[97] Additional mutational analysis of PR-11 revealed that a positive charge on the three N-terminal amino acids imparts activity.[98] Substitution with alanine at one or more of these residues resulted in an additive loss in activity. PR-39 has been shown to induce angiogenesis in cell cultures and mice and possess anti-inflammatory activity.[95,96] It also stimulated angiogenesis by increasing cellular HIF-1α protein levels via inhibition of ubiquitin dependent proteasomal degradation.[96] Anti-inflammatory activity resulted from inhibition of IκBα degradation which in turn prevents activation of NFκB-dependent gene expression, yet overall proteasomal protein degradation is not impaired.[95] While it is not a druggable compound, PR-39 may serve as a lead for the development of proteasome assembly inhibitors.

The anti-malarial drug chloroquine (**24**) was reported to inhibit both eukaryotic and archaeal 20S proteasomes.[99] NMR experiments identified chloroquine as uniquely binding between the α and β subunits. Binding distal from the active sites was confirmed by the simultaneous binding of MG132. However, chloroquine is clinically irrelevant as it only inhibits the proteasome at high μM concentrations. A screening of compounds with the chloroquine pharmacophore identified 5-amino-8-hydroxyquinoline (**25**, 5AHQ) as a more potent inhibitor of the 20S proteasome with an IC_{50} was low to sub μM range.[100] 5AHQ inhibited CT-L proteasome activity (T-L and

C-L activities were not tested) in both intact cells and cellular extracts of various myeloma and leukemia cell lines. Oral administration in mice was shown to inhibit tumor growth and cell death was also preferentially induced in cancerous cells. 5AHQ was found to act as a non-competitive inhibitor of the α7 subunit in NMR experiments with the α_7-α_7 "half-proteasome". However, it has yet to be verified that it does not also bind to any β-subunits or if there are other cellular targets of 5AHQ. 5AHQ shows promising activity in many bortezomib resistant cell lines resulting from β5-subunit mutation or overexpression[101,102] and no resistance has been observed yet to 5AHQ, which remains effective in bortezomib resistant cell lines.[101,103]

1.5: Biosynthesis of the Salinosporamides and Analogs

Bioactive natural products often possess intricate and unique chemical structures. In the study of biosynthesis, the objective is to understand how organisms assemble natural products from common chemical building blocks utilizing enzymatic or spontaneous transformations. Many natural products are produced by a variable assembly-line mechanism. Polyketide synthases (PKSs) are analogous to the fatty acid synthases which chain together two carbon monomers by decarboxylative Claisen condensation reactions.[3] However, unlike fatty acid synthases, PKSs generate chemical diversity by incorporating variable starter units and extender units and by differential reduction of each incorporated ketide segments.[3] Non-ribosomal peptide synthetases (NRPSs) incorporate amino acid monomers, including those of a non-proteinogenic

origin, to form peptides which may additionally be modified by processes such as methylation, epimerization, dehydration, and cyclization.[3]

One consequence of this assembly-line style biosynthesis is that many natural products are produced as a family of highly similar compounds. The PKS or NRPS machinery may allow flexibility in the incorporation of PKS extender units or amino acids, respectively, as well as differential activity of tailoring enzymes.[3] A solid understanding of a natural product's biosynthesis may also allow for the production of novel "unnatural products" in a process termed mutasynthesis, in which biosynthetic genes are manipulated and unnatural biosynthetic precursors are introduced. The objectives of expanding structural diversity within a natural product family by mutasynthesis are similar to those of the traditional medicinal chemist: improving potency, reducing toxicity, circumventing resistance mechanisms and eliminating off-target effects. Knowledge of how biosynthetic pathways are regulated may also allow us to activate or increase production of natural products which cannot be practically produced by organic synthesis. Biosynthetic genes may even be cloned from the natural producing organism and inserted into a host organism for greater production. This was famously achieved in the case of the antimalarial drug artemisinin, in which genes required for the biosynthesis of artemesinic acid, a precursor to artemisinin, were transplanted from the sweet wormwood plant (*Artemisia annua*) into yeast (*Saccharomyces cerevisiae*), resulting in a substantial decrease in the production cost of this drug.[104] The following is a broad overview of salinosporamide biosynthesis. My extensive efforts to characterize one specific enzymatic transformation in this pathway,

the oxidation of 5-chloro-5-deoxy-D-ribose by the enzyme SalM, are the subject of Chapter 2 of my dissertation.

Salinispora tropica produces a suite of γ-lactam-β-lactone natural product PIs differing in the substitution at C-2 of the γ-lactam ring. The salinosporamides originate from a mixed PKS/NRPS assembly (Figure 1.7) which incorporates three core building blocks: the nonproteinogenic amino acid cyclohexenylalanine, an acetyl-CoA PKS starter unit, and a variable PKS extender unit.[105] Salinosporamides with methyl (salinosporamide D, **26**), ethyl (B, **19**), propyl (E, **27**), and chloroethyl (A, **18**) substitutions have been isolated which incorporate methyl-, ethyl-, propyl-, and chloroethyl-malonyl-CoA PKS extender units, respectively. The unsubstituted γ-lactone ring, the product of malonyl-CoA incorporation, was not identified in *S. tropica*. However, this analog, salinosporamide K (**28**), was isolated from "*Salinispora pacifica"* CNT-133.[13] "*S. pacifica"* CNT-133 also produced salinosporamide D but not B indicating that the extender unit AT domain requires shorter or unsubstituted extender units. This is opposed to the extender unit AT domain of *S. tropica* which requires substituted extender units.

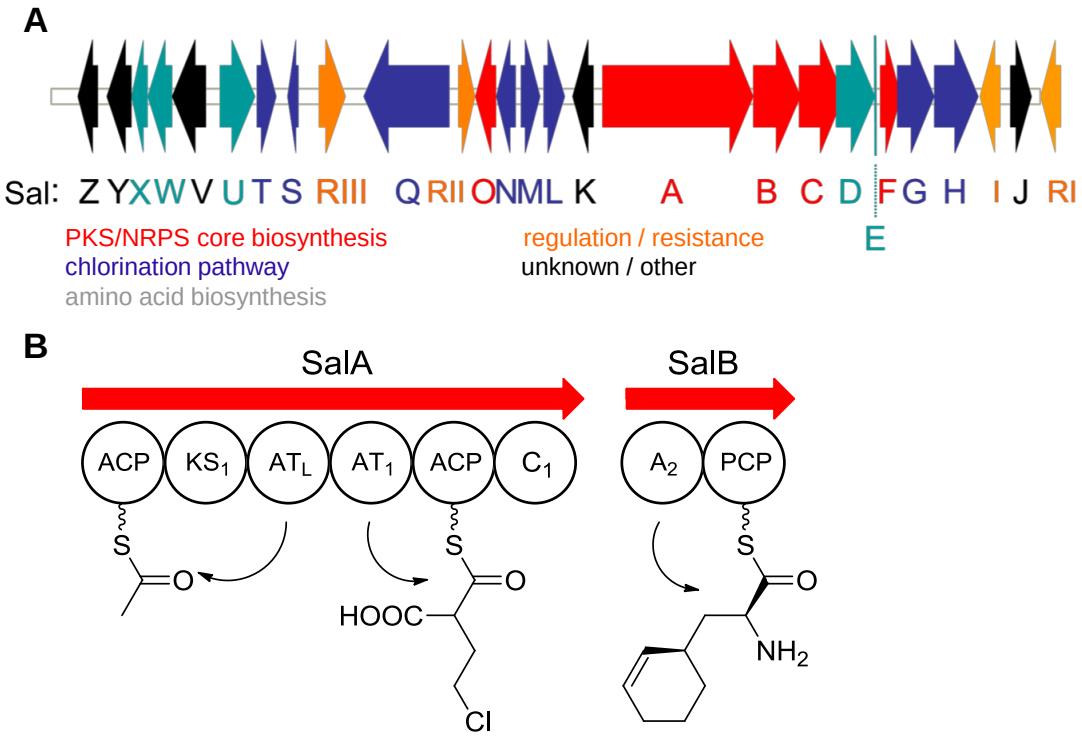

Figure 1.7. Organization of the biosynthetic gene cluster for the salinosporamides in *S. tropica* CNB-440. (A) This biosynthetic gene cluster encodes for the biosynthesis of salinosporamides A, B, D, and E. Genes are color-coded based on function. The genes required for the core PKS/NRPS genes (red), the shared cyclohexenylalanine (gray) and the salinosporamide A specific chloroethylmalonyl-CoA (blue) biosynthesis are present. (B) Domain analysis of the SalA multi-domain type I polyketide synthase and the SalB non-ribosomal peptide synthetase didomain. The AT_L domain of SalA loads an acetyl-CoA starter unit and the AT_1 domain loads a 2-substututed malonyl-CoA extender unit, such as chloroethylmalonyl-CoA. The SalB non-ribosomal peptide synthetase A_2 domain adenylates and loads cyclohexenylalanine.

Salinosporamide A incorporates the unprecedented chloroethylmalonyl-CoA PKS extender unit which substantially increases its potency as a PI relative to the other salinosporamides. Biosynthesis of chloroethylmalonyl-CoA PKS extender unit (Figure 1.8A) is initiated by the nucleophilic chlorination of S-adenosyl-L-methionine (SAM) by the chlorinase enzyme SalL.[106] SalL bears sequence homology to the 36% identical

fluorinase enzyme FlA of the fluoroacetate producing *Streptomyces cattleya*.[107] In both pathways, adenine is then removed from the 5-halo-5-deoxyadenosine by the action of a purine nucleoside phosphorylase, SalT or FlB.[108] At this point, the two pathways diverge. The biosynthesis of chloroethylmalonyl-CoA was characterized by a combination of bioinformatics analysis, *in vivo* gene replacement and chemical complementation, and *in vitro* enzyme characterization (in the cases of SalL,[95] SalG,[108] and SalM[109]). Our understanding of the terminal reaction, reductive carboxylation of chlorocrotonyl-CoA, arose from the recharacterization of the crotonyl-CoA reductase (CCR) enzymes as also possessing carboxylase functionality.[110] Carboxylation of α,β-unsaturated-CoA thioesters results in the formation of 2-substituted malonyl-CoA PKS extender units.[111] Through gene inactivation experiments, it was determined that the housekeeping CCR enzyme Strop_3612 is sufficient to generate the ethylmalonyl-CoA derived salinosporamide B (Figure 1.8B). The salinosporamide gene cluster encoded CCR enzyme SalG was shown to be solely responsible for synthesis of choroethylmalonyl-CoA as well as propionyl-CoA.[108,112] Longer C_6-C_8 2-alkenoates were not incorporated into salinosporamides. However, in the production of cinnabaramide A from *Streptomyces* sp. JS360, the SalG homolog CinF catalyzes the reductive carboxylation of oct-2-enoyl-CoA to from hexylmalonyl-CoA, leading to the C_6 alkyl chain at C-2 of the γ-lactam.[113]

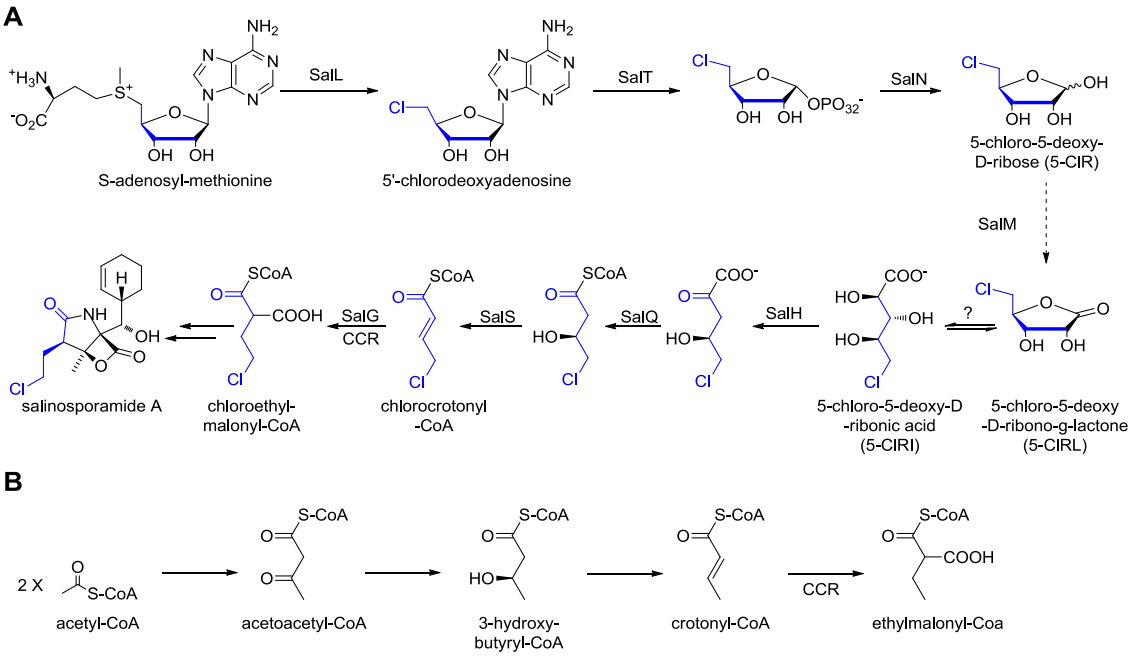

Figure 1.8. Biosynthesis of polyketide synthase extender units. (A) The chloroethylmalonyl-CoA biosynthetic pathway encoded within the salinosporamide biosynthetic gene cluster of *S. tropica* CNB-440. The SalM reaction (dashed line) is the subject of Chapter 2. (B) The ethylmalonyl-CoA biosynthetic pathway.

As the halide leaving group of salinosporamide A renders this PI significantly more potent than the non-halogenated salinosporamides, it would be advantageous to selectively overproduce salinosporamide A by upregulating the incorporation of the chloroethylmalonyl-CoA extender unit. A selective doubling of salinosporamide A production was accomplished via upregulation the LuxR-type regulator SalR2.[114] SalR2 activates two operons, one of which encodes the chlorinase gene *salL*, the first committed step of chloroethylmalonyl-CoA, and therefore salinosporamide A, biosynthesis. The increased production of salinosporamide A by chloroethylmalonyl-CoA upregulation revealed that PKS extender unit incorporation of the salinosporamides may be dictated by the supply of extender units.

The complete biosynthetic pathway of the cyclohexenylalanine amino acid has not been conclusively established, but it does utilize the recently described prephenate decarboxylase SalX (Figure 1.9).[115] Inactivation of the *salX* gene abolished production of the salinosporamides. Chemical complementation of the Δ*salX* strain with alternative amino acids afforded the mutasynthetically derived compounds[90,91] salinosporamides X1-X7 (**29**-**35**), as well as the previously synthesized antiprotealide (**36**).[116] With the exception of salinosporamide X7, all P1 modifications reduced *in vivo* potency and *in vitro* CT-L inhibition. However, salinosporamide X7 (**35**, Figure 1.4) had equipotent activity *in vitro* and 3-fold more potency against the HCT-116 cell line than the parent compound.

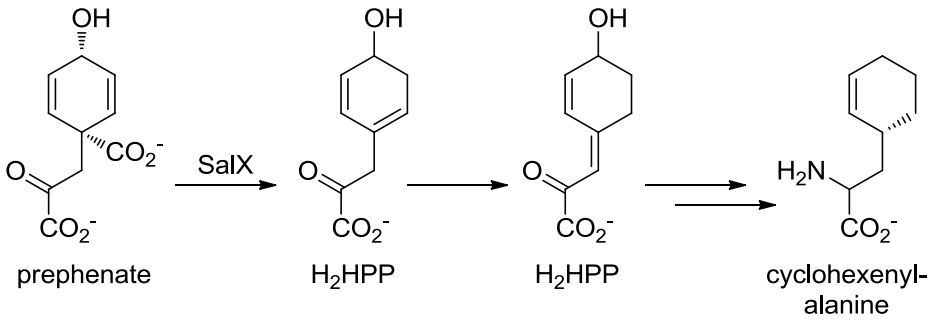

Figure 1.9. Biosynthesis of cyclohexenylalanine. SalX catalyzes the non-aromatizing decarboxylation of prephenate to the endocyclic diene dihydro-4-hydroxyphenylpyruvate (H_2HPP), followed by spontaneous isomerization to the exocyclic diene H_2HPP. The following steps have yet to be elucidated but are believed to require transamination by the aminotransferase SalW which may also catalyze dehydration through the conjugated system.

1.6: Proteasome Inhibition in Cancer Therapy

Proteasome inhibitors have flourished as anticancer agents because they potently and preferentially induce apoptosis in certain malignant cell types. The natural product lactacystin was first identified to induce apoptosis in the human monoblast U937 cell line[117] while chronic lymphocytic leukemia cells were found to be significantly more sensitive to lactacystin-induced TNFα-mediated apoptosis than were normal human lymphocytes.[118] Tumor growth was also suppressed *in vivo* by proteasome inhibition in mouse models of Burkitt's lymphoma and the induction of apoptosis preferentially targeted cancerous cells.[119] Finding that malignant cells were more susceptible to PI-induced apoptosis lead to speculation that malignant cells may rely more heavily on proteasomal degradation for survival.[120] Elevated proteasome expression has indeed been observed in neoplastic cells, including various types of leukemia, indicating that increased proteasome activity is required to maintain survival during rapid proliferation.[121] Defects in ubiquitinating and deubiquitinating enzymes have also been linked to certain cancers.[24] Basal proteasome activities have been shown to differ among cell lines and correlate to intrinsic bortezomib sensitivity[102] with cells intrinsically resistant to bortezomib displaying higher CT-L and C-L activities.[102,122] However, while basal proteasome activities may serve as an indicator of intrinsic resistance, there is no evidence that they serve as a predictor of acquired resistance.

The specific mechanism by which proteasome inhibition translates into anticancer therapy is complex and may vary depending on the specific transformation. While many biochemical pathways have been identified to be affected, the unifying theme is that proteasome inhibition diminishes the degradation of regulatory proteins.[24]

Inhibition of the NF-κB pathway is a frequently sited consequence of proteasome inhibition. Functional proteasomes are required to degrade IκBα, an inhibitor of NF-κB function. Proteasome inhibition allows IκBα levels to rise, thereby inhibiting NF-κB which leads to a decreased production of antiapoptotic factors, angiogenic factors and apoptosis inhibitors.[24] As the NF-κB pathway is activated by many chemotherapeutic agents, PIs such as bortezomib may, when used in combination therapy, increase the effectiveness of such drugs.[123] Proteasome inhibition has also been reported to cause disregulation of cyclins, cyclin-dependent kinases and other cell cycle regulatory proteins that disrupt cell division. Proteasome inhibition may favor apoptosis by stabilizing proapoptotic proteins such as Bax and p53 while reducing antiapoptotic proteins such as the Bcl-2-family proteins.[24,123] Additionally, antitumor activity has been attributed to the formation of reactive oxygen species and aggresomes, the unfolded protein response, the intrinsic mitochondrial apoptotic pathway, the death receptor pathway, and ER stress response pathway.[24] For more detailed reviews on the mechanisms of action of PIs in cancer therapy, see the following reviews.[24,120,123,124]

1.7: Resistance to Proteasome Inhibitors

1.7.1: Introduction to Proteasome Inhibitor Resistance.

Despite bortezomib being more efficacious than other chemotherapeutic agents in the treatment of certain hematological malignancies, as many as 65% of patients do not respond and all patients eventually see progression of the disease.[125] Why some patients are intrinsically resistant and the rest ultimately acquire resistance is poorly

understood. Many recent studies have greatly improved our understanding of PI resistance by establishing cell lines of various malignancies that are resistant to bortezomib.[101-103,126-132] The results of these studies are summarized here.

1.7.2: Multidrug Resistance.

One generalist strategy for drug resistance is achieved through multidrug resistance (MDR) efflux pumps. Resistance to the peptidyl aldehyde ALLN in Chinese hamster ovary cells was reportedly caused by the upregulation of P-glycoprotein (Pgp) transmembrane pump via upregulation of the encoding multidrug resistance gene *mdr1*.[133] This verified that Pgp could export linear peptides, the primary structural scaffold of most PIs. Another MDR pump, MRP1, was later established to export hydrophobic linear peptides as well.[134] Over-expression of MRP1 lead to multidrug resistance, which included ALLN, in various cancer cell lines used.[134] Acute myeloid leukemia cell lines over-expressing Pgp were shown to display slight (~2X) bortezomib resistance whereas cell lines overexpressing MRP1 were not resistant.[135] However, no additional reports have attributed MDR resistance to bortezomib, and several studies have ruled it out,[102,103,126-128] suggesting that multi-drug resistance is not a significant factor in PI resistance.

1.7.3: Changes in Proteasome Subunit Levels.

To elucidate other potential PI resistance mechanisms, bortezomib resistant cell lines have been established by chronic exposure to increasing concentrations of the PI.[101-103,126-132] Table A1.1 summarizes the results of these studies. The results, while far from uniform, illustrate a common theme: upregulation of proteasome subunits and/or mutation of the β5-subunit encoding gene *PSMB5*. Upregulation at both the mRNA

transcription and protein translation level have been observed. The maximum bortezomib tolerance achieved and the time required for development of resistance varied widely by cell line. The data presented in Table A1.1 come from PI resistant lines which were established and analyzed by multiple groups. The table represents the level of detail and quantification provided by the authors of these studies.

Alterations in mRNA transcription of the β5-subunit encoding *PSMB5* gene have varied from slightly decreased,[103] to unchanged,[128,131] to slightly increased,[101,127,129] to substantially increased (5-15 fold).[101,132] In cases where transcription levels of other proteasome related genes were quantified, *PSMB6* and *PSMB7* also varied from unchanged[103] to a five-fold increase.[101] Transcription of genes related to the 11S immunoproteasome regulatory cap were also upregulated in one study.[129] Oerlemans *et al.* performed microarray transcriptional analysis on their 30 nM and 100 nM bortezomib resistant human monocytic lines as well as their 100 nM resistant line after 6 months in absence of bortezomib. No discernible link between gene expression and resistance was observed.[103]

Evaluating proteasomal subunit upregulation at the protein level is a more direct measurement of proteasome upregulation. In most case where bortezomib resistance was observed, β5-subunit protein levels increased. Although many studies did not quantify the change in proteasome subunit protein levels, the degree of β5 increase has ranged from minor to as much as 60-fold.[103] No clear quantitative correlation between level of resistance and the extent of β5-subunit expression has been observed.

Many of these studies quantified either mRNA or protein levels but not both. In cases were both were analyzed,[101,103,129,131,132] it appears that mRNA transcription levels are not a strong indicator of protein expression levels. In one case, *PSMB5* transcription was unchanged but a 60-fold increase in β5-subunit protein was observed.[103] Silencing of *PSMB5* mRNA expression in these cells did prevent upregulation of the β5-subunit and restore bortezomib sensitivity and induce apoptosis. In another case, *PSMB5* transcription from 7 nM and 100 nM bortezomib resistant lines increased by 5X and 15X, respectively, relative to the parental cells.[101] However, while both showed β5-subunit protein upregulation relative to the parental line, there was no difference in protein concentration between these two resistant cell lines despite the 3-fold difference in mRNA transcription. Based on these studies, mRNA transcription levels should not be used as a proxy for proteasome content or activity.

Bortezomib resistant cell lines displayed conflicting regulation of the immunoproteasome components. One study found a complete shift in favor of the 19S-20S proteasome at the expense of the 11S and immunosubunits[126] while another study found upregulation of the 11S and downregulation of the 19S regulatory particle with no change in immunosubunit expression.[129] Franke *et al.* observed a specific shift away from β5i toward β5 in resistant MM cells but no alteration of β5/β5i ratio was demonstrated in resistant acute lymphoblastic lymphoma cells.[101] The 11S cap was also upregulated in resistant the acute myeloid leukemia cell line.[101] In a study of three bortezomib resistant non-small cell lung cancer lines, two showed upregulation of the immunosubunits while the third showed no change.[102] Taken together,

immunoproteasome regulation appears to vary widely among and within bortezomib resistant cancer types.

1.7.4: Proteasome β-subunit Mutations.

Many bortezomib resistant cell lines have been found to possess mutations in the β5-subunit encoding gene *PSMB5*. Most of these mutations encode amino acid substitutions located in the S1 binding pocket. Substitution of Ala49 with Thr or Val has been observed independently in six different studies.[101-103,127,128,130] Additional S1 binding pocket mutations include A50V, C52F, M45V, M45I and T21A. X-ray crystallographic analysis of bortezomib bound to the 20S proteasome β5-subunits of the *Saccharomyces cerevisiae* revealed a hydrogen bonding network between bortezomib, a structured water molecule, and several amino acid residues of the S1 binding pocket, including Ala49, Ala50 and Thr21 (Figure 1.10A).[136] Although these hydrogen bonding interactions originate from backbone atoms, side chain substitutions may alter backbone positioning and disrupt the bonding network. Met45 was additionally shown to move 2.7 Å to accommodate bortezomib's P1 leucine residue.[136] Mutation of Met45 may diminish binding by constricting the S1 pocket or reducing favorable hydrophobic interactions. Cys52 is located behind the S1 binding pocket and may hinder movement of Met45. Ala49 is positioned at the entrance of the S1 binding pocket (Figure 1.10B). Increasing the size of the side chain may stearically hinder the binding of both inhibitors and substrates. Indeed, computational modeling of these mutations showed that they should decrease both substrate and inhibitor binding.[101,127] Cleavage of the fluorogenic substrate succinyl-Leu-Leu-Val-Tyr-amc (LLVY-amc) also appears to be reduced in the

resistant cell lines. However, no alternative fluorogenic substrates have been tested to check for a shift in proteolytic specificity.

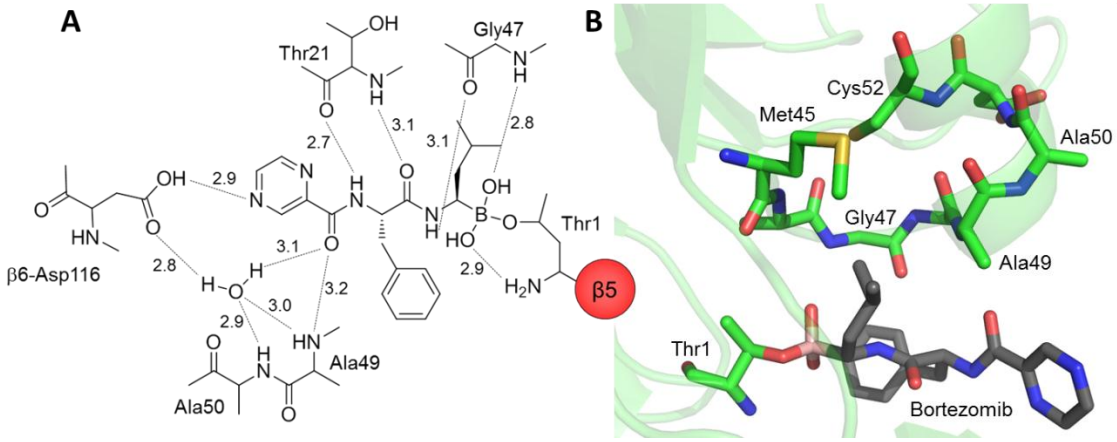

Figure 1.10. Substrate binding analysis of bortezomib and the β5-subunit of the *Saccharomyces cerevisiae* 20S proteasome. (A) Dashed lines represent H-bonding with distances shown in Å. Mutations observed at Ala49, Ala50 and Thr21 may disrupt H-bonding and decrease PI binding. Figure adapted from Groll *et al.*[136] (B) Crystal structure of the S1 binding pocket with bortezomib bound. Image created using PDB file 2F16, chain K rendered in PyMol.[137]

The role of one *PSMB5* mutation in acquired PI resistance was verified in T cell lymphoblastic lymphoma cells. The parental line was mutated by retroviral infection to encode the same A49T seen in the bortezomib resistant line.[127] These cells were resistant to bortezomib induced apoptosis and the inhibition of CT-L activity was decreased. The same mutation was also transfected into parental KMS-11 MM cells and shown to induce bortezomib resistance, but not to the full extent of KMS-11/BTZ cells suggesting that other factors also contribute to resistance.[130]

Mutations were observed at resistance levels as low as 7 nM bortezomib[101] which is below the clinically used concentration of 12.5 nM.[126] Franke *et al.* showed that mutations were observed in cell lines which were developed in as little as four months and that upon repeating the bortezomib desensitizing process, the same cell line developed a different set of mutations.[101] They argued that this supports de novo mutation as opposed to the selection of preexisting mutations. Although cell lines with different mutations varied greatly in their level of bortezomib resistance, it has not been conclusively shown *in vitro* that any specific mutation is fully responsible for the acquired level of resistance or that one mutation confers greater resistance than another.

Few studies have searched for mutations in other proteasome subunits. Ri *et al.* reported no mutations in the β1 or β6 subunit encoding genes[130] and the study by Franke *et al.* did not find mutations in *PSMB6* or *PSMB7*.[101] It should also be noted that not all bortezomib resistant cell lines contained *PSMB5* mutations. MM[132] and MCL[131] cell lines, each resistant to 100 nM bortezomib, were both found to be free of mutations.

1.7.5: Actinobacterial Self-Resistance to Endogenously Produced PIs.

Many PIs, including salinosporamide A, lactacystin and epoxomicin, are produced by members of the actinobacteria.[91] As the actinobacteria are the only family of eubacteria known to possess 20S proteasome machinery, it raises the question of how such potent inhibitors can be produced within an organism that possesses the target protein. Sequencing of the complete genome of the salinosporamide producing actinobacteria *S. tropica* CNB-440 revealed a secondary 20S proteasome β-subunit (SalI) encoded within the salinosporamide biosynthetic gene cluster.[11] We hypothesized

that SalI may function as a target modification resistance mechanism by complexing with the lone α-subunit to form a salinosporamide resistant 20S proteasome complex. My efforts to characterize the biochemical functionality of SalI and its potential role as a self-resistance mechanism are the subject of Chapter 3 of this dissertation.[138]

1.7.6: Stability of Resistance Phenotype.

In most cases, acquired bortezomib resistance appears to be a stable transformation. In resistant monocytic/macrophage cells transferred to bortezomib free media for 7 days, *PSMB5* expression was unaltered but β5 levels decreased by 2.5-fold.[103] After 6 months, these cells still retained 35-fold bortezomib resistance. β5-subunit levels and the encoding mRNA both decreased over this time but were rapidly restored upon reintroduction of bortezomib.[103] Rüchrick *et al.* confirmed that the resistance phenotype was stable over 14 days and de Wilt *et al.* and Lü *et al.* both confirmed resistance after 2 months in the absence of bortezomib.[102,128,129] However, Pérez-Galán *et al.* reported that resistance to bortezomib, which was not caused by a β5-subunit mutation, was gradually lost over time as the IC_{50} increased 80-fold after one month in the absence of bortezomib.[131]

1.7.7: PI Resistance in Human Patients.

It should be noted that the bortezomib resistance mechanisms discussed above were only observed in cell lines. Although the sample size is small, no *PSMB5* mutations have yet been observed in primary patient cell samples.[130,131,139] Screening patients who develop bortezomib resistance for *PSMB5* mutations does not appear to be common practice in the clinic. Microarray analysis was used on over one hundred

patients with myeloma to identify changes in gene regulation which correlated to progression of the malignancy.[140] Several proteasome pathway genes were upregulated 48 hours after bortezomib was administered in combination with thalidomide and dexamethasone relative to treatment with only thalidomide and dexamethasone. These genes included *PSMD4,* encoding one of the non-ATPase 19S regulatory cap proteins, and *PSMB2*, *PSMB3*, and *PSMB4,* all encoding non-catalytic 20S β-subunits. Shaughnessy *et al.* suggested that this upregulation is due to preferential killing of normal plasma cells and survival of cells with existing upregulation as opposed to drug induced upregulation in all cells. None of the catalytic β-subunit encoding genes were found to be differentially regulated. In another study, proteasome activity was visualized in primary cells taken from patients with chronic lymphocytic leukemia, acute lymphoblastic leukemia, and acute myeloid leukemia using fluorescent probes.[141] While the stoichiometry of the β1, β2 and β5-subunits remained the same, the activity varied even within the same cancer types but remained consistent per patient over several weeks. A correlation was observed that in myeloma and non-Hodgkin's lymphoma cells with the lowest (β1 + β5) activity levels, relative to β2, were the most sensitive to bortezomib.

1.7.8: Resistance Mechanisms Beyond Proteasome Modification.

Many of the studies reviewed here explored changes in cellular biochemistry beyond the proteasome. Several reports showed that poly-ubiquitinated proteins failed to accumulate under bortezomib treatment in resistant lines.[101-103,126,129,130,132] However, poly-Ub proteins did accumulate when bortezomib levels significantly higher than the

selective concentration were used.[101-103] No changes in growth rate or morphology were observed for most of the resistant cell lines.[103,127,129] Balsas *et al.* observed that resistant cells were significantly larger in size and nearly doubled in cellular DNA content.[132] Rückrich *et al.* observed a 75% reduction of total protein biosynthesis,[129] whereas Ri *et al.* observed no alteration of protein synthesis levels in bortezomib resistant lines.[130] Pérez-Galán *et al.* also observed that intrinsically resistance cells and those which acquired resistance were associated with plasmacytic differentiation.[131]

Many PI resistance mechanisms function independently of alterations to the Ub-proteasome system. As McConkey and Zhu comprehensively surveyed these PI resistance mechanisms in 2008,[124] I will only mention a few new studies published since that time. Constitutive NF-κB expression has been observed in MCL lines which were less susceptible to bortezomib induced apoptosis.[142] In bortezomib resistant mesothelioma I-45 cell lines, generated by exposure to increasing concentrations of bortezomib, growth kinetics slowed significantly as compared to the parental line but no change in β-subunit expression or *PSMB5* gene mutations was observed.[143] β5-subunit activity was not altered in resistant lines and bortezomib retained the ability inhibition of the β5-subunit. Bortezomib resistance was attributed to a reduction in the level of ubiquitinated protein and suppression of the pro-apoptotic genes *NOXA*, *Mcl-1S*, and *p53*.[143] Bortezomib induced apoptosis was also diminished by Bcl-2 overexpression. Bcl-2 bound to Noxa thereby preventing Noxa-induced apoptosis in human lymphoid cells.[144] Bortezomib has also been shown to induce stress granules which inhibit apoptosis in HeLa cells.[145] In this case, the cyclin-dependent kinase inhibitor p21 is

suggested to arrest cell cycle and promote apoptosis. The RNA binding protein CUGBP1 stabilized p21 mRNA and increased expression during bortezomib therapy, which prohibited apoptosis through a yet to be defined mechanism. The authors of this study suggest that both CUGPB1 and p21 could be drug targets to sensitize for proteasome inhibitor treatment. Solid tumor cell lines, but not MM lines, excreted the chaperone protein GRP-78 which caused bortezomib resistance.[146] Knockdown of the encoding gene restored bortezomib sensitivity.

1.8: Circumventing PI Resistance

Overcoming intrinsic and acquired resistance to PIs such as bortezomib will greatly improve efficacy in the clinic. As it is apparent that multiple mechanisms of resistance are possible, no one solution will be adequate to ensure effective treatment in all patients. Strategies to improve the efficacy of PI therapy may include the use of irreversible β-subunit inhibitors, modifying the P1 residue to target mutated β5-subunits, targeting alternate proteasome subunits or proteasome complex assembly as discussed earlier, inhibiting upstream ubiquitination pathway enzymes, and targeting proteins outside of the ubiquitin-proteasome pathway.

Several reports have identified acquired mutations of the *PSMB5* gene in bortezomib resistant cell lines. These mutations appear to alter the S1 binding pocket which slows or prevents PI binding and often confer resistance to other PIs that target the catalytic site of the β5-subunit. As all inhibitors currently being explored in the clinic primarily target the β5-subunit active site, they will all likely be susceptible to

this mechanism of inhibition. However, the administration of CEP-18770 along with bortezomib did delay progression of MM in a patient whom had become resistant to bortezomib.[147] As both bortezomib and CEP-18770 are boronates that target the β5-subunit, it is unclear how CEP-18870 was able to overcome resistance. Irreversible inhibitors such as carfilzomib and salinosporamide A may be less susceptible to mutated β-subunits. While a modified S1 binding site may slow binding kinetics, as evidenced by elevated IC_{50}s, the binding event must only take place once before permanently deactivating the catalytic site. As an example, MM 8226/BTZ100 cells, which possess an A49T mutation, showed 39.5-fold resistance to bortezomib but only 9.7-fold resistance to carfilzomib and 10.1-fold resistance to ONX 0912.[101] In one study, bortezomib resistant MM cell lines were established by prolonged exposure to bortezomib to examine the ability of carfilzomib to overcome bortezomib resistance. While some cross resistance was observed for carfilzomib, it did retain greater antiproliferative effectiveness.[148] Carfilzomib also demonstrated antiproliferative and cytotoxic effectiveness on bortezomib resistant primary patient samples as well.[148] ONX 0912 has also been shown to induce apoptosis *in vitro* in two bortezomib resistant patient samples, although the specific mechanism of this bortezomib resistance was not known in this case.[149] The irreversible PI salinosporamide A induced apoptosis in MM cells that were resistant to bortezomib which was attributed to activation of different apoptotic pathways.[64] It remains to be seen what level of resistance develops to these irreversible inhibitors when they are used as the selecting agent.

If target sequence modification is confirmed as a clinically relevant form of PI resistance, it would be ideal to develop inhibitors with specificity for the mutated proteasomes. As the same mutations, such as A49T or A49V, have been observed in several independently derived bortezomib resistant cell lines as well as the salinosporamide A producing bacterium *S. tropica*,[138] a second generation of PIs tuned specifically for these active site alterations could be developed. A library of PI analogs with various P1 residues, as has been established previously when developing inhibitors for the wild-type proteasome,[22] could be assayed *in vitro* against a 20S complex containing a mutated β5-subunit. Such PIs could either be utilized if mutations are detected in the patient or concurrently with bortezomib to decrease the selecting pressure for mutations.

Multiple strategies to treat PI resistant cancers by inhibition of alternative targets have been recently reported. As inhibition of the proteasome appears to combat cancer by decreasing proteolysis of regulatory proteins, this effect could also be achieved by inhibiting the upstream ubiquitinating enzymes E1, E2, and E3 or deubiquitinating enzymes. As the specificity of E1, E2, and E3 increases, so too does the enzyme diversity. Targeting the primary E1 enzyme in humans should prevent proteasomal degradation of most cellular proteins and therefore have a similar effect to inhibition of the proteasome. For example, the E1 inhibitor PYZD-4409 was recently shown to preferentially induce cell death in malignant leukemia cells and delay tumor growth in a murine leukemia model, achieving a similar affect as a PI with an alternative target.[30] Inhibiting a specific E3 could target individual cellular proteins, allowing for more

controlled therapy. Disruption of the ubiquitination system with small molecule inhibitors is an active area of study and has been recently reviewed.[150]

Inhibition of several targets outside of the Ub-proteasome pathway has successfully destroyed bortezomib resistant cancer cells. Fuchs *et al.* reported that the HMG-CoA reductase inhibitors simvastatin (Zocor) and lovastatin effectively induced apoptosis in both parental Namalwa Burkitt's lymphoma and their bortezomib resistant Namalwa^{ad} cell lines.[151] Simvastatin was shown not to inhibit the proteasome nor did it reduce proteasome subunit expression. In another case, low expression levels of caspase-8 and caspase-3 were observed in bortezomib resistant DHL-4 cells.[152] This could be countered by inhibition of the lysophosphatidic acid acyl-transferase (LPAAT) with the LPAAT-β inhibitor CT-32615. The galectin-3 inhibitor GCS-100, a polysaccharide derived from citrus pectin, was also shown to induce apoptosis in MM cell lines, including those resistant to bortezomib.[153] GCS-100 induced apoptosis independent of the proteasome by modulating several cellular apoptosis and cell cycle regulators.[154] Finally, MCL cells resistant to bortezomib displayed a marked increase in BiP/Grp78 due to increased activity of the chaperone Hsp90.[155] Inhibition of Hsp90 with the ansamycin IPI-504 effectively overcame bortezomib resistance.

1.9: Conclusion

For centuries, chemical entities derived from natural sources have played an instrumental role in the treatment of human illnesses. The discovery of proteasome inhibitors, many of which were isolated from a variety of natural sources, has improved our understanding of both the mechanism of proteasome mediated proteolysis and the

greater role of proteasome mediated protein degradation in the cell. This knowledge has allowed proteasome inhibitors to be developed as therapeutic agents for many applications, primarily in the treatment of hematological malignancies.

In this dissertation, I report my efforts to characterize the biosynthetic origin of the potent proteasome inhibitor, salinosporamide A, produced by the marine bacterium *Salinispora tropica*. This organism and the PI it produces were previously discovered by fellow scientists at the Scripps Institution of Oceanography. A better understanding of the biosynthesis of this molecule has enabled us to produce analogous structures by mutasynthesis, probe structure activity relationships, increase fermentation yields, and consider the evolutionary origin of this family of pharmaceutically relevant molecules.

Furthermore, I have characterized a potential self-resistance mechanism for this organism to protect itself against the endogenously produced salinosporamide A. The modified sequence of a duplicated β-subunit target appears to confer resistance to salinosporamide A and cross-resistance to other PIs. Similar mutations have recently been observed in the β5-subunit of PI resistant human cell lines, validating the medicinal relevance of this resistance mechanism. Additionally, we may now utilize secondary 20S proteasome β-subunit genes as a marker to locate PI biosynthetic gene clusters in actinobacteria genomes.

1.10: Acknowledgements

Chapter 1, in part, was submitted as Uncovering the Molecular Mechanisms of Proteasome Inhibitor Resistance (2012). Kale, Andrew J. and Moore, Bradley S., Journal of Medicinal Chemistry. The dissertation author was the primary author of this submission.

1.11: Appendix

Table A1.1. Comparative summary of cell lines with acquired bortezomib resistance.

[a]The data shown matches the level of quantitation provided in each publication. Experiments not performed are indicated as ND (not determined) whereas data that appears to have been obtained but not reported is indicated as NR (not reported). Symbols used: ↑, increase; ↓, decrease; ⊗, no change

[b]Abbreviations: 5AHQ, 5-amino-8-hydroxyquinole; 5fl, 5-fluorouacil; ALLN, Ac-LLnL-al; ble, bleomycin; chl, chloroquine; cis, cisplatin; cyc, cyclosporin A; daun, daunoribicin; dox, doxorubicin; epox, epoxomicin; eto, etoposide; fld, fludarabine; gef, gefitnib; gel, geldanamycin; hct, hydrocortisone; het, heterozygous; hom, homozygous; lact, lactacystin; mel, melphalan; mtx, methotrexate; mpr, methylprednisolone; mit, mitoxantrone; NLVS, 4-hydroxy-5-iodo-3-nitrophenylacetyl-Leu-Leu-Leu-vinylsulfone; 0912, ONX 0912; 0914, ONX 0914; sts, stauroporine; sulf, sulfasalazine; vinc, vincristine; vind, vindesine; ZL_3VS, Z-Leu-Leu-Leu-vinylsulfone

[c]In cases where resistant vs. sensitive were not designated by the authors, an arbitrary resistance factor cutoff of 1.3 was used

[d]Estimated from figure in publication

[e]Assayed in the absence of bortezomib

[f]β5 level proportional to level of resistance

[g]Activity varied by selective concentration, but each line was not quantified

[h]CT-L activity relative to the same cell line in the absence of bortezomib

[i]Assays performed after 2 weeks in the absence of bortezomib

[j]An additional silent mutation was observed

[k]After more than 2 mo in the absence of bortezomib

[l]IC_{50} did not change when grown without bortezomib for 14 days.

[m]β5 and β1 activity could not be differentiated from each other

[n]After 1 mo in the absence of bortezomib

[o]Estimated from on-gel assay

[p]Relative luminescence, 1 = 100,000 units

[q]Assay performed after 72 hours in the absence of bortezomib

Ref.	Cancer cell type	Cell line	Selective concentation (bortezomib)	Selection time	mRNA transcription regulation	Protein expression regulation	Cellular bortezomib sensitivity IC_{50} (resistance factor)	Proteasome activity/resistance	β5-subunit mutation	Cross-resistace[b,c] (resistance factor)	Sensitivity[b,c] (resistance factor)
Fuchs *et al.*[126]	Namalwa Burkitt lymphoma	Namalwa (parental)	-	-	-	-	-	-	ND	-	Lact inhibited β1 & β5 @ 5 μM
		Namalwa[ad]	12.5 nM	3-4 wks	ND	↑: 19S & 20S components; ↓: 11S & immunosubunits	Hyperproliferation only slightly inhibited at 100 nM	↑: CT-L, T-L, and C-L activities (< 1.5X)[d], 50 nM bortezomib failed to inhibit CT-L activity	ND	apoptosis resistance: lact (slight), γ-radiation, sts	Lact inhibited β5 activity @ 10 μM, not β1 or β2
Oerlemans *et al.*[103]	Monocytic/ macrophage	THP1/WT (parental)	-	-	relative *PSMB5*, *PSMB7*, *PSMB6* levels:	-	3.3 ± 0.6 nM (growth inhibition)	CT-L (1X), C-L (1X), & T-L (1X)[e]	None	MG132 (237 nM), MG262 (2.1 nM), ALLN (3.7 μM), 4A6 (0.26 μM)	-
		$THP1/BTZ_{30}$	30 nM	6 mo	0.4, 1, 1.3[d] ↓: β5i & β1i (2X)	↑: β5 (up to 60X)[f], β1 & β2 (< 2X)	NR	↑ activity: CT-L (1.3-1.4X), C-L (1.8-2.3X), & T-L (1.4-1.7X)[e,g]	A49T	NR	NR
		$THP1/BTZ_{50}$	50 nM	6 mo	0.5, 0.7, 1.1[d] No microarray	↑: β5 (up to 60X)[f], β1 & β2 (< 2X)	148 ± 54 nM (45)	↑ activity: CT-L (1.3-1.4X), C-L (1.8-2.3X), & T-L (1.4-1.7X)[e,g]	NR	MG132 (8.1), MG262 (8.3), ALLN (5.8), 4A6 (44)	mtx, sulf, 5fl, chl, ble, gef, cis, cyc, mpr, geld, dox, mit, eto
		$THP1/BTZ_{100}$	100 nM	6 mo	0.6, 0.8, 1.2[d] ↓: β5i & β1i (2X)	↑: β5 (up to 60X)[f], β1 & β2 (< 2X)	261 ± 71 nM (79)	↑ activity: CT-L (1.3-1.4X), C-L (1.8-2.3X), & T-L (1.4-1.7X)[e,g]	A49T	MG132 (11.9), MG262 (10.3), ALLN (10.0), 4A6 (117)	mtx, sulf, 5fl, chl, ble, gef, cis, cyc, mpr, geld, dox, mit, eto
		$THP1/BTZ_{200}$	200 nM	6 mo	0.9, 0.9, 1.5[d] No microarray	↑: β5 (up to 60X)[f], β1 & β2 (< 2X)	426 ± 72 nM (129)	↑ activity: CT-L (1.3-1.4X), C-L (1.8-2.3X), & T-L (1.4-1.7X)[e,g]	NR	MG132 (15.8), MG262 (10.8), ALLN (18.1), 4A6 (287)	mtx, sulf, 5fl, chl, ble, gef, cis, cyc, mpr, geld, dox, mit, eto
		$THP1/BTZ_{(-100)}$	100 nM, 0 nM for 6 mo	6 mo	0.4, 0.7, 1.0[d] ⊗: all proteasome genes	↑: β5 (minor), β1 & β2 (< 2X)	NR	↑ activity: CT-L (1.3-1.4X), C-L (1.8-2.3X), & T-L (1.4-1.7X)[e,g]	A49T	NR	NR
Lü *et al.*, 2008[127]	Lymphoblastic lymphoma/ leukemia	Jurkat (parental)	-	-	-	-	10, 3 nM @ 24, 48 h	15% CT-L (10 nM bortezomib @ 18 h)[d,h]	none	-	-
		JurkatB1	NR (> 200 nM)	6 mo[i]	↑: *PSMB5*	ND	ND	ND	A49T (het)[b]	ND	daun, dox, vind, eto
		JurkatB2	500 nM	6 mo[i]	NR	ND	26, 12 nM @ 24, 48 h	60% CT-L (10 nM bortezomib @ 18 h)[d,h]	A49T (het)[j]	ND	daun, dox, vind, eto
		JurkatB3	NR (> 200 nM)	6 mo[i]	NR	ND	ND	ND	A49T (het)	ND	daun, dox, vind, eto
		JurkatB4	NR (> 200 nM)	6 mo[i]	NR	ND	ND	ND	NR	ND	daun, dox, vind, eto
		JurkatB5	500 nM	6 mo[i]	↑: *PSMB5*	ND	ND	ND	A49T (het)	ND	daun, dox, vind, eto
		JurkatB2/1000	1000 nM	9 mo[i]	NR	ND	268, 164 nM @ 24, 48 h	90% CT-L (80 nM bortezomib @ 24 h)[h]	A49T (hom)[b]	ND	daun, dox, vind, eto
Lü *et al.*, 2009[128]	Lymphoblastic lymphoma/ leukemia	Jurkat (parental)	-	-	Relative *PSMB5* mRNA levels: 1.0 ± 0.12	ND	4.1 nM @ 48 h	Parental CT-L activity, IC_{50}: 75 nM[d]	-	ND	ND
		JurkatB-G322A	1000 nM	7-9 mo[k]	1.71 ± 0.49	ND	90.4 nM @ 48 h (22)	⊗: CT-L activity; IC_{50}: 175 nM[d]	A49T	ND	ND
		JurkatB-C323T	1000 nM	7-9 mo[k]	0.86 ± 0.07	ND	161.4 nM @ 48 h (39.4)	⊗: CT-L activity; IC_{50}: 240 nM[d]	A49V	ND	ND
		JurkatB-G322A/C326T	1000 nM	7-9 mo[k]	1.31 ± 0.20	ND	273.5 nM @ 48 h (66.7)	⊗: CT-L activity; IC_{50}: > 300 nM[d]	A49T/A50V	ND	ND
Ruchrick *et al.*[129], Kraus *et al.*[141]	Acute myeloid leukemia	HL-60 (parental)	-	-	-	-	30 nM	-	ND	-	-
		HL-60a	40 nM, maintained @ 20 nM	several wks	↑: 20S and 11S subunit genes; ↓: ER stress and UPR genes	↑: 11S; ⊗: immuno-subunits; ↓: 19S	> 600 nM (>20)[l]	↑ activity[d,m]: β1/β5 (50%) and β2 (50%); β1/β5 activity less succeptible to inhibiton	ND	NLVS & ZL_3VS, lact & epox to a lesser extent	daun
	Myeloma	AMO-1 (parental)	-	-	-	-	8 nM	-	ND	-	-
		AMO-1a	NR, maintained @ 20 nM	several wks	ND	Similar to HL-60a; ↑: β2, β5 & β1	> 160 nM (>20)	↑ activity[d,m]: β1/β5 (4.5X) and β2 (8X); β1/β5 activity less succeptible to inhibiton	ND	NLVS & ZL_3VS, lact & epox to a lesser extent, daun	None
	Plasmocytoid lymphoma	ARH-77 (parental)	-	-	-	-	20 nM	-	ND	-	-
		ARH-77a	NR, maintained @ 20 nM	several wks	ND	Similar to HL-60a; ↑: β2, β5	500 nM (25)	↑ activity[d]: β2 (2.3X); β1/β5 activity less succeptible to inhibiton	ND	NLVS & ZL_3VS, lact & epox to a lesser extent	daun
Ri *et al.*[130]	Multiple myeloma	KMS-11 (parental)	-	-	-	-	6 nM @ 72 h	↓: CT-L activity @ 6 h of 10 nM bortezomib exposure (30-37% retained)[h]	None	None	-
		KMS-11/BTZ	NR	6 mo[i]	ND	⊗: β5, β1; ↑: β2 (slight)	148.3 nM @ 72 h (24.7)	↓: CT-L activity @ 48 h of 10 nM bortezomib exposure (47-51% retained)[h]	A49T	MG132	dox
		OPM-2 (parental)	-	-	-	-	3.1 nM @ 72 h	↓: CT-L activity @ 6 h of 10 nM bortezomib exposure (10-13% retained)[h]	None	None	-
		OPM-2/BTZ	NR	6 mo[i]	ND	⊗: β5, β1; ↑: β2 (slight)	51.6 nM @ 72 h (16.6)	↓: CT-L activity @ 48 h of 10 nM bortezomib exposure (21-23% retained)[h]	A49T	MG132	dox

Table A1.1. Comparative summary of cell lines with acquired bortezomib resistance, continued.

Ref.	Cancer cell type	Cell line	Selective concentation (bortezomib)	Selection time	mRNA transcription regulation	protein expression regulation	Cellular bortezomib sensitivity IC_{50} (resistance factor)	Proteasome activity/resistance	β5-subunit mutation	Cross-resistace[b,c] (resistance factor)	Sensitivity[b,c] (resistance factor)
Pérez-Galán *et al.*[131]	Mantle cell lymphoma	HBL2 (parental)	-	-	-	-	6 nM @ 48 h	-	None	-	-
		HBL2-BR	100 nM	> 1 yr	*PSMB5* unchanged	↑: β5	489.7 nM @ 48 h (81.6)[n]	↑: CT-L (< 2X), T-L (1.3X), and C-L (1.4X)[d]	None	MG132 (3.4), NLVS (7.8)	eto (0.48), fld (0.34), hct (0.74)
		JEKO (parental)	-	-	-	-	4.9 nM @ 48 h	-	None	-	-
		JEKO-BR	100 nM	> 1 yr	*PSMB5* unchanged	↑: β5	213.8 nM @ 48 h (43.6)[n]	↑: CT-L (1.4X), T-L (1.7X), and C-L (1.7X)[d]	None	MG132 (3.7), NLVS (6.4)	eto (0.50), fld (0.64), hct (0.29)
Franke *et al.*[101]	Multiple myeloma RPMI-8226	8226 WT (parental)	-	-	-	-	2.6 ± 0.3 nM	complete inhibition of CT-L @ 25 nM[o]	None	Parental sensitivites: MG132 (307.8 nM), MG262 (6.7 nM), 4A6 (133.2 nM), Cfl (2.4 nM), 0912 (122 nM), 0914 (26 nM), 5AHQ (2.9 μM)	
		8226/BTZ7	7 nM	3-6 mo	↑: *PSMB5*, *PSMB6*, & *PSMB7* (all about 5X)[d]	↑: β5; ⊗: β2 & β1; ↓: β5i	12.1 ± 0.7 nM (4.5)	↓: CT-L activity rel. to parental, CT-L inhibition with bortezomib[o]	T21A	MG132 (3.9), MG262 (3.2), 4A6 (8.7), 0912 (1.5), 0914 (1.4)	Cfl (1.2), 5AHQ (ND)
		8226/BTZ100	100 nM	15 mo	↑: *PSMB5* (15X), *PSMB6* & *PSMB7* (5X)[d]	↑: β5; ⊗: β2 & β1; ↓: β5i	105.9 ± 14.9 nM (39.5)	↓: CT-L activity rel. to parental, CT-L inhibition with bortezomib[o]	A49T	MG132 (12.6), MG262 (8.3), 4A6 (28.2), Cfl (9.7), 0912 (10.1), 0914 (60)	5AHQ (1.3)
	Acute lymphoblastic leukemia (CCRF-CEM)	CEM WT (parental)	-	-	-	-	1.5 ± 0.4 nM	complete inhibition of CT-L @ 25 nM[o]	None	Parental sensitivities: MG132 (32.6 nM), MG262 (1.41 nM), 4A6 (97.0 nM), Cfl (0.84 nM), 0912 (14.8 nM), 0914 (46.6 nM), 5AHQ (5.7 μM)	
		CEM/BTZ7	7 nM	< 4 mo	↑: *PSMB5*, *PSMB6,* and *PSMB7* (all minor)	↑: β1, β2, β5 & α7	12.4 ± 5.8 nM (10.4)	↑: CT-L activity rel. to parental; ↓: CT-L inhibition with bortezomib[o]	C52F	MG132 (43.8), MG262 (5.7), 4A6 (24.7), Cfl (13.3), 0912 (27), 0914 (5.4)	5AHQ (ND)
		CEM/BTZ200	200 nM	4 mo	↑: *PSMB5*, *PSMB6,* and *PSMB7* (all minor)	↑: β1, β2, β5 & α7	189.1 ± 43.5 nM (170.4)	↓: CT-L inhibition with bortezomib[o]	A49V/C52F	MG132 (122.4), MG262 (23.2), 4A6 (24.1), Cfl (38.8), 0912 (147), 0914 (35.2)	5AHQ (1.1)
	monocytic/ macrophage	THP1/BTZ100N	100 nM	NR	NR	NR	NR	NR	M45V	NR	NR
		THP1/BTZ500	500 nM	NR	NR	NR	NR	NR	M45I/A49T	NR	NR
de Wilt *et al.*[102]	Non-small cell lung cancer (NSCLC)	H460 (parental)	-	-	ND	β1i & β5i: 3X rel. to A549 or SW1573	13 ± 2 nM @ 72 h	Comparative activies of parental strains[d,p]: CT-L (4.3), T-L (1.0), C-L (3.2)	None	-	-
		$H460BTZR_{80}$	80 nM	> 6 mo[q]	ND	↑: β5, β2, β1, β5i, β2i, β1i & α7	173 ± 24 nM (14) @ 72 h	↑: bortezomib IC_{50} CT-L, C-L rel. to parental (1.5-2.5X); no T-L inhibtion	A49T	MG132 (2.8), 4A6 (2.9), 0912 (2.0)	Cfl (1.3) 0914 (1.1), 5AHQ (1.2), dox (NR)
		$H460BTZR_{200}$	300 nM	> 6 mo[q]	ND	↑: 20S subunits	276 ± 51 nM (22) @ 72 h	↑: bortezomib IC_{50} CT-L, C-L rel. to parental (1.5-2.5X); no T-L inhibtion	A49T	Cfl (1.5), MG132 (5.9), 4A6 (2.8), 0914 (1.6), 0912 (12.4)	5AHQ (0.6), dox (NR)
	Non-small cell lung cancer (NSCLC)	A549 (parental)	-	-	ND	-	8.7 ± 2 nM @ 72 h	Comparative activities of parental strains[d,p]: CT-L (3.2), T-L (1.2), C-L (2.2)	None	-	-
		$A549BTZR_{40}$	40 nM	> 6 mo[q]	ND	↑: β5, β2, β1, β5i, β2i, β1i & α7	70 ± 9 nM (8) @ 72 h	sym: bortezomib IC_{50} CT-L, C-L rel. to parental (1.5-2.5X); no T-L inhibtion	M45V	Cfl (8.1), MG132 (4.3), 4A6 (3.3), 0914 (2.6), 0912 (9.9)	5AHQ (1.1), dox (NR)
		$A549BTZR_{100}$	100 nM	> 6 mo[q]	ND	↑: 20S subunits	167 ± 16 nM (19) @ 72 h	↑: bortezomib IC_{50} CT-L, C-L rel. to parental (1.5-2.5X); no T-L inhibtion	M45V/A49T	Cfl (21), MG132 (10.3), 4A6 (>11), 0914 (12.8), 0912 (55.5)	5AHQ (0.8), dox (NR)
	Non-small cell lung cancer (NSCLC)	SW1573 (parental)	-	-	ND	-	1.7 ± 0.4 nM @ 72 h	Comparative activities of parental strains[d,p]: CT-L (1.5), T-L (0.8), C-L (0.8)	None	-	-
		$SW1573BTZR_{30}$	30 nM	> 6 mo[q]	ND	↑: β5, β2, β1, & α7; ⊗: β5i, β2i, β1i	30 ± 1.4 nM (18) @ 72 h	↑: bortezomib IC_{50} CT-L, C-L rel. to parental (1.5-2.5X); no T-L inhibtion	C52F	Cfl (6.7), MG132 (8.6), 4A6 (>8.8), 0912 (13.8)	0914 (1.1), 5AHQ (1.1) dox (NR)
		$SW1573BTZR_{150}$	150 nM	> 6 mo[q]	ND	↑: 20S subunits	119 ± 28 nM (70) @ 72 h	↑: bortezomib IC_{50} CT-L, C-L rel. to parental (1.5-2.5X); no T-L inhibtion	C52F	Cfl (12), MG132 (>19.8), 4A6 (>14.6), 0914 (3.2), 0912 (125)	5AHQ (0.8), dox (NR)
Balsas *et al.*[132]	Multiple Myeloma (RPMI 8226)	8226	-	-	-	-	Growth IC_{50}: 15 nM, apoptosis LD_{50}: 15 nM	ND	None	-	-
		8226/7B	100 nM	18 mo	↑: *PSMB5* transcription (very large)	↑: β5 & β2, β1 to a lesser extent	Growth IC_{50}: 75 nM, apoptosis LD_{50}: 85 nM	ND	None	MG-132, epoxomicin (below 50 nM)	dox, mel, BMS-214662, vinc, IKK-i, BMS-345541

1.12: References

1. Paul, V. J., Puglisi, M. P., and Ritson-Williams, R. (2006) Marine chemical ecology, *Nat. Prod. Rep.* 23, 153-180.

2. O'Brien, J., and Wright, G. D. (2011) An ecological perspective of microbial secondary metabolism, *Curr. Opin. Biotechnol.* 22, 552-558.

3. Dewick, P. M. (2009) *Medicinal Natural Products: A Biosynthetic Approach*, 3rd ed., John Wiley & Sons, Ltd., Chichester, West Sussex, United Kingdom.

4. Faulkner, D. J. (2000) Highlights of marine natural products chemistry (1972-1999), *Nat. Prod. Rep.* 17, 1-6.

5. Molinski, T. F., Dalisay, D. S., Lievens, S. L., and Saludes, J. P. (2009) Drug development from marine natural products, *Nat. Rev. Drug Discovery* 8, 69-85.

6. Gulder, T. A. M., and Moore, B. S. (2009) Chasing the treasures of the sea - bacterial marine natural products, *Curr. Opin. Microbiol.* 12, 252-260.

7. Berdy, J. (2005) Bioactive microbial metabolites - a personal view, *J. Antibiot.* 58, 1-26.

8. Jensen, P. R., Dwight, R., and Fenical, W. (1991) Distribution of actinomycetes in near-shore tropical marine sediments, *Appl. Environ. Microbiol.* 57, 1102-1108.

9. Mincer, T. J., Jensen, P. R., Kauffman, C. A., and Fenical, W. (2002) Widespread and persistent populations of a major new marine actinomycete taxon in ocean sediments, *Appl. Environ. Microbiol.* 68, 5005-5011.

10. Maldonado, L. A., Fenical, W., Jensen, P. R., Kauffman, C. A., Mincer, T. J., Ward, A. C., Bull, A. T., and Goodfellow, M. (2005) *Salinispora arenicola* gen. nov., sp nov and *Salinispora tropica* sp nov., obligate marine actinomycetes belonging to the family *Micromonosporaceae*, *Int. J. Syst. Evol. Microbiol.* 55, 1759-1766.

11. Udwary, D. W., Zeigler, L., Asolkar, R. N., Singan, V., Lapidus, A., Fenical, W., Jensen, P. R., and Moore, B. S. (2007) Genome sequencing reveals complex secondary metabolome in the marine actinomycete *Salinispora tropica*, *Proc. Natl. Acad. Sci. U. S. A.* 104, 10376-10381.

12. Penn, K., Jenkins, C., Nett, M., Udwary, D. W., Gontang, E. A., McGlinchey, R. P., Foster, B., Lapidus, A., Podell, S., Allen, E. E., Moore, B. S., and Jensen, P.

R. (2009) Genomic islands link secondary metabolism to functional adaptation in marine Actinobacteria, *ISME Journal* 3, 1193-1203.

13. Eustáquio, A. S., Nam, S. J., Penn, K., Lechner, A., Wilson, M. C., Fenical, W., Jensen, P. R., and Moore, B. S. (2011) The discovery of salinosporamide K from the marine bacterium "*Salinispora pacifica*" by genome mining gives insight into pathway evolution, *ChemBioChem* 12, 61-64.

14. Gulder, T. A. M., and Moore, B. S. (2010) Salinosporamide natural products: potent 20S proteasome inhibitors as promising cancer chemotherapeutics, *Angew. Chem. Int. Ed.* 49, 9346-9367.

15. Wilson, M. C., Gulder, T. A. M., Mahmud, T., and Moore, B. S. (2010) Shared biosynthesis of the saliniketals and rifamycins in *Salinispora arenicola* is controlled by the sare1259-encoded cytochrome P450, *J. Am. Chem. Soc.* 132, 12757-12765.

16. Schultz, A. W., Oh, D.-C., Carney, J. R., Williamson, R. T., Udwary, D. W., Jensen, P. R., Gould, S. J., Fenical, W., and Moore, B. S. (2008) Biosynthesis and structures of cyclomarins and cyclomarazines, prenylated cyclic peptides of marine actinobacterial origin, *J. Am. Chem. Soc.* 130, 4507-4516.

17. Buchanan, G. O., Williams, P. G., Feling, R. H., Kauffman, C. A., Jensen, P. R., and Fenical, W. (2005) Sporolides A and B: structurally unprecedented halogenated macrolides from the marine actinomycete *Salinispora tropica*, *Org. Lett.* 7, 2731-2734.

18. Feling, R. H., Buchanan, G. O., Mincer, T. J., Kauffman, C. A., Jensen, P. R., and Fenical, W. (2003) Salinosporamide A: a highly cytotoxic proteasome inhibitor from a novel microbial source, a marine bacterium of the new genus *Salinospora*, *Angew. Chem. Int. Ed.* 42, 355-358.

19. Williams, P. G., Buchanan, G. O., Feling, R. H., Kauffman, C. A., Jensen, P. R., and Fenical, W. (2005) New cytotoxic salinosporamides from the marine Actinomycete *Salinispora tropica*, *J. Org. Chem.* 70, 6196-6203.

20. Fenical, W., Jensen, P. R., Palladino, M. A., Lam, K. S., Lloyd, G. K., and Potts, B. C. (2009) Discovery and development of the anticancer agent salinosporamide A (NPI-0052), *Biorg. Med. Chem.* 17, 2175-2180.

21. Murata, S., Yashiroda, H., and Tanaka, K. (2009) Molecular mechanisms of proteasome assembly, *Nat. Rev. Mol. Cell Biol.* 10, 104-115.

22. Borissenko, L., and Groll, M. (2007) 20S proteasome and its inhibitors: crystallographic knowledge for drug development, *Chem. Rev.* 107, 687-717.

23. Genin, E., Reboud-Ravaux, M., and Vidal, J. (2010) Proteasome inhibitors: recent advances and new perspectives in medicinal chemistry, *Curr. Top. Med. Chem.* 10, 232-256.

24. Nencioni, A., Grunebach, F., Patrone, F., Ballestrero, A., and Brossart, P. (2007) Proteasome inhibitors: antitumor effects and beyond, *Leukemia* 21, 30-36.

25. Woodle, E. S., Walsh, R. C., Alloway, R. R., Girnita, A., and Brailey, P. (2011) Proteasome inhibitor therapy for antibody-mediated rejection, *Pediatr. Transplant* 15, 548-556.

26. Kisselev, Alexei F., van der Linden, W. A., and Overkleeft, Herman S. (2012) Proteasome inhibitors: an expanding army attacking a unique target, *Chem. Biol.* 19, 99-115.

27. Cheriyath, V., Jacobs, B. S., and Hussein, M. A. (2007) Proteasome inhibitors in the clinical setting: benefits and strategies to overcome multiple myeloma resistance to proteasome inhibitors, *Drugs R. D.* 8, 1-12.

28. Finley, D. (2009) Recognition and processing of ubiquitin-protein conjugates by the proteasome, *Annu. Rev. Biochem.* 78, 477-513.

29. Groll, M., Bochtler, M., Brandstetter, H., Clausen, T., and Huber, R. (2005) Molecular machines for protein degradation, *ChemBioChem* 6, 222-256.

30. Xu, G. W., Ali, M., Wood, T. E., Wong, D., Maclean, N., Wang, X. M., Gronda, M., Skrtic, M., Li, X. M., Hurren, R., Mao, X. L., Venkatesan, M., Zavareh, R. B., Ketela, T., Reed, J. C., Rose, D., Moffat, J., Batey, R. A., Dhe-Paganon, S., and Schimmer, A. D. (2010) The ubiquitin-activating enzyme E1 as a therapeutic target for the treatment of leukemia and multiple myeloma, *Blood* 115, 2251-2259.

31. Hochstrasser, M. (2009) Origin and function of ubiquitin-like proteins, *Nature* 458, 422-429.

32. De Mot, R. (2007) Actinomycete-like proteasomes in a Gram-negative bacterium, *Trends Microbiol.* 15, 335-338.

33. Maupin-Furlow, J. (2012) Proteasomes and protein conjugation across domains of life, *Nat. Rev. Microbiol.* 10, 100-111.

34. Striebel, F., Hunkeler, M., Summer, H., and Weber-Ban, E. (2010) The mycobacterial Mpa-proteasome unfolds and degrades pupylated substrates by engaging Pup's N-terminus, *EMBO J.* 29, 1262-1271.

35. Darwin, K. H., Ehrt, S., Gutierrez-Ramos, J. C., Weich, N., and Nathan, C. F. (2003) The proteasome of *Mycobacterium tuberculosis* is required for resistance to nitric oxide, *Science* 302, 1963-1966.

36. Burns, K. E., and Darwin, K. H. (2010) Pupylation versus ubiquitylation: tagging for proteasome-dependent degradation, *Cell. Microbiol.* 12, 424-431.

37. Burns, K. E., Liu, W. T., Boshoff, H. I. M., Dorrestein, P. C., and Barry, C. E. (2009) Proteasomal protein degradation in Mycobacteria is dependent upon a prokaryotic ubiquitin-like protein, *J. Biol. Chem.* 284, 3069-3075.

38. Pearce, M. J., Mintseris, J., Ferreyra, J., Gygi, S. P., and Darwin, K. H. (2008) Ubiquitin-like protein involved in the proteasome pathway of *Mycobacterium tuberculosis*, *Science* 322, 1104-1107.

39. Chen, X., Solomon, W. C., Kang, Y., Cerda-Maira, F., Darwin, K. H., and Walters, K. J. (2009) Prokaryotic ubiquitin-like protein pup is intrinsically disordered, *J. Mol. Biol.* 392, 208-217.

40. Liao, S. H., Shang, Q., Zhang, X. C., Zhang, J. H., Xu, C., and Tu, X. M. (2009) Pup, a prokaryotic ubiquitin-like protein, is an intrinsically disordered protein, *Biochem. J.* 422, 207-215.

41. Burns, K. E., Pearce, M. J., and Darwin, K. H. (2010) Prokaryotic ubiquitin-like protein provides a two-part degron to Mycobacterium proteasome substrates, *J. Bacteriol.* 192, 2933-2935.

42. Striebel, F., Imkamp, F., Sutter, M., Steiner, M., Mamedov, A., and Weber-Ban, E. (2009) Bacterial ubiquitin-like modifier Pup is deamidated and conjugated to substrates by distinct but homologous enzymes, *Nat. Struct. Mol. Biol.* 16, 647-651.

43. Imkamp, F., Rosenberger, T., Striebel, F., Keller, P. M., Amstutz, B., Sander, P., and Weber-Ban, E. (2010) Deletion of dop in *Mycobacterium smegmatis* abolishes pupylation of protein substrates in vivo, *Mol. Microbiol.* 75, 744-754.

44. Cerda-Maira, F. A., Pearce, M. J., Fuortes, M., Bishai, W. R., Hubbard, S. R., and Darwin, K. H. (2010) Molecular analysis of the prokaryotic ubiquitin-like protein (Pup) conjugation pathway in *Mycobacterium tuberculosis*, *Mol. Microbiol.* 77, 1123-1135.

45. Sutter, M., Damberger, F. F., Imkamp, F., Allain, F. H. T., and Weber-Ban, E. (2010) Prokaryotic ubiquitin-like protein (Pup) is coupled to substrates via the side chain of its C-terminal glutamate, *J. Am. Chem. Soc.* 132, 5610-5612.

46. Burns, K. E., Cerda-Maira, F. A., Wang, T., Li, H. L., Bishai, W. R., and Darwin, K. H. (2010) "Depupylation" of prokaryotic ubiquitin-like protein from mycobacterial proteasome substrates, *Mol. Cell* 39, 821-827.

47. Imkamp, F., Striebel, F., Sutter, M., Ozcelik, D., Zimmermann, N., Sander, P., and Weber-Ban, E. (2010) Dop functions as a depupylase in the prokaryotic ubiquitin-like modification pathway, *EMBO Rep.* 11, 791-797.

48. Watrous, J., Burns, K., Liu, W. T., Patel, A., Hook, V., Bafna, V., Barry, C. E., Bark, S., and Dorrestein, P. C. (2010) Expansion of the mycobacterial "PUPylome", *Mol. Biosyst.* 6, 376-385.

49. Poulsen, C., Akhter, Y., Jeon, A. H.-W., Schmitt-Ulms, G., Meyer, H. E., Stefanski, A., Stuhler, K., Wilmanns, M., and Song, Y.-H. (2010) Proteome-wide identification of mycobacterial pupylation targets, *Mol Syst Biol* 6, 386.

50. Festa, R. A., McAllister, F., Pearce, M. J., Mintseris, J., Burns, K. E., Gygi, S. P., and Darwin, K. H. (2010) Prokayrotic ubiquitin-like protein (Pup) proteome of *Mycobacterium tuberculosis*, *Plos One* 5, e8589.

51. Cerda-Maira, F. A., McAllister, F., Bode, N. J., Burns, K. E., Gygi, S. P., and Darwin, K. H. (2011) Reconstitution of the *Mycobacterium tuberculosis* pupylation pathway in *Escherichia coli*, *EMBO Rep.* 12, 863-870.

52. Groll, M., Nazif, T., Huber, R., and Bogyo, M. (2002) Probing structural determinants distal to the site of hydrolysis that control substrate specificity of the 20S proteasome, *Chem. Biol.* 9, 655-662.

53. Lowe, J., Stock, D., Jap, R., Zwickl, P., Baumeister, W., and Huber, R. (1995) Crystal-structure of the 20S proteasome from the archaeon *T. acidophilum* at 3.4-angstrom resolution, *Science* 268, 533-539.

54. Vinitsky, A., Michaud, C., Powers, J. C., and Orlowski, M. (1992) Inhibition of the chymotrypsin-like activity of the pituitary multicatalytic proteinase complex, *Biochemistry* 31, 9421-9428.

55. Aoyagi, T., Takeuchi, T., Matsuzak.A, Kawamura, K., Kondo, S., Hamada, M., Maeda, K., and Umezawa, H. (1969) Leupeptins, new protease inhibitors from Actinomycetes, *J. Antibiot.* 22, 283-286.

56. Kondo, S., Kawamura, K., Iwanaga, J., Hamada, M., Aoyagi, T., Maeda, K., Takeuchi, T., and Umezawa, H. (1969) Isolation and characterization of leupeptins produced by *Actinomycetes*, *Chem. Pharm. Bull. (Tokyo)* 17, 1896-1901.

57. Wilk, S., and Orlowski, M. (1980) Cation-sensitive neutral endopeptidase: isolation and specificity of the bovine pituitary enzyme, *J. Neurochem.* 35, 1172-1182.

58. Hines, J., Groll, M., Fahnestock, M., and Crews, C. M. (2008) Proteasome inhibition by fellutamide B induces nerve growth factor synthesis, *Chem. Biol.* 15, 501-512.

59. Groll, M., Schellenberg, B., Bachmann, A. S., Archer, C. R., Huber, R., Powell, T. K., Lindow, S., Kaiser, M., and Dudler, R. (2008) A plant pathogen virulence factor inhibits the eukaryotic proteasome by a novel mechanism, *Nature* 452, 755-758.

60. Oka, M., Nishiyama, Y., Ohta, S., Kamei, H., Konishi, M., Miyaki, T., Oki, T., and Kawaguchi, H. (1988) Glidobactin A, B, and C, new antitumor antibiotics. 1. Production, isolation, chemical properties and biological activity, *J. Antibiot.* 41, 1331-1337.

61. Clerc, J., Groll, M., Illich, D. J., Bachmann, A. S., Huber, R., Schellenberg, B., Dudler, R., and Kaiser, M. (2009) Synthetic and structural studies on syringolin A and B reveal critical determinants of selectivity and potency of proteasome inhibition, *Proc. Natl. Acad. Sci. U. S. A.* 106, 6507-6512.

62. Adams, J., Behnke, M., Chen, S. W., Cruickshank, A. A., Dick, L. R., Grenier, L., Klunder, J. M., Ma, Y. T., Plamondon, L., and Stein, R. L. (1998) Potent and selective inhibitors of the proteasome: dipeptidyl boronic acids, *Bioorg. Med. Chem. Lett.* 8, 333-338.

63. Dick, L. R., and Fleming, P. E. (2010) Building on bortezomib: second-generation proteasome inhibitors as anti-cancer therapy, *Drug Discov. Today* 15, 243-249.

64. Chauhan, D., Catley, L., Li, G., Podar, K., Hideshima, T., Velankar, M., Mitsiades, C., Mitsiades, N., Yasui, H., Letai, A., Ovaa, H., Berkers, C., Nicholson, B., Chao, T.-H., Neuteboom, S. T. C., Richardson, P., Palladino, M. A., and Anderson, K. C. (2005) A novel orally active proteasome inhibitor induces apoptosis in multiple myeloma cells with mechanisms distinct from Bortezomib, *Cancer Cell* 8, 407-419.

65. Ruschak, A. M., Slassi, M., Kay, L. E., and Schimmer, A. D. (2011) Novel proteasome inhibitors to overcome bortezomib resistance, *J. Natl. Cancer Inst.* 103, 1007-1017.

66. Kupperman, E., Lee, E. C., Cao, Y. Y., Bannerman, B., Fitzgerald, M., Berger, A., Yu, J., Yang, Y., Hales, P., Bruzzese, F., Liu, J., Blank, J., Garcia, K., Tsu, C., Dick, L., Fleming, P., Yu, L., Manfredi, M., Rolfe, M., and Bolen, J. (2010) Evaluation of the proteasome inhibitor MLN9708 in preclinical models of human cancer, *Cancer Res.* 70, 1970-1980.

67. Piva, R., Ruggeri, B., Williams, M., Costa, G., Tamagno, I., Ferrero, D., Giai, V., Coscia, M., Peola, S., Massaia, M., Pezzoni, G., Allievi, C., Pescalli, N., Cassin, M., di Giovine, S., Nicoli, P., de Feudis, P., Strepponi, I., Roato, I., Ferracini, R., Bussolati, B., Camussi, G., Jones-Bolin, S., Hunter, K., Zhao, H., Neri, A., Palumbo, A., Berkers, C., Ovaa, H., Bernareggi, A., and Inghirami, G. (2008) CEP-18770: A novel, orally active proteasome inhibitor with a tumor-selective pharmacologic profile competitive with bortezomib, *Blood* 111, 2765-2775.

68. Dorsey, B. D., Iqbal, M., Chatterjee, S., Menta, E., Bernardini, R., Bernareggi, A., Cassara, P. G., D'Arasmo, G., Ferretti, E., De Munari, S., Oliva, A., Pezzoni, G., Allievi, C., Strepponi, I., Ruggeri, B., Ator, M. A., Williams, M., and MallamoT, J. P. (2008) Discovery of a potent, selective, and orally active proteasome inhibitor for the treatment of cancer, *J. Med. Chem.* 51, 1068-1072.

69. Millennium Pharmaceuticals, Inc. (Accessed April 6, 2012) Oncology development pipeline, http://www.millennium.com/OurScience.aspx.

70. Hanada, M., Sugawara, K., Kaneta, K., Toda, S., Nishiyama, Y., Tomita, K., Yamamoto, H., Konishi, M., and Oki, T. (1992) Epoxomicin, a new antitumor agent of microbial origin, *J. Antibiot.* 45, 1746-1752.

71. Sugawara, K., Hatori, M., Nishiyama, Y., Tomita, K., Kamei, H., Konishi, M., and Oki, T. (1990) Eponemycin, a new antibiotic active against B16 melanoma. I. Production, isolation, structure and biological activity, *J. Antibiot.* 43, 8-18.

72. Meng, L. H., Mohan, R., Kwok, B. H. B., Elofsson, M., Sin, N., and Crews, C. M. (1999) Epoxomicin, a potent and selective proteasome inhibitor, exhibits in vivo antiinflammatory activity, *Proc. Natl. Acad. Sci. U. S. A.* 96, 10403-10408.

73. Groll, M., Kim, K. B., Kairies, N., Huber, R., and Crews, C. M. (2000) Crystal structure of epoxomicin : 20S proteasome reveals a molecular basis for selectivity of α',β'-epoxyketone proteasome inhibitors, *J. Am. Chem. Soc.* 122, 1237-1238.

74. Pereira, A. R., Kale, A. J., Fenley, A. T., Byrum, T., Debonsi, H. M., Gilson, M. K., Valeriote, F. A., Moore, B. S., and Gerwick, W. H. (2012) The carmaphycins: new proteasome inhibitors exhibiting an α,β-epoxyketone warhead from a marine cyanobacterium, *ChemBioChem* 13, 810-817.

75. Demo, S. D., Kirk, C. J., Aujay, M. A., Buchholz, T. J., Dajee, M., Ho, M. N., Jiang, J., Laidig, G. J., Lewis, E. R., Parlati, F., Shenk, K. D., Smyth, M. S., Sun, C. M., Vallone, M. K., Woo, T. M., Molineaux, C. J., and Bennett, M. K. (2007) Antitumor activity of PR-171, a novel irreversible inhibitor of the proteasome, *Cancer Res.* 67, 6383-6391.

76. Zhou, H. J., Aujay, M. A., Bennett, M. K., Dajee, M., Demo, S. D., Fang, Y., Ho, M. N., Jiang, J., Kirk, C. J., Laidig, G. J., Lewis, E. R., Lu, Y., Muchamuel, T., Parlati, F., Ring, E., Shenk, K. D., Shields, J., Shwonek, P. J., Stanton, T., Sun, C. C. M., Sylvain, C., Woo, T. M., and Yang, J. F. (2009) Design and synthesis of an orally bioavailable and selective peptide epoxyketone proteasome inhibitor (PR-047), *J. Med. Chem.* 52, 3028-3038.

77. Roccaro, A. M., Sacco, A., Aujay, M., Ngo, H. T., Azab, A. K., Azab, F., Quang, P., Maiso, P., Runnels, J., Anderson, K. C., Demo, S., and Ghobrial, I. M. (2010) Selective inhibition of chymotrypsin-like activity of the immunoproteasome and constitutive proteasome in Waldenstrom macroglobulinemia, *Blood* 115, 4051-4060.

78. Onxy Pharmaceuticals, Inc. (Accessed April 6, 2012) Clinical development - carfilzomib, http://www.onyx.com/clinical-development/carfilzomib.

79. Onxy Pharmaceuticals, Inc. (Accessed April 6, 2012) Clinical development - oprozomib, http://www.onyx.com/clinical-development/oprozomib.

80. Omura, S., Fujimoto, T., Otoguro, K., Matsuzaki, K., Moriguchi, R., Tanaka, H., and Sasaki, Y. (1991) Lactacystin, a novel microbial metabolite, induces neuritogenesis of neuroblastoma cells, *J. Antibiot.* 44, 113-116.

81. Fenteany, G., Standaert, R. F., Lane, W. S., Choi, S., Corey, E. J., and Schreiber, S. L. (1995) Inhibition of proteasome activities and subunit-specific amino-terminal threonine modification by lactacystin, *Science* 268, 726-731.

82. Dick, L. R., Cruikshank, A. A., Grenier, L., Melandri, F. D., Nunes, S. L., and Stein, R. L. (1996) Mechanistic studies on the inactivation of the proteasome by lactacystin A central role for clasto-lactacystin beta-lactone, *J. Biol. Chem.* 271, 7273-7276.

83. Corey, E. J., and Li, W. D. Z. (1999) Total synthesis and biological activity of lactacystin, omuralide and analogs, *Chem. Pharm. Bull. (Tokyo)* 47, 1-10.

84. Macherla, V. R., Mitchell, S. S., Manam, R. R., Reed, K. A., Chao, T. H., Nicholson, B., Deyanat-Yazdi, G., Mai, B., Jensen, P. R., Fenical, W. F., Neuteboom, S. T. C., Lam, K. S., Palladino, M. A., and Potts, B. C. M. (2005)

Structure-activity relationship studies of salinosporamide a (NPI-0052), a novel marine derived proteasome inhibitor, *J. Med. Chem.* 48, 3684-3687.

85. Groll, M., Huber, R., and Potts, B. C. M. (2006) Crystal structures of salinosporamide A (NPI-0052) and B (NPI-0047) in complex with the 20S proteasome reveal important consequences of β-lactone ring opening and a mechanism for irreversible binding, *J. Am. Chem. Soc.* 128, 5136-5141.

86. Denora, N., Potts, B. C. M., and Stella, V. J. (2007) A mechanistic and kinetic study of the β-lactone hydrolysis of salinosporamide A (NPI-0052), a novel proteasome inhibitor, *J. Pharm. Sci.* 96, 2037-2047.

87. Stadler, M., Bitzer, J., Mayer-Bartschmid, A., Muller, H., Benet-Buchholz, J., Gantner, F., Tichy, H. V., Reinemer, P., and Bacon, K. B. (2007) Cinnabaramides A-G: analogues of lactacystin and salinosporamide from a terrestrial streptomycete, *J. Nat. Prod.* 70, 246-252.

88. Asai, A., Hasegawa, A., Ochiai, K., Yamashita, Y., and Mizukami, T. (2000) Belactosin A, a novel antitumor antibiotic acting on cyclin/CDK mediated cell cycle regulation, produced by *Streptomyces* sp., *J. Antibiot.* 53, 81-83.

89. Asai, A., Tsujita, T., Sharma, S. V., Yamashita, Y., Akinaga, S., Funakoshi, M., Kobayashi, H., and Mizukami, T. (2004) A new structural class of proteasome inhibitors identified by microbial screening using yeast-based assay, *Biochem. Pharmacol.* 67, 227-234.

90. Groll, M., Larionov, O. V., Huber, R., and de Meijere, A. (2006) Inhibitor-binding mode of homobelactosin C to proteasomes: new insights into class I MHC ligand generation, *Proc. Natl. Acad. Sci. U. S. A.* 103, 4576-4579.

91. Moore, B. S., Eustáquio, A. S., and McGlinchey, R. P. (2008) Advances in and applications of proteasome inhibitors, *Curr. Opin. Chem. Biol.* 12, 434-440.

92. Koguchi, Y., Kohno, J., Nishio, M., Takahashi, K., Okuda, T., Ohnuki, T., and Komatsubara, S. (2000) TMC-95A, B, C, and D, novel proteasome inhibitors produced by *Apiospora montagnei* Sacc. TC 1093 - taxonomy, production, isolation, and biological activities, *J. Antibiot.* 53, 105-109.

93. Groll, M., Koguchi, Y., Huber, R., and Kohno, J. (2001) Crystal structure of the 20 S proteasome: TMC-95A complex: A non-covalent proteasome inhibitor, *J. Mol. Biol.* 311, 543-548.

94. Agerberth, B., Lee, J. Y., Bergman, T., Carlquist, M., Boman, H. G., Mutt, V., and Jornvall, H. (1991) Amino acid sequence of PR-39. Isolation from pig

intestine of a new member of the family of proline-arginine-rich antibacterial peptides, *Eur. J. Biochem.* 202, 849-854.

95. Gao, Y. H., Lecker, S., Post, M. J., Hietaranta, A. J., Li, J., Volk, R., Li, M., Sato, K., Saluja, A. K., Steer, M. L., Goldberg, A. L., and Simons, M. (2000) Inhibition of ubiquitin-proteasome pathway-mediated IκBα degradation by a naturally occurring antibacterial peptide, *J. Clin. Invest.* 106, 439-448.

96. Li, J., Post, M., Volk, R., Gao, Y., Li, M., Metais, C., Sato, K., Tsai, J., Aird, W., Rosenberg, R. D., Hampton, T. G., Li, J., Sellke, F., Carmeliet, P., and Simons, M. (2000) PR39, a peptide regulator of angiogenesis, *Nat. Med.* 6, 49-55.

97. Gaczynska, M., Osmulski, P. A., Gao, Y., Post, M. J., and Simons, M. (2003) Proline- and arginine-rich peptides constitute a novel class of allosteric inhibitors of proteasome activity, *Biochemistry* 42, 8663-8670.

98. Anbanandam, A., Albarado, D. C., Tirziu, D. C., Simons, M., and Veeraraghavan, S. (2008) Molecular basis for proline- and arginine-rich peptide inhibition of proteasome, *J. Mol. Biol.* 384, 219-227.

99. Sprangers, R., Li, X. M., Mao, X. L., Rubinstein, J. L., Schimmer, A. D., and Kay, L. E. (2008) TROSY-based NMR evidence for a novel class of 20S proteasome inhibitors, *Biochemistry* 47, 6727-6734.

100. Li, X. M., Wood, T. E., Sprangers, R., Jansen, G., Franke, N. E., Mao, X. L., Wang, X. M., Zhang, Y., Verbrugge, S. E., Adomat, H., Li, Z. H., Trudel, S., Chen, C., Religa, T. L., Jamal, N., Messner, H., Cloos, J., Rose, D. R., Navon, A., Guns, E., Batey, R. A., Kay, L. E., and Schimmer, A. D. (2010) Effect of noncompetitive proteasome inhibition on bortezomib resistance, *J. Natl. Cancer Inst.* 102, 1069-1082.

101. Franke, N. E., Niewerth, D., Assaraf, Y. G., van Meerloo, J., Vojtekova, K., van Zantwijk, C. H., Zweegman, S., Chan, E. T., Kirk, C. J., Geerke, D. P., Schimmer, A. D., Kaspers, G. J. L., Jansen, G., and Cloos, J. (2011) Impaired bortezomib binding to mutant β5 subunit of the proteasome is the underlying basis for bortezomib resistance in leukemia cells, *Leukemia* 26, 757-768.

102. de Wilt, L. H. A. M., Jansen, G., Assaraf, Y. G., van Meerloo, J., Cloos, J., Schimmer, A. D., Chan, E. T., Kirk, C. J., Peters, G. J., and Kruyt, F. A. E. (2012) Proteasome-based mechanisms of intrinsic and acquired bortezomib resistance in non-small cell lung cancer, *Biochem. Pharmacol.* 83, 207-217.

103. Oerlemans, R., Franke, N. E., Assaraf, Y. G., Cloos, J., van Zantwijk, I., Berkers, C. R., Scheffer, G. L., Debipersad, K., Vojtekova, K., Lemos, C., van

der Heijden, J. W., Ylstra, B., Peters, G. J., Kaspers, G. L., Dijkmans, B. A. C., Scheper, R. J., and Jansen, G. (2008) Molecular basis of bortezomib resistance: proteasome subunit β5 (*PSMB5*) gene mutation and overexpression of PSMB5 protein, *Blood* 112, 2489-2499.

104. Ro, D. K., Paradise, E. M., Ouellet, M., Fisher, K. J., Newman, K. L., Ndungu, J. M., Ho, K. A., Eachus, R. A., Ham, T. S., Kirby, J., Chang, M. C. Y., Withers, S. T., Shiba, Y., Sarpong, R., and Keasling, J. D. (2006) Production of the antimalarial drug precursor artemisinic acid in engineered yeast, *Nature* 440, 940-943.

105. Beer, L. L., and Moore, B. S. (2007) Biosynthetic convergence of salinosporamides A and B in the marine actinomycete *Salinispora tropica*, *Org. Lett.* 9, 845-848.

106. Eustáquio, A. S., Pojer, F., Noe, J. P., and Moore, B. S. (2008) Discovery and characterization of a marine bacterial SAM-dependent chlorinase, *Nat. Chem. Biol.* 4, 69-74.

107. Deng, H., O'Hagan, D., and Schaffrath, C. (2004) Fluorometabolite biosynthesis and the fluorinase from *Streptomyces cattleya*, *Nat. Prod. Rep.* 21, 773-784.

108. Eustáquio, A. S., McGlinchey, R. P., Liu, Y., Hazzard, C., Beer, L. L., Florova, G., Alhamadsheh, M. M., Lechner, A., Kale, A. J., Kobayashi, Y., Reynolds, K. A., and Moore, B. S. (2009) Biosynthesis of the salinosporamide A polyketide synthase substrate chloroethylmalonyl-coenzyme A from S-adenosyl-L-methionine, *Proc. Natl. Acad. Sci. U. S. A.* 106, 12295-12300.

109. Kale, A. J., McGlinchey, R. P., and Moore, B. S. (2010) Characterization of 5-chloro-5-deoxy-D-ribose 1-dehydrogenase in chloroethylmalonyl coenzyme A biosynthesis: substrate and reaction profiling, *J. Biol. Chem.* 285, 33710-33717.

110. Erb, T. J., Berg, I. A., Brecht, V., Muller, M., Fuchs, G., and Alber, B. E. (2007) Synthesis Of C-5-dicarboxylic acids from C-2-units involving crotonyl-CoA carboxylase/reductase: The ethylmalonyl-CoA pathway, *Proc. Natl. Acad. Sci. U. S. A.* 104, 10631-10636.

111. Wilson, M. C., and Moore, B. S. (2012) Beyond ethylmalonyl-CoA: The functional role of crotonyl-CoA carboxylase/reductase homologs in expanding polyketide diversity, *Nat. Prod. Rep.* 29, 72-86.

112. Liu, Y., Hazzard, C., Eustáquio, A. S., Reynolds, K. A., and Moore, B. S. (2009) Biosynthesis of salinosporamides from alpha,beta-unsaturated fatty acids: Implications for extending polyketide synthase diversity, *J. Am. Chem. Soc.* 131, 10376-10377.

113. Rachid, S., Huo, L. J., Herrmann, J., Stadler, M., Kopcke, B., Bitzer, J., and Muller, R. (2011) Mining the cinnabaramide biosynthetic pathway to generate novel proteasome inhibitors, *ChemBioChem* 12, 922-931.

114. Lechner, A., Eustaquio, A. S., Gulder, T. A. M., Hafner, M., and Moore, B. S. (2011) Selective overproduction of the proteasome inhibitor salinosporamide A via precursor pathway regulation, *Chem. Biol.* 18, 1527-1536.

115. Mahlstedt, S., Fielding, E. N., Moore, B. S., and Walsh, C. T. (2010) Prephenate decarboxylases: a new prephenate-utilizing enzyme family that performs nonaromatizing decarboxylation en route to diverse secondary metabolites, *Biochemistry* 49, 9021-9023.

116. Reddy, L. R., Fournier, J. F., Reddy, B. V. S., and Corey, E. J. (2005) An efficient, stereocontrolled synthesis of a potent omuralide-salinosporin hybrid for selective proteasome inhibition, *J. Am. Chem. Soc.* 127, 8974-8976.

117. Imajoh-Ohmi, S., Kawaguchi, T., Sugiyama, S., Tanaka, K., Omura, S., and Kikuchi, H. (1995) Lactacystin, a specific inhibitor of the proteasome, induces apoptosis in human monoblast U937 cells, *Biochem. Biophys. Res. Commun.* 217, 1070-1077.

118. Delic, J., Masdehors, P., Omura, S., Cosset, J. M., Dumont, J., Binet, J. L., and Magdelenat, H. (1998) The proteasome inhibitor lactacystin induces apoptosis and sensitizes chemo- and radioresistant human chronic lymphocytic leukaemia lymphocytes to TNF-α-initiated apoptosis, *Br. J. Cancer* 77, 1103-1107.

119. Orlowski, R. Z., Eswara, J. R., Lafond-Walker, A., Grever, M. R., Orlowski, M., and Dang, C. V. (1998) Tumor growth inhibition induced in a murine model of human Burkitt's lymphoma by a proteasome inhibitor, *Cancer Res.* 58, 4342-4348.

120. Hideshima, T., Richardson, P. G., and Anderson, K. C. (2011) Mechanism of action of proteasome inhibitors and deacetylase inhibitors and the biological basis of synergy in multiple myeloma, *Mol. Cancer Ther.* 10, 2034-2042.

121. Naujokat, C., and Hoffmann, S. (2002) Role and function of the 26S proteasome in proliferation and apoptosis, *Lab. Invest.* 82, 965-980.

122. Masdehors, P., Merle-Beral, H., Maloum, K., Omura, S., Magdelenat, H., and Delic, J. (2000) Deregulation of the ubiquitin system and p53 proteolysis modify the apoptotic response in B-CLL lymphocytes, *Blood* 96, 269-274.

123. Orlowski, R. Z., and Kuhn, D. J. (2008) Proteasome inhibitors in cancer therapy: lessons from the first decade, *Clin. Cancer. Res.* 14, 1649-1657.

124. McConkey, D. J., and Zhu, K. (2008) Mechanisms of proteasome inhibitor action and resistance in cancer, *Drug Resist. Update* 11, 164-179.

125. Richardson, P. G., Barlogie, B., Berenson, J., Singhal, S., Jagannath, S., Irwin, D., Rajkumar, S. V., Srkalovic, G., Alsina, M., Alexanian, R., Siegel, D., Orlowski, R. Z., Kuter, D., Limentani, S. A., Lee, S., Hideshima, T., Esseltine, D.-L., Kauffman, M., Adams, J., Schenkein, D. P., and Anderson, K. C. (2003) A phase 2 study of bortezomib in relapsed, refractory myeloma, *New Engl. J. Med.* 348, 2609-2617.

126. Fuchs, D., Berges, C., Opelz, G., Daniel, V., and Naujokat, C. (2008) Increased expression and altered subunit composition of proteasomes induced by continuous proteasome inhibition establish apoptosis resistance and hyperproliferation of Burkitt lymphoma cells, *J. Cell. Biochem.* 103, 270-283.

127. Lü, S. Q., Yang, J. M., Song, X. M., Gong, S. L., Zhou, H., Guo, L. P., Song, N. X., Bao, X. C., Chen, P. P., and Wang, J. M. (2008) Point mutation of the proteasome β5 subunit gene is an important mechanism of bortezomib resistance in bortezomib-selected variants of Jurkat T cell lymphoblastic lymphoma/leukemia line, *J. Pharmacol. Exp. Ther.* 326, 423-431.

128. Lü, S. Q., Yang, J. M., Chen, Z. L., Gong, S. L., Zhou, H., Xu, X. Q., and Wang, J. M. (2009) Different mutants of PSMB5 confer varying bortezomib resistance in T lymphoblastic lymphoma/leukemia cells derived from the Jurkat cell line, *Exp. Hematol.* 37, 831-837.

129. Rückrich, T., Kraus, M., Gogel, J., Beck, A., Ovaa, H., Verdoes, M., Overkleeft, H. S., Kalbacher, H., and Driessen, C. (2009) Characterization of the ubiquitin-proteasome system in bortezomib-adapted cells, *Leukemia* 23, 1098-1105.

130. Ri, M., Iida, S., Nakashima, T., Miyazaki, H., Mori, F., Ito, A., Inagaki, A., Kusumoto, S., Ishida, T., Komatsu, H., Shiotsu, Y., and Ueda, R. (2010) Bortezomib-resistant myeloma cell lines: a role for mutated *PSMB5* in preventing the accumulation of unfolded proteins and fatal ER stress, *Leukemia* 24, 1506-1512.

131. Pérez-Galán, P., Mora-Jensen, H., Weniger, M. A., Shaffer, A. L., Rizzatti, E. G., Chapman, C. M., Mo, C. C., Stennett, L. S., Rader, C., Liu, P. C., Raghavachari, N., Stetler-Stevenson, M., Yuan, C., Pittaluga, S., Maric, I., Dunleavy, K. M., Wilson, W. H., Staudt, L. M., and Wiestner, A. (2011) Bortezomib resistance in mantle cell lymphoma is associated with plasmacytic differentiation, *Blood* 117, 542-552.

132. Balsas, P., Galan-Malo, P., Marzo, I., and Naval, J. (2012) Bortezomib resistance in a myeloma cell line is associated to PSMβ5 overexpression and polyploidy, *Leukemia Res.* 36, 212-218.

133. Sharma, R. C., Inoue, S., Roitelman, J., Schimke, R. T., and Simoni, R. D. (1992) Peptide transport by the multidrug resistance pump, *J. Biol. Chem.* 267, 5731-5734.

134. de Jong, M. C., Slootstra, J. W., Scheffer, G. L., Schroeijers, A. B., Puijk, W. C., Dinkelberg, R., Kool, M., Broxterman, H. J., Meloen, R. H., and Scheper, R. J. (2001) Peptide transport by the multidrug resistance protein MRP1, *Cancer Res.* 61, 2552-2557.

135. Minderman, H., Zhou, Y. F., O'Loughlin, K. L., and Baer, M. R. (2007) Bortezomib activity and in vitro interactions with anthracyclines and cytarabine in acute myeloid leukemia cells are independent of multidrug resistance mechanisms and p53 status, *Cancer Chemother. Pharmacol.* 60, 245-255.

136. Groll, M., Berkers, C. R., Ploegh, H. L., and Ovaa, H. (2006) Crystal structure of the boronic acid-based proteasome inhibitor bortezomib in complex with the yeast 20S proteasome, *Structure* 14, 451-456.

137. The PyMOL Molecular Graphics System, Version 1.5.0.1 ed., Schrödinger, LLC.

138. Kale, A. J., McGlinchey, R. P., Lechner, A., and Moore, B. S. (2011) Bacterial self-resistance to the natural proteasome inhibitor salinosporamide A, *ACS Chem. Biol.* 6, 1257-1264.

139. Politou, M., Karadimitris, A., Terpos, E., Kotsianidis, I., Apperley, J. F., and Rahemtulla, A. (2006) No evidence of mutations of the PSMB5 (beta-5 subunit of proteasome) in a case of myeloma with clinical resistance to bortezomib, *Leukemia Res.* 30, 240-241.

140. Shaughnessy, J. D., Qu, P., Usmani, S., Heuck, C. J., Zhang, Q., Zhou, Y., Tian, E., Hanamura, I., van Rhee, F., Anaissie, E., Epstein, J., Nair, B., Stephens, O., Williams, R., Waheed, S., Alsayed, Y., Crowley, J., and Barlogie, B. (2011) Pharmacogenomics of bortezomib test-dosing identifies hyperexpression of proteasome genes, especially PSMD4, as novel high-risk feature in myeloma treated with total therapy 3, *Blood* 118, 3512-3524.

141. Kraus, M., Rückrich, T., Reich, M., Gogel, J., Beck, A., Kammer, W., Berkers, C. R., Burg, D., Overkleeft, H., Ovaa, H., and Driessen, C. (2007) Activity patterns of proteasome subunits reflect bortezomib sensitivity of hematologic

malignancies and are variable in primary human leukemia cells, *Leukemia* 21, 84-92.

142. Yang, D. T., Young, K. H., Kahl, B. S., Markovina, S., and Miyamoto, S. (2008) Prevalence of bortezomib-resistant constitutive NF-kappaB activity in mantle cell lymphoma, *Mol. Cancer* 7, 40.

143. Zhang, L. D., Littlejohn, J. E., Cui, Y., Cao, X. B., Peddaboina, C., and Smythe, W. R. (2010) Characterization of bortezomib-adapted I-45 mesothelioma cells, *Mol. Cancer* 9, 110.

144. Smith, A. J., Dai, H. M., Correia, C., Takahashi, R., Lee, S. H., Schmitz, I., and Kaufmann, S. H. (2011) Noxa/Bcl-2 protein interactions contribute to bortezomib resistance in human lymphoid cells, *J. Biol. Chem.* 286, 17682-17692.

145. Gareau, C., Fournier, M. J., Filion, C., Coudert, L., Martel, D., Labelle, Y., and Mazroui, R. (2011) p21(WAF1/CIP1) upregulation through the stress granule-associated protein CUGBP1 confers resistance to bortezomib-mediated apoptosis, *Plos One* 6, e20254.

146. Kern, J., Untergasser, G., Zenzmaier, C., Sarg, B., Gastl, G., Gunsilius, E., and Steurer, M. (2009) GRP-78 secreted by tumor cells blocks the antiangiogenic activity of bortezomib, *Blood* 114, 3960-3967.

147. Sanchez, E., Li, M. J., Steinberg, J. A., Wang, C., Shen, J., Bonavida, B., Li, Z. W., Chen, H. M., and Berenson, J. R. (2010) The proteasome inhibitor CEP-18770 enhances the anti-myeloma activity of bortezomib and melphalan, *Br. J. Haematol.* 148, 569-581.

148. Kuhn, D. J., Chen, Q., Voorhees, P. M., Strader, J. S., Shenk, K. D., Sun, C. M., Demo, S. D., Bennett, M. K., van Leeuwen, F. W. B., Chanan-Khan, A. A., and Orlowski, R. Z. (2007) Potent activity of carfilzomib, a novel, irreversible inhibitor of the ubiquitin-proteasome pathway, against preclinical models of multiple myeloma, *Blood* 110, 3281-3290.

149. Chauhan, D., Singh, A. V., Aujay, M., Kirk, C. J., Bandi, M., Ciccarelli, B., Raje, N., Richardson, P., and Anderson, K. C. (2010) A novel orally active proteasome inhibitor ONX 0912 triggers in vitro and in vivo cytotoxicity in multiple myeloma, *Blood* 116, 4906-4915.

150. Edelmann, M. J., Nicholson, B., and Kessler, B. M. (2011) Pharmacological targets in the ubiquitin system offer new ways of treating cancer, neurodegenerative disorders and infectious diseases, *Expert Rev. Mol. Med.* 13, e35.

151. Fuchs, D., Berges, C., Opelz, G., Daniel, V., and Naujokat, C. (2008) HMG-CoA reductase inhibitor simvastatin overcomes bortezomib-induced apoptosis resistance by disrupting a geranylgeranyl pyrophosphate-dependent survival pathway, *Biochem. Biophys. Res. Commun.* 374, 309-314.

152. Hideshima, T., Chauhan, D., Ishitsuka, K., Yasui, H., Raje, N., Kumar, S., Podar, K., Mitsiades, C., Hideshima, H., Bonham, L., Munshi, N. C., Richardson, P. G., Singer, J. W., and Anderson, K. C. (2005) Molecular characterization of PS-341 (bortezomib) resistance: implications for overcoming resistance using lysophosphatidic acid acyltransferase (LPAAT)-beta inhibitors, *Oncogene* 24, 3121-3129.

153. Chauhan, D., Li, G. L., Podar, K., Hideshima, T., Neri, P., He, D. L., Mitsiades, N., Richardson, P., Chang, Y., Schindler, J., Carver, B., and Anderson, K. C. (2005) A novel carbohydrate-based therapeutic GCS-100 overcomes bortezomib resistance and enhances dexamethasone-induced apoptosis in multiple myeloma cells, *Cancer Res.* 65, 8350-8358.

154. Streetly, M. J., Maharaj, L., Joel, S., Schey, S. A., Gribben, J. G., and Cotter, F. E. (2010) GCS-100, a novel galectin-3 antagonist, modulates MCL-1, NOXA, and cell cycle to induce myeloma cell death, *Blood* 115, 3939-3948.

155. Roue, G., Pérez-Galán, P., Mozos, A., Lopez-Guerra, M., Xargay-Torrent, S., Rosich, L., Saborit-Villarroya, I., Normant, E., Campo, E., and Colomer, D. (2011) The Hsp90 inhibitor IPI-504 overcomes bortezomib resistance in mantle cell lymphoma in vitro and in vivo by down-regulation of the prosurvival ER chaperone BiP/Grp78, *Blood* 117, 1270-1279.

Chapter 2:

Characterization of 5-Chloro-5-Deoxy-D-Ribose-1-Dehydrogenase in Chloroethylmalonyl-Coenzyme A Biosynthesis: Substrate and Reaction Profiling

2.1: Abstract

SalM is a short-chain dehydrogenase/reductase enzyme from the marine actinomycete *Salinispora tropica* that is involved in the biosynthesis of chloroethylmalonyl-CoA, a novel halogenated polyketide synthase extender unit of the proteasome inhibitor salinosporamide A. SalM was heterologously overexpressed in *Escherichia coli* and characterized *in vitro* for its substrate specificity, kinetics, and reaction profile. A sensitive, real-time ^{13}C NMR assay was developed to visualize the oxidation of 5-chloro-5-deoxy-D-ribose to 5-chloro-5-deoxy-D-ribono-γ-lactone in a NAD^+-dependent reaction followed by spontaneous lactone hydrolysis to 5-chloro-5-deoxy-D-ribonate. While short-chain dehydrogenase/reductase enzymes are widely regarded as metal independent, a strong divalent metal cation dependence for Mg^{2+}, Ca^{2+}, or Mn^{2+} was observed with SalM. Oxidative activity was also measured with the alternative substrates D-erythrose and D-ribose, making SalM the first reported stereospecific non-phosphorylated ribose-1-dehydrogenase.

2.2: Introduction

The marine actinomycete *Salinispora tropica* produces a suite of γ-lactam-β-lactone natural products identified as potent 20S proteasome inhibitors.[1] Exploration into the biosynthesis of the most bioactive family member, salinosporamide A, resulted in the characterization of a pathway for the biosynthesis of chloroethylmalonyl-CoA, a novel polyketide synthase substrate (Figure 2.1).[2] A broad overview of the biosynthesis of salinosporamide A and chloroethylmalonyl-CoA was introduced in Chapter 1.

Chapter 2 of this dissertation details my extensive efforts to elucidate the role of the SalM enzyme in the chloroethylmalonyl-CoA biosynthetic pathway.

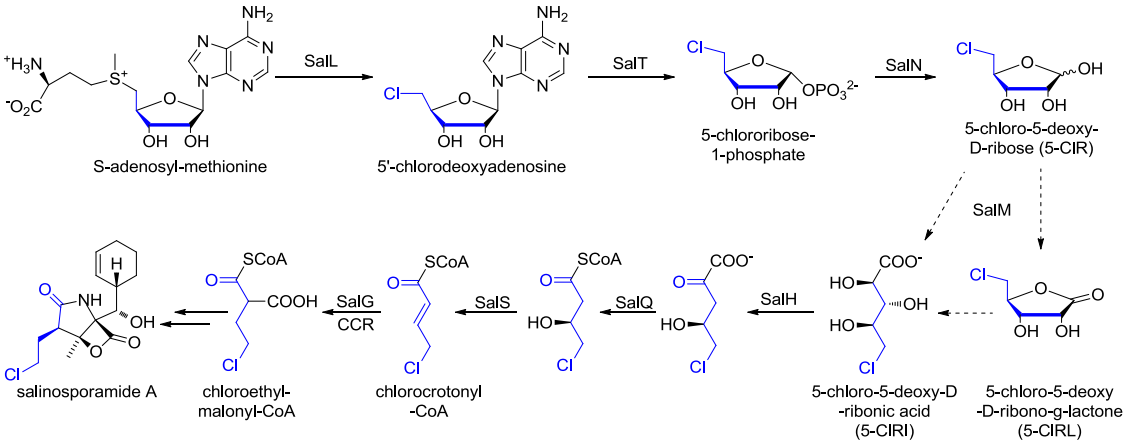

Figure 2.1. The biosynthetic pathway of chloroethylmalonyl-CoA in salinosporamide A production in *S. tropica* CNB-440. The dashed arrows represent the postulated enzymatic role(s) of the short-chain dehydrogenase/reductase SalM in the oxidation of 5-ClR. Blue coloring indicates the fate of 5-ClR incorporation into salinosporamide A.

To probe which genes were responsible for chloroethylmalonyl-CoA biosynthesis, salinosporamide cluster (*sal*) genes were individually replaced with an antibiotic resistance cassette and the production of salinosporamides A and B were quantified (Table 2.1).[2] A selective loss of salinosporamide A production relative to salinosporamide B indicated the gene was involved in chloroethylmalonyl-CoA biosynthesis as salinosporamide B is alternatively produced from ethylmalonyl-CoA (see Chapter 1, Figure 1.8B). As discussed in Chapter 1, the first two steps of chloroethylmalonyl-CoA biosynthesis, catalyzed by the chlorinase SalL and the purine nucleoside phosphorylase SalT, were believed to parallel fluoroacetate production in *Streptomyces cattleya*.[3] This was supported by the complete loss or significant reduction

of salinosporamide A production in the *ΔsalL* and *ΔsalT* strains, respectively, and the *in vitro* characterization of SalL.[4] This would result in 5-chlororibose-1-phosphate as the product of SalT. At this point the pathways appeared to diverge. The presence of a pathway specific phosphatase, SalN, suggested that 5-chlororibose-1-phosphate is dephosphorylated to 5-chloro-5-deoxy-D-ribose (5-ClR). We hypothesized that 5-ClR is then oxidized at C1 which would ultimately lead to a sugar acid, which could serve as the substrate for the dihydroxyacid dehydratase, SalH.

Table 2.1. Production of salinosporamides in *S. tropica* CNB-440 gene inactivation strains. Table adapted from Eustáquio *et al.*[2] [a]salinosporamide A production relative to the wild-type strain, [b]salinosporamide B production relative to the wild-type strain, [c]N.D. = not detected.

Strain	Annotated function	% Sal. A[a]	% Sal. B[b]
wild-type	-	100 ± 10	100 ± 13
ΔsalA	PKS	N.D.[c]	N.D.
ΔsalL	Chlorinase	N.D.	90 ± 20
ΔsalT	Purine nucleotide phosphorylase	50 ± 8	91 ± 10
ΔsalN	Phosphatase	16 ± 3	92 ± 9
ΔsalM	Short-chain dehydrogenase/reductase	2.2 ± 0.2	120 ± 20
ΔsalH	Dihydroxyacid dehydratase	3.8 ± 0.7	70 ± 15
ΔsalQ	α-ketoacid decarboxylase	25 ± 6	98 ± 16
ΔsalS	Acyl dehydratase	39 ± 14	95 ± 30
ΔsalG	Crotonyl-CoA reductase/carboxylase	N.D.	94 ± 30

Gene replacement of *salM*, which encodes a short-chain dehydrogenase/ reductase (SDR) enzyme, dramatically and selectively reduced the production of salinosporamide A by ~98% relative to the wild-type organism while production of the

non-chlorinated salinosporamide B remained unchanged.[2] As SalM was predicted to be an oxidoreductase, it was selected as the most likely candidate for oxidation of 5-ClR. The *in vivo* substrate of SalM was then verified to be 5-ClR by derivatization of the accumulated fermentation product of the *ΔsalM* strain.[2] Furthermore, chemical complementation with 5-ClR to the separate upstream *ΔsalL* strain restored salinosporamide A production.[2] Thus, based on the information available, we predicted that SalM would oxidize 5-ClR at the anomeric carbon by acting as a pentose-1-dehydrogenase.

Our understanding of the product of SalM oxidation on 5-ClR was less clear. A BRENDA enzyme database search for ribose-1-dehydrogenases (1.1.1.115) revealed a single report of an enzyme reported to convert D-ribose to D-ribonate.[5] This led us to predict that the SalM product would be 5-chloro-5-deoxy-D-ribonate (5-ClRI). However, a closer reading of this publication revealed that the enzyme product was not actually reported. Alternatively, a bioinformatic analysis of SDR enzymes (discussed in detail later) such as SalM lead us to believe that 5-ClR would be oxidized to 5-chloro-5-deoxy-D-ribono-γ-lactone (5-ClRL). Chemical complementation of the *ΔsalM* strain with 5-ClRL increased production of salinosporamide A while complementation with 5-ClRI did not.[2] However, it was not clear if these experiments had biological significance as it was unknown if 5-ClRI was taken up by the cell. Furthermore, we suspected that 5-ClRL may spontaneously hydrolyze to 5-ClRI in the cell. Thus we decided to characterize SalM *in vitro* to verify the structure of the enzymatic reaction product.

It is intuitive to presume that SalM evolved from a primary metabolic ribose-1-dehydrogenase to oxidize a halogenated sugar derivative. However, despite the ubiquitous nature of ribose in biology, non-phosphorylated ribose-1-dehydrogenases have not been well characterized. Instead, pentose catabolism utilizes phosphorylated intermediates in the pentose phosphate pathway, nucleotide metabolism, and pentose-glucuronate conversion. Phosphorylated pentoses are also used in anabolic pathways such as the Calvin-Benson cycle and in the generation of nucleosides. The only previously reported "ribose-1-dehydrogenase" was isolated from pig liver and oxidized both D-ribose and D-xylose with approximately equal activity.[5] Oxidative enzyme activity for ribose has been reported as an alternative substrate for other sugar oxidoreductase enzymes with broad substrate specificity;[6-10] however, a non-phosphorylated pentose-1-dehydrogenase specific to the stereochemistry of ribose has yet to be reported.

Potentially related pentose-1-dehydrogenases such as L-arabinose-1-dehydrogenase and D-xylose-1-dehydrogenase have been shown to oxidize a cyclical hemiacetal substrate to the corresponding lactone.[8,9,11,12] Glucose-1-dehydrogenase has also been reported to possess "gluconolactonase" activity, catalyzing both the oxidation of glucose to gluconolactone and the subsequent hydrolysis to gluconate.[9] Since SalH is a dihydroxyacid dehydratase and expected to accept 5-ClRI as its substrate and the salinosporamide biosynthetic gene cluster does not encode a putative lactonase enzyme,[2] we were compelled to determine if a lactone intermediate (5-ClRL) exists and if so, to decipher the fate of this pathway product. We thus set out to explore whether

SalM produces a lactone, an acid, or possesses bi-functional dehydrogenase/lactonase activity.

Traditional analysis of oxidoreductase enzymes such as SalM utilize changes in optical absorption corresponding to the conversion of cofactors such as NAD(P)(H) or FAD(H). While this method provides a simple, non-invasive way to monitor redox kinetics, it fails to identify the structure of the enzymatic product. Subsequent cofactor-independent reactions such as hydrolysis are thus not observed. Therefore, real-time visualization of product structures is imperative when transient intermediates are formed. A sensitive time-arrayed NMR approach was consequently developed to monitor the progress of the SalM reaction and to identify structures of intermediates and products. Chapter 2 describes my efforts to develop a real-time ^{13}C-NMR based characterization of SalM, a novel 5-chloro-5-deoxy-D-ribose-1-dehydrogenase.

2.3: Results

2.3.1: Bioinformatic Analysis.

Amino acid sequence similarity to SalM was used to identify potential enzymatic homologs. BLAST analysis of the 255 amino acid sequence of SalM indicated a classical short-chain dehydrogenase/reductase enzyme.[13] Based on previously reported phylogenetic analyses of the SDR superfamily, it was expected that SalM should perform a simple ketone/alcohol redox reaction and would not participate in any additional chemistry such as epimerization, decarboxylation, or dehydration.[13,14] The highest scoring sequence was an uncharacterized 67% identical protein (accession number YP_638874) from several terrestrial *Mycobacteria* species (strains KMS, MCS,

JCS). SalM does show 40% sequence similarity to annotated glucose-1-dehydrogenases from *Listeria grayi* DSM 20601 and *Brevibacillus brevis* NBRC 100599 (accession numbers ZP_04443055 and YP_002770578, respectively).

2.3.2: Enzyme Purification and Cofactor Identification.

Recombinant SalM was expressed in *E. coli* BL21 (DE3) for *in vitro* characterization. The N-terminal octahistidyl-tagged enzyme was purified by Ni-NTA affinity chromatography and afforded approximately 20 mg L^{-1} recombinant protein in greater than 90% purity. All enzyme activity assays utilized the tagged protein without further purification since SalM was prone to aggregation and eluted over a very broad range of sizes via size exclusion chromatography.

To assay SalM, we first identified the appropriate redox cofactor. The SDR family of enzymes contain a Rossmann fold for the binding of dinucleotide cofactors[14] with many SDR enzymes having a preference for either the phosphorylated or non-phosphorylated cofactor.[13] While no activity was observed with $NADP^+$, the addition of NAD^+ as cofactor resulted in its conversion to NADH as monitored spectrophotometrically. The preference for NAD^+ is further supported by the bioinformatics analysis of the primary sequence of the cofactor binding region.[13] Alignment of SalM with 3α-20β-hydroxysteroid dehydrogenase (PDB 2hsd) revealed a conserved aspartic acid residue at position 40 equivalent to Asp36 of 2hsd. This would place SalM into the cD1d subfamily of SDRs in which NAD^+ is the expected enzyme cofactor. Asp40 of SalM likely forms hydrogen bonds to the 2' and 3' hydroxyls of the adenine ribose moiety.[15] Our initial attempts to assay SalM with 5-ClR and NAD^+ resulted in minimal activity. While optimizing assay conditions, we observed that the

addition of the divalent metal cations magnesium, manganese, or calcium increased its activity 10-fold at low millimolar concentrations.

Increasing concentrations of Mg^{2+} and Ca^{2+} were shown to have a positive relationship with activity (Figure 2.2). Maximum activity is reached by 20 mM. Additional cation failed to increase activity or was inhibitory. At all concentrations, enzyme activity was slow to reach the linear kinetic phase. However, presoaking concentrated enzyme stock solutions with 10 mM $MgCl_2$ for several days at -20 °C and then adding enzyme to a Mg^{2+} free buffer at the time of the assay resulted in equivalent activity. Additionally, this method allowed steady state kinetics to be reached much sooner than adding divalent cation at the start of the assay, suggesting that the metal ion is a slow binding structural component that reaches saturation.

When using the cation pre-soaked enzyme, subsequent addition of metal ions to the assay buffer was found to inhibit activity, indicating that the cation reaches saturation and then becomes inhibitory. As expected, the addition of EDTA into the assay mixture significantly inhibited enzyme activity. Mn^{2+} was shown to stimulate SalM activity strongly in the 1-2 mM range but inhibitory at higher concentrations. At 2 mM $MnCl_2$, activity was equal to that of 20 mM $MgCl_2$. However, at concentrations above 20 mM, activity was less than SalM devoid of divalent cation. Fe^{2+}, Cu^{2+}, Zn^{2+}, and Ni^{2+} were also tested but found to be inactive or inhibitory (data not shown). Addition of $MgCl_2$ or $MgSO_4$ resulted in equivalent activity indicating that the counterion was not responsible for changes in enzyme activity.

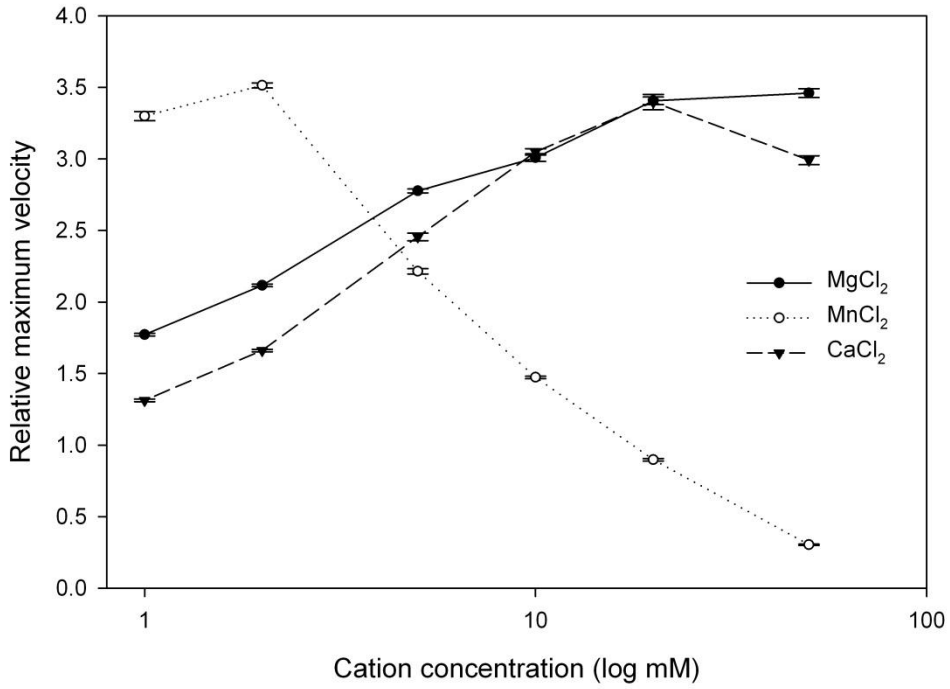

Figure 2.2. Metal dependence of SalM activity. SalM enzyme was assayed for activity with 1 mM NAD^+ and 1 mM 5-ClR in the presence of various concentrations of $MgCl_2$, $MnCl_2$ or $CaCl_2$ between 1 mM and 50 mM. The maximum velocity of the reaction at steady-state was normalized to the maximum velocity of the SalM reaction without addition of metal (Activity = 1).

2.3.3: C-terminus Mutations.

Metal dependence within the SDR family is rare, however, there is precedence. Two distinct, isolated cases of structural metal dependence in SDR enzymes have been previously characterized structurally. In the first case, dTDP-6-deoxy-L-lyxo-4-hexulose reductase (RmlD) from *Salmonella enterica* (PDB 1kbz) was shown to require Mg^{2+} for dimerization.[16] Its high resolution crystal structure showed that the magnesium ion was bound by two glutamate residues per monomer to stabilize the dimer.[17] In the second case, R-specific alcohol dehydrogenase (RADH) from *Lactobacillus brevis* (PDB 1nxq)

was shown to be a homotetramer stabilized by two structured magnesium ions per tetramer.[18] The carboxylate of the C-terminal glutamine residue coordinates water molecules that bind magnesium. As with SalM, RADH had a slow binding rate with Mg^{2+}. Mn^{2+} was also shown to be a suitable cofactor (activity vs. concentration was not reported in this study).

Although we were unable to discern the monomeric state of SalM due to extensive aggregation, SalM does contain a C-terminal glutamine residue as with RADH. To probe the importance of Gln255 in SalM, eight mutants, including truncations (Q255 deletion, A254-Q255 deletion), substitutions (Q255E, Q255S, Q255N, Q255V), and extension (256V, Q255N/256Q) were generated. In all cases, highly expressed yet entirely insoluble protein was produced, suggesting an important structural role of Gln255.

2.3.4: Substrate Specificity and Kinetics.

To identify enzyme substrate specificity ten different sugars were assayed (Figure 2.3). Only 5-ClR, D-ribose, and D-erythrose showed activity with 5-ClR being the preferred substrate. Sugars tested and found inactive (less than 2% activity relative to 5-ClR) included 2-deoxy-D-ribose, D-ribose-5-phosphate, D-xylose, D-arabinose, L-arabinose, D-allose, and D-glucose. The K_m differed significantly among the three substrates with 5-ClR binding to SalM two orders of magnitude greater than D-erythrose and three orders of magnitude greater than D-ribose (Table 2.2). V_{max} values were comparable for all three substrates, indicating that K_m is the driver of differential activity among the three preferred substrates. k_{cat} values were not calculated due to

enzyme aggregation, which led to an unknown fraction of the total SalM enzyme being inactive.

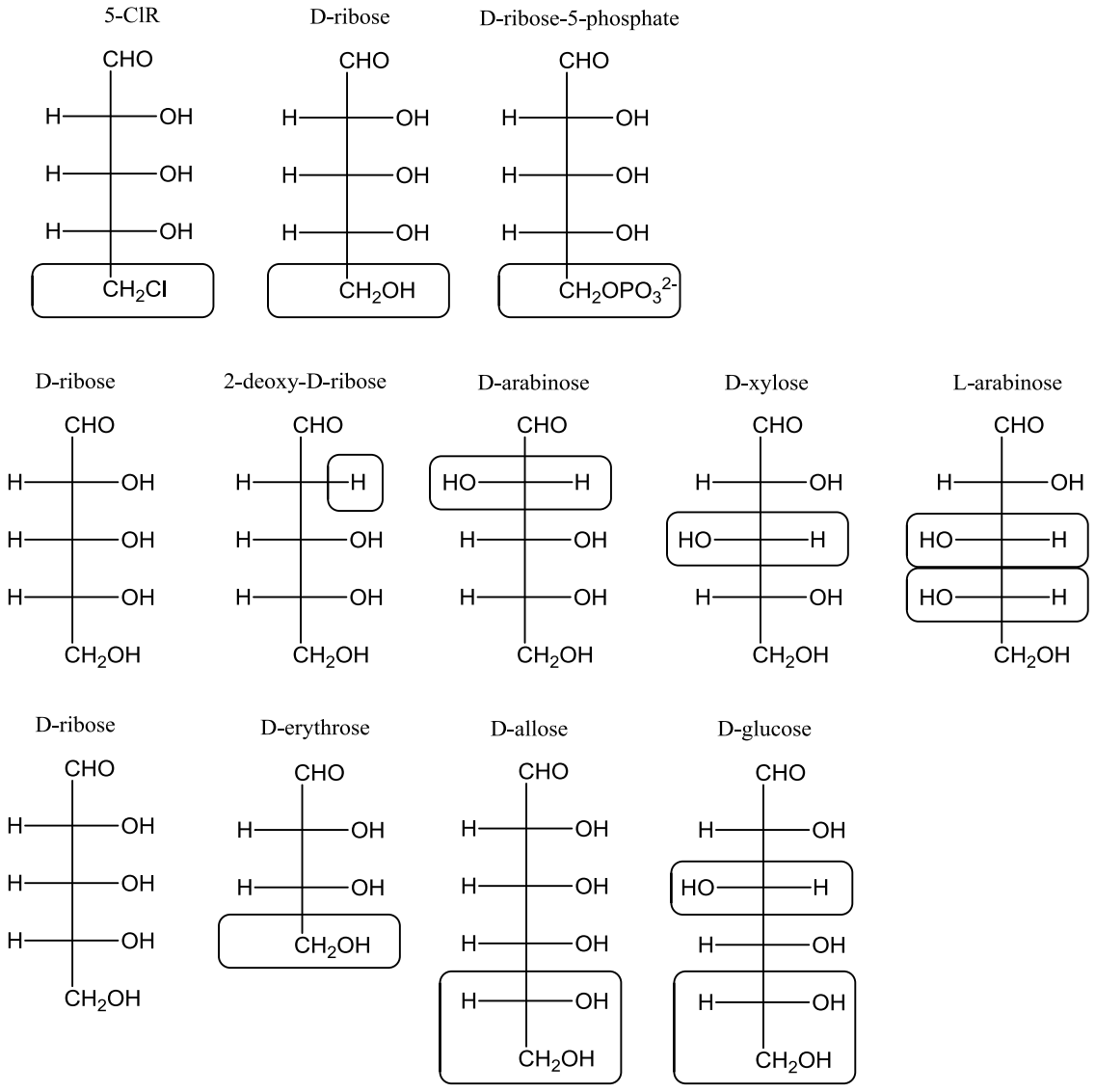

Figure 2.3. Carbohydrates assayed for SalM activity. Top row: C5 modifications to 5-ClR. Middle line: pentose stereoisomers of D-ribose. Bottom row: carbon chain length subtraction and addition with retention of stereochemistry relative to D-ribose. Glucose was also tested. SalM only oxidized 5-ClR, D-ribose, and D-erythrose.

Table 2.2. Kinetic values for accepted substrates of SalM.

	K_m (mM)	V_{max} (μMols $min^{-1}mg^{-1}$)
D-ribose	19 ± 3	4.8 ± 0.2
D-erythrose	2.5 ± 0.5	5.4 ± 0.4
5-ClR	0.02 ± 0.01	6.8 ± 0.1

2.3.5: Carbon NMR Assays of SalM.

In order to explore the product structure(s) of SalM, we first assayed activity with [U-^{13}C]ribose in an arrayed NMR experiment (Figure 2.4). A standard ^{1}H-decoupled ^{13}C-NMR spectrum of 256 scans was recorded of the reaction mixture immediately prior to the addition of SalM. After enzyme addition, equivalent scans were repeated at selected time points extending up to 72 hours. The short scan time of approximately 9 minutes allowed only the labeled ribose carbon signals to be readily detected in the assay mixture that also contained NAD^+ and its two ribose residues. However, as ribose adopts four cyclical anomeric forms in solution, its NMR spectrum is rather complex for a five-carbon molecule. It has been reported previously that the α and β six-membered pyranoses account for approximately 21.5% and 58.5%, respectively, of the total sugar at a temperature of 30 °C, while the α and β five-membered furanoses account for the remaining 6.5% and 13.5%, respectively.[19] The open chain aldehyde, on the other hand, is only a transient intermediate and thus not observed by NMR analysis. Upon oxidation of the anomeric C1 carbon, we anticipated that the spectrum would significantly simplify as the reaction progresses to give a single product.

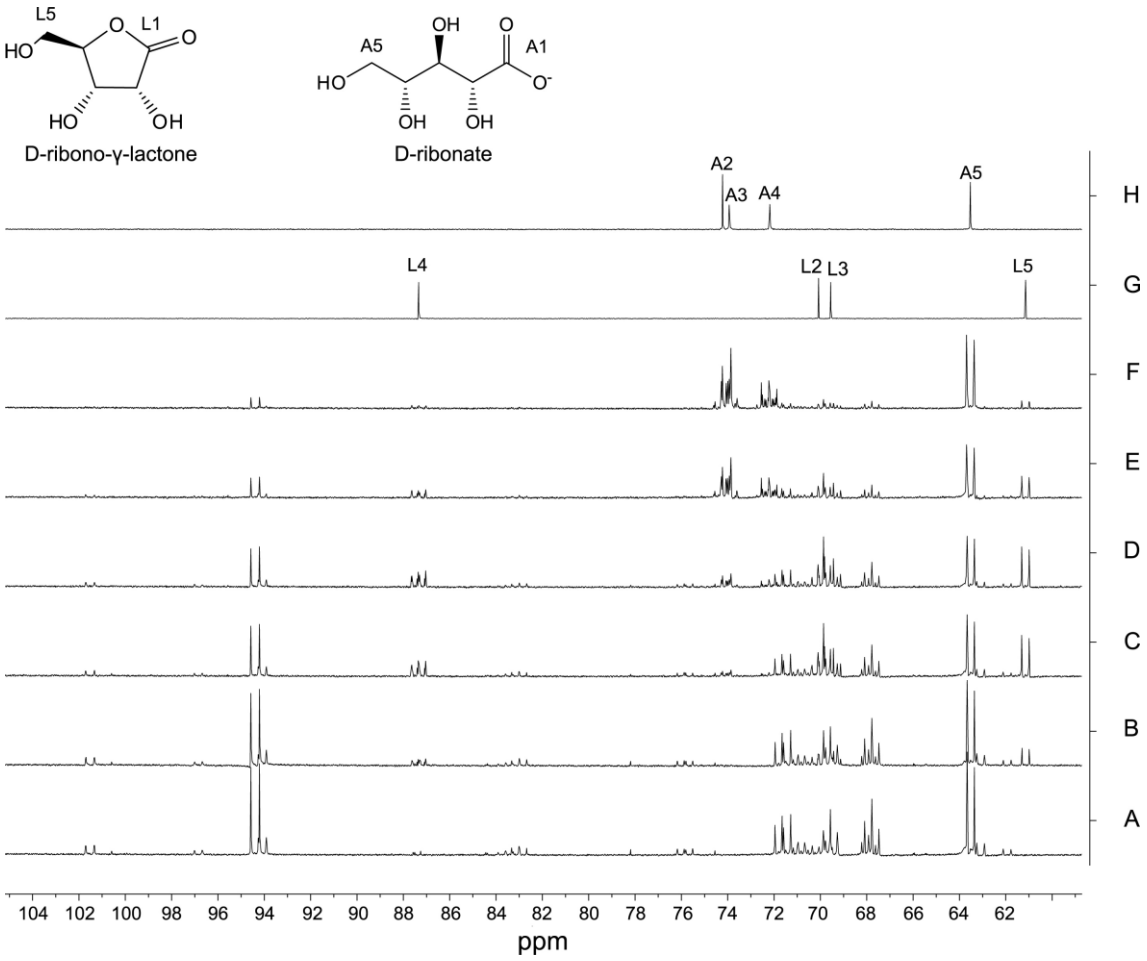

Figure 2.4. Partial 125 MHz ^{13}C NMR spectra of [U-^{13}C]ribose and NAD^{+} assayed with SalM. Spectra acquired over 9 min were taken prior to the addition of enzyme (**A**) and then after enzyme addition at 45 min (**B**), 115 min (**C**), 210 min (**D**), 21 h (**E**), and 72 h (**F**). Standards of unlabeled ribono-γ-lactone (**G**) and ribonate (**H**) are provided for reference with carbons 2-5 labeled as L2-L5 and A2-A5, respectively. Lactone formation is clearly apparent with the emergence of L4 and L5 at 87.5 and 61.0 ppm, respectively, beginning with trace **B**. As the lactone peaks fade over time, several new peaks emerge at 70-72 ppm that correspond to A2-A4 of ribonate. ^{13}C NMR peak assignments for unlabeled D-ribose have been previously reported (all peaks shifted 2.3 ppm down field relative to **A**).[20] Resonances for carbon 1 of D-ribono-γ-lactone and D-ribonate are not shown.

Upon the addition of SalM, the consumption of ribose was observed as the four ^{13}C doublets between 93 and 102 ppm representing the anomeric C1 positions of the

ribose congeners decreased in intensity over time. With the oxidation of C1, a new doublet of weak intensity likewise emerged at 178.9 ppm. Unfortunately since the chemical shifts of the C1 carbonyls of ribono-γ-lactone and ribonate standards are nearly identical, we turned our attention to other more diagnostic signals for analysis. Significantly, two clear signals emerged characteristic of ribono-γ-lactone – a doublet of doublets centered at 87.4 ppm and a doublet centered at 61.1 ppm corresponding to C4 and C5, respectively. No peaks corresponding to ribono-δ-lactone were observed suggesting that the less abundant furanose is the preferred enzyme substrate. As the reaction progresses further, these characteristic lactone peaks decreased in intensity with the concomitant emergence of a new cluster of signals at 72 to 74 ppm corresponding to C2 to C4 of ribonate. It is evident that the initial product of SalM is a five-membered lactone, which is then hydrolyzed to an acid. However, the role of SalM in lactone hydrolysis remained unclear.

We next explored the putative natural substrate, 5-ClR, using a complementary NMR spectroscopic strategy. Since we instead used unlabeled material, we utilized the coherence transfer spectroscopic technique Distortionless Enhancement of Polarization Transfer (DEPT) that resulted in enhanced four-fold sensitivity.[21] The DEPT-135 experiment allowed the visualization of all protonated carbons with differential phasing of methylene versus methyl and methine carbons.

While the use of 5-ClR simplified the NMR spectrum by eliminating the carbon signals pertaining to the two pyranose anomers, the increased scan time of this assay from nine to 68 minutes complicated the analysis by allowing the two ribose moieties

per NAD(H) cofactor molecule to be equally visible. This scenario posed a challenge to differentiate the product profile from that of the cofactor. To simplify this dilemma, we identified a diagnostic set of signals to monitor throughout the enzymatic reaction pertaining to the C5 ribose methylene carbons. Carbon 5 of the chlorinated sugar substrate is significantly upfield shifted in relation to the phosphate-attached cofactor riboses. This is true as well in the potential products 5-ClRL and 5-ClRI standards (Figure 2.5). Carbon 5 of the β anomer of 5-ClR was clearly visible at 45.8 ppm in the first time point before addition of SalM with the less prevalent α anomer at 45.2 ppm being less visible under these conditions. After enzyme addition, a new peak appeared at 43.2 ppm correlating to C5 of 5-ClRL that eventually gave way to a second product peak at 48.0 ppm relating to C5 of 5-ClRI, confirming the result of the labeled ribose experiment.

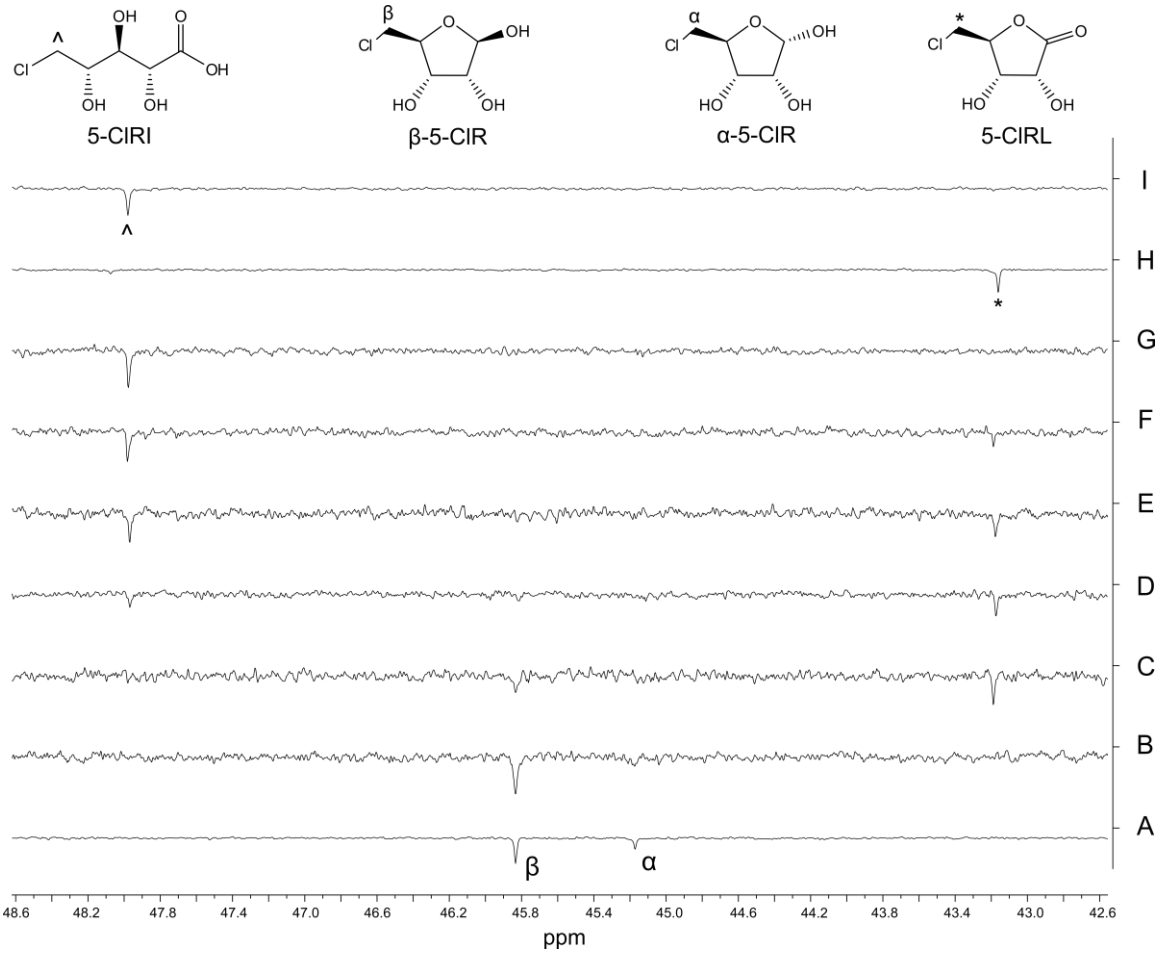

Figure 2.5. Partial 125 MHz DEPT NMR spectra of the SalM assay with unlabeled 5-ClR. A 135° DEPT NMR assay was used to monitor the oxidation of 4 mM unlabeled 5-ClR by SalM. C5 resonances are shown. Spectra acquired over 1 hour were taken prior to the addition of SalM (**A**) and then sequentially after enzyme addition at 0-1 h (**B**), 1-2 h (**C**), 2-3 h (**D**), 3-4 h (**E**), and 8-9 h (**F**). Standards of 5-ClRL (**H**) and 5-ClRI (**I**) are shown for reference. C5 of the substrate 5-ClR is populated between two resonances at 45.2 and 45.8 ppm and relate to the α- and β-anomers, respectively (trace A). 5-ClRL appears within the first hour after the addition of SalM as noted with the characteristic emergence of C5 at 43.2 ppm as noted by the asterisk (*). C5 of 5-ClRI (^) subsequently appears in the second hour and increases in intensity to become the sole product after 9 hours.

2.3.6: Lactone Opening Assay.

The NMR assays established that the SalM reaction involves the enzymatic oxidation of a furanose hemiacetal to a lactone. To identify SalM's role in the subsequent hydrolysis of the lactone to the corresponding carboxylic acid, a colorimetric assay was employed. Active and boiled SalM were separately added to solutions of 10 mM 5-ClRL in 100 mM Tris pH 7.5 and periodically analyzed colorimetrically for lactone concentration at periodic time points. At all time points, the concentration of lactone was approximately equal regardless of whether active or boiled control enzyme was added (Figure 2.6, Table A2.1), indicating that SalM does not actively participate in the hydrolysis of the lactone.

The hydrolysis rate of lactones in aqueous solution is known to follow second order kinetics, dependent on both lactone concentration and hydroxide concentration (pH).[22] Lactone hydrolysis may liberate a proton in basic solutions which alters the pH. However, if a sufficiently strong buffer is used, this effect is minimal, converting the hydrolysis rate to a pseudo first order equation. The hydrolysis rate of 5-ClRL in the presence of active SalM or absence of SalM was -0.0035 ± 0.0001 per minute and -0.0036 ± 0.0002 per minute, respectively.

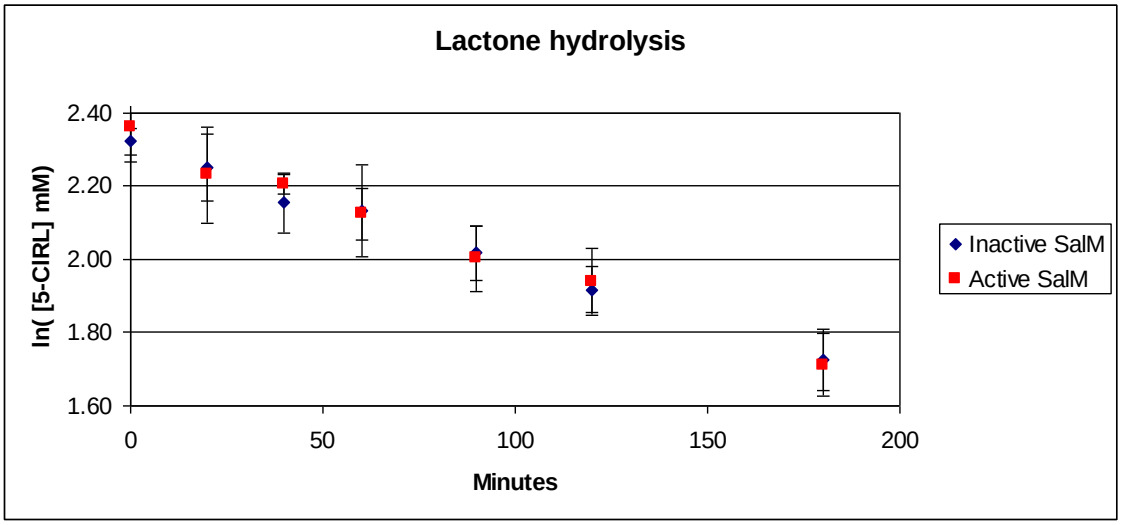

Figure 2.6. Graphical comparison of 5-ClRL hydrolysis rates in the presence and absence of active SalM enzyme.

2.4: Discussion

2.4.1: Substrate Specificity and Kinetic Analysis.

In this study, we have shown that SalM accepts 5-ClR, D-ribose, and D-erythrose as substrates with varying activity (Figure 2.7). In addition to 5-ClR, the 5-fluoro and 5-bromo analogs are presumed as substrates based on previous *in vivo* experiments with the upstream SalL mutant to produce fluoro- and bromo-salinosporamide.[4,23] However, examination of non-accepted substrates can be equally informative in structure activity relationship analysis. Carbohydrates provide a unique opportunity to individually probe minor alterations in substrate structure and stereochemistry. Inversion of stereochemistry at either C2 or C3 (D-arabinose and D-xylose, respectively) led to abolishment of activity, indicating that SalM is specific to the stereochemistry of ribose. This observation, however, is complicated by the decreased furanoses prevalence of

these two pentoses relative to D-ribose.[19] The biologically relevant 2-deoxy-D-ribose was also found to be an inactive substrate indicating that the C2 hydroxyl of ribose is required for activity and possibly forms key binding interactions with SalM at this position.

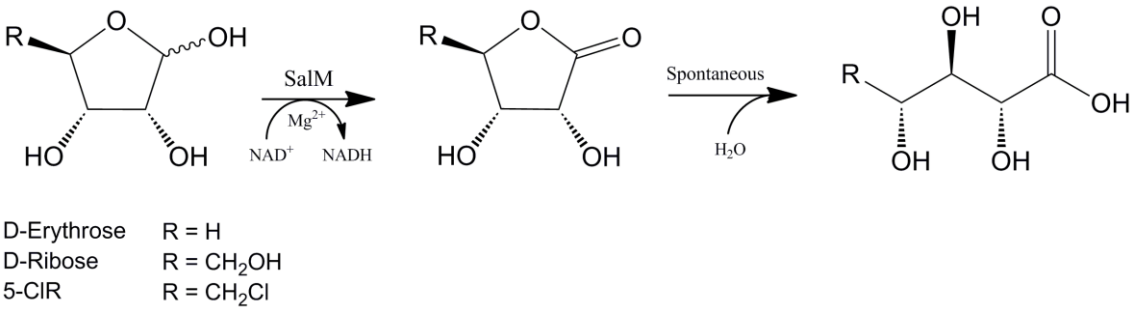

Figure 2.7. SalM-mediated transformation of select furanoses. SalM oxidizes C1 of furanose carbohydrates with stereochemistry of D-ribose at C2 and C3 to the corresponding γ-lactone. The four-carbon D-erythrose was accepted, while the six-carbon D-allose was not, thereby indicating a limit to the size of the C4 furanose substituent. Lactone hydrolysis was found to be not mediated by SalM.

Carbon chain length and ring size also influence SalM activity. Both 5-ClR and D-erythrose are only capable of forming five-membered rings, establishing furanoses as valid substrates. The observation of D-ribose being converted solely to the γ-lactone also supports the exclusive acceptance of five-membered rings. SalM did not accept D-allose, the hexose with identical stereochemistry to D-ribose at C2, C3, and C4. As D-allose adopts a furanose form of 8-10% at the assay temperature, this observation suggests that the enzyme cannot accommodate more than one carbon extending from C4 of the furanose ring.[19]

To further analyze the structure-activity relationship of SalM, we compared the kinetic parameters of the three accepted substrates. The minor differences in V_{max} indicate that enzyme-substrate binding accounts for the majority of change in activity. The significantly lower K_m of 5-ClR over ribose likely has two sources. Firstly, the replacement of the C5 hydroxyl with a chloro group in 5-ClR prevents the formation of a pyranose ring. As the true enzyme substrate appears to be one of the furanose anomers, which comprise only 20% of total ribose in solution at 30 °C, the effective substrate concentration of ribose is actually five-fold lower as compared to 5-ClR. Secondly, the switch from chloro to the more polar hydroxyl group likely creates unfavorable binding interactions with the enzyme. Erythrose, like 5-ClR, only adopts a furanose ring structure yet has a 100-fold increase in K_m. The lack of a fifth carbon and attached chloride extending from C4 of the furanose ring eliminates the possibility of any favorable binding interactions that 5-ClR may generate with SalM at this site.

2.4.2: Metal Dependence and Lactonase Activity.

Convergent evolution has produced multiple strategies for catalyzing the oxidation of hydroxyls to carbonyls. Two of the most prominent families of such enzymes are the short-chain dehydrogenase reductases (SDR) and the medium-chain dehydrogenase reductases (MDR). While the reactions catalyzed may be similar, their mechanisms are distinct. Metal dependence is synonymous within the MDR family with zinc acting as a catalytic component to activate a coordinated water molecule for abstraction of the hydroxyl proton of the substrate.[24] Glucose-1-dehydrogenase from the MDR family has been reported to oxidize glucose to gluconolactone followed by

"lactonase" activity to hydrolyze the lactone.[10,25,26] However, no mechanism has been reported for catalysis of this additional functionality.

Unlike the MDR family, the metal-independent SDRs are typically catalyzed by a lysine-activated tyrosine.[14] Since the mechanism of classical SDRs is well established to be metal independent and SalM possesses the highly conserved YX_3K catalytic group, it is likely that the metal ion is not contributing to substrate oxidation.[14] Our initial speculation as to the atypical metal dependence of SalM included the possibility of additional lactonase activity. Lactonase enzymes such as Drp35 from *Staphylococcus aureus* bind a catalytic zinc cation to activate water for hydrolysis of lactones.[27] This enzyme was also shown to exhibit lactonase activity when bound to Mg^{2+} or Mn^{2+}. However, when SalM was assayed without Mg^{2+}, 5-ClR was not oxidized to 5-ClRL indicating that the metal ion is required for the first step of the reaction and not the latter. As SalM does possess a C-terminal glutamine as in the case of RADH in *L. brevis*, we anticipate the divalent metal cation to play a similar structural role. This hypothesis is supported by the total loss of solubility for all C-terminal mutations to SalM.

Having established that SalM does not participate in lactone hydrolysis, we explored the possibility of a missing chloroethylmalonyl-CoA biosynthetic enzyme. In metabolic pathways that require lactone hydrolysis, a lactonase is often employed to facilitate the reaction.[8,12,28,29] While the salinosporamide gene cluster does not contain a lactonase, a search of the total genome sequence of *S. tropica* CNB-440 resulted in one annotated gluconolactonase.[30] This gene (Stro_0658) is located approximately 400 open reading frames from the *sal* locus. While it is not known if this enzyme participates in

the lactone opening of 5-ClRL, it seems unlikely to be specialized for this reaction since *Salinispora arenicola* CNS-205, the closest sequenced relative of *S. tropica*, contains a 92% similar gluconolactonase yet does not contain the salinosporamide gene cluster.[31] It is therefore possible that the biosynthesis of chloroethylmalonyl-CoA depends on the spontaneous hydrolysis of 5-ClRL. This may result in a specific bottleneck in salinosporamide A production, suggesting that fermentation yields of this prospective drug candidate may be increased by engineering a lactonase into *S. tropica*.

2.4.3: Evolution of SalM and the Chloroethylmalonyl-CoA Pathway.

Previously characterized pentose dehydrogenases for D-arabinose (1.1.1.117), L-arabinose (1.1.1.46), and D-xylose (1.1.1.179) have been linked to non-phosphorylative pentose catabolism (Figure 2.8).[8] In such pathways, the pentose is oxidized to a sugar lactone, followed by lactonase mediated hydrolysis to the pentonic acid. A pentonic acid dehydratase then creates a 2-keto-3-deoxy-pentonic acid, which may be subsequently oxidized to α-ketoglutarate or pyruvate.[29] The transformation of 5-ClR in salinosporamide biosynthesis follows a strikingly similar route. In the initial step, 5-ClR is oxidized to 5-ClRL by SalM, followed by hydrolysis to 5-ClRI. The acid dehydratase SalH then putatively dehydrates 5-ClRI to 5-chloro-4-hydroxy-2-oxopentanoate followed by SalQ-mediated α-oxidation to 4-chloro-3-hydroxy-2-oxopentanoate.[2]

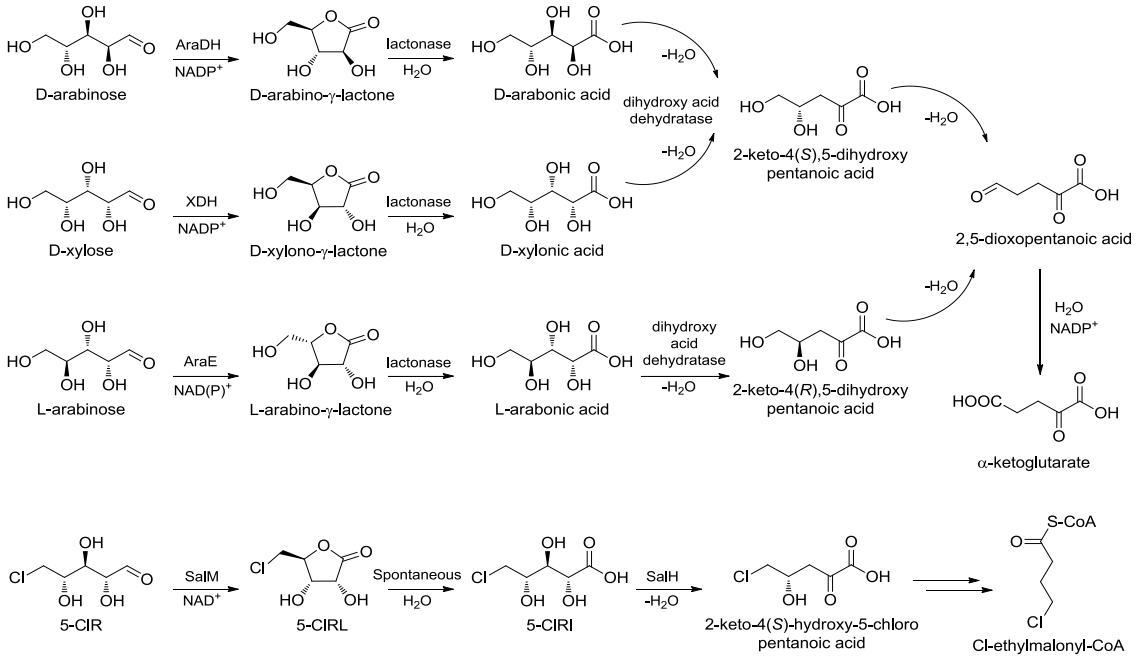

Figure 2.8. Parallel pathways in pentose oxidation. The oxidation of 5-ClR by SalM to a pentose lactone, followed by hydrolysis to the pentonic acid and dehydration by the dihydroxyacid dehydratase SalH, parallels previously reported non-phosphorylated pentose oxidation pathways for other pentoses in archaea. Figure adapted from Brouns *et al.*[8]

It is tempting to envision this portion of chloroethylmalonyl-CoA biosynthesis as being recruited from non-phosphorylated pentose oxidation. SalM has been shown here to act as a furanose-1-dehydrogenase with activity for both D-ribose and D-erythrose. Neither substrate has a previously characterized stereospecific 1-dehydrogenase. The lack of activity for SalM with the pentoses L-arabinose and D-xylose implies that SalM was not likely recruited from previously identified pathways. If SalM did evolve from a pentose oxidation pathway, it would likely be specific to D-ribose. As the enzymes of such a putative pathway have yet to be elucidated, it creates

the potential to use secondary metabolic enzymes, SalM and SalH, as probes for primary metabolic non-phosphorylative ribose oxidation pathways.

2.5: Methods

2.5.1: Chemicals.

All purchased chemicals were of reagent grade from Sigma-Aldrich unless otherwise noted. Isopropyl β-D-1-thiogalactopyranoside (IPTG) was obtained from Denville Scientific, D-erythrose from Alfa Aesar as a 70% w/v syrup, [U-^{13}C]ribose (98% ^{13}C) from Cambridge Isotope Laboratories, and nickle-nitrilotriacetic acid (Ni-NTA) from QIAGEN. The putative SalM substrate and products 5-chloro-5-deoxy-D-ribose (5-ClR),[32] 5-chloro-5-deoxy-D-ribono-γ-lactone (5-ClRL),[33] and 5-chloro-5-deoxy-D-ribonate (5-ClRI)[2] were all synthesized according to literature procedures (Schemes A2.1 and A2.2).

2.5.2: Expression and Purification of Recombinant SalM.

Genomic DNA was obtained from cultures of *Salinispora tropica* CNB-440 as previously described and used as a template for PCR.[4] The 768 bp *salM* gene (Stro_1027) was PCR amplified from genomic DNA using *Pfu* polymerase (Stratagene) with the forward 5'-CGTGGTTCCCATGGCATGACGAA CGGTGGGCGCC-3' and reverse 5'-GCTCGAA TTCAAGCTTTCACTGCGCGAGGTAACCTC-3' primers. The PCR product was digested with NcoI and HindIII (the introduced restriction sites are underlined), ligated into NcoI/HindIII-digested pHIS8,[34] and its sequence verified (Seqxcel). Plasmid preparation and isolation was performed in *Escherichia coli*

DH5$_\alpha$ as previously described.[4] The N-terminal octahistadyl tagged SalM was overexpressed in *E. coli* BL21(DE3). A 10 ml starter culture was grown overnight from a single colony in terrific broth with 50 μg ml^{-1} kanamycin sulfate at 37 °C with shaking and then used to inoculate 1 L of terrific broth media at 28 °C with 50 μg ml^{-1} kanamycin sulfate. Growth was monitored to an optical density of 0.47, and then 0.2 mM IPTG was added to induce protein expression. The culture was grown overnight at 28 °C with shaking.

All protein purification steps took place at 4 °C. Protein purification buffers contained 300 mM NaCl, 50 mM sodium phosphate adjusted to pH 8.0, and increasing concentrations of imidazole. Buffers A (lysis), B (wash), and C (elution) contained 10, 20, and 250 mM imidazole, respectively. Cells were pelleted at 6,300 g for 45 minutes, resuspended in buffer A and lysed with six 30 second bursts of probe sonication with resting periods of 30 seconds. The lysate was centrifuged for 30 minutes at 10,000 g. Soluble protein was collected and purified on a Ni-NTA column by washing with several volumes of buffer B and eluting with 2.5 ml of buffer C. Eluant was desalted using a PD-10 desalting column (GE Life Sciences) and resuspended in 50 mM sodium phosphate buffer adjusted to pH 8.0. Desalted protein was concentrated on a Vivaspin 6 10 kDa membrane centrifuge concentrator (Sartorius Stedim) and then subjected to size exclusion chromatography on a Superdex 200 column (GE Life Sciences) with 100 mM Tris-HCl adjusted to pH 8.0, 500 mM NaCl, and 2 mM dithiothreitol.

2.5.3: Construction of C-terminal Mutants.

SalM C-terminal mutants were PCR amplified from genomic DNA with the forward primer 5’-GCATACCATAGAATTCATGACGAACGGTGGGCGCCTAT-3’ and the following reverse primer for the specified mutant:

-Q255E - 5’-GCTCGAATTCAAGCTTTCACTC CGCGAGGTAACCTC-3’

-Q255N - 5’-ATTGAGAGCTGCGGCCGCTCA GTTCGCGAGGTAACCTCCGTCGA-3’

-Q255S - 5’-ATTGAGAGCTGCGGCCGCTCAG CTCGCGAGGTAACCTCCGTCGA-3’

-Q255V - 5’-ATTGAGAGCTGCGGCCGCTCAC ACCGCGAGGTAACCTCCGTCGA-3’

-Extension 256N - 5’-ATTGAGAGCT GCGGCCGCTCAGTTCTGCGCGAGGTAACCTCCGTCGA-3’

-Q255V/Extension 256Q - 5’-ATTGAGAGCT GCGGCCGCTCACTGCACCGCGAGGTAACCTCCGTCGA-3’

-A254-Q255 deletion - 5’-ATTGAGAGCT GCGGCCGCTCAGAGGTAACCTCCGTCGA-3’

-Q255 deletion - 5’-ATTGAGAGCTGCGGCCG CTCACGCGAGGTAACCTCCGTCGA-3’

With the exception of the Q255E mutant, PCR products were digested with EcoRI and NotI (the introduced restriction sites are underlined), ligated into EcoRI/NotI-digested pHIS8, and sequence verified. The Q255E mutant was constructed as above with HindIII in place of NotI. Proteins were expressed via the autoinduction expression system Overnight Express I (EMD Chemicals) in 1 L Luria broth in 50 μg

ml^{-1} kanamycin sulfate at 28 °C for 24 hours. A wild-type SalM control was concurrently expressed under the same conditions to verify expression and solubility. Protein purification was carried out in a manner analogous to that described for wild-type SalM.

2.5.4: Enzyme Assays.

In vitro enzyme assays were performed in a 96-well half-area microtiter plate. Conversion of NAD^+ to NADH was monitored at a wavelength of 340 nm using a SpectraMax M2 spectrometer (Molecular Devices, Sunnyvale, CA). All microplate assays were performed at 30 °C in 50 μl volume with 100 mM Tris-HCl buffer pH 7.5 unless otherwise noted.

2.5.5: Divalent Cation Analysis.

To identify suitable metal cofactors, SalM was assayed for activity with 0.5 mM 5-ClR, 0.5 mM NAD^+, and 2.4 μg (0.048 mg ml^{-1}) SalM. 2 mM $FeSO_4$, $NiSO_4$, $ZnSO_4$, $CuCl_2$, $CaCl_2$ $MnCl_2$, $MgSO_4$, $MgCl_2$, or no divalent cation was added.

As $MgCl_2$, $CaCl_2$, and $MnCl_2$ were identified as accelerating the SalM catalyzed reaction, an activity vs. concentration assay was performed with cation concentration varying between 1–50 mM. 1 mM 5-ClR, 1 mM NAD^+ and 2.4 μg (0.048 mg ml^{-1}) SalM were used. These assays were performed in triplicate and averaged. The maximum velocity at steady state conditions for each concentration was fitted with a linear line using SigmaPlot 11.0 (Systat Software, Inc., Chicago, Il).

2.5.6: Comparative Substrate Analysis.

Ten sugars were assayed for activity with SalM: D-ribose, 2-deoxy-D-ribose, D-ribose-5-phosphate, 5-chloro-5-deoxy-D-ribose, D-erythrose, D-allose, D-glucose, D-xylose, D-arabinose, and L-arabinose. A final concentration of 2 mM carbohydrate was used for all substrates with excess NAD^+ cofactor at 2.5 mM. SalM (1.6 μg; 0.032 mg ml^{-1}) was added to each 50 μl reaction buffered with 100 mM Tris-HCl pH 8.0 containing 2 mM $MgCl_2$. After enzyme addition, absorbance measurements were recorded every minute for three hours.

2.5.7: Kinetic Assays.

Kinetic data were determined for D-ribose, D-erythrose, and 5-chloro-5-deoxy-D-ribose. All reactions contained 2.4 μg SalM (0.048 mg ml^{-1}), presoaked in 10 mM $MgCl_2$, and 4 mM NAD^+ cofactor. Substrate concentrations vs. initial velocities were plotted in SigmaPlot 11.0 (Systat Software, Inc.) and fit with a non-linear Michaelis-Menten curve. Concentrations of D-ribose ranged from 0.5 mm to 200 mM, representing a range of 0.3 to 10.8 K_m, whereas concentrations of D-erythrose ranged from 0.10 mM to 40 mM representing a range of 0.4 to 16 K_m. The K_m for 5-ClR, however, was at the lower limit of detection for NADH absorbance. Therefore, kinetic assays with 5-ClR were repeated on a 100 μl scale to increase the absorbance path length. The concentration of SalM was reduced to 1.2 μg per reaction (0.012 mg ml^{-1}). Concentrations tested for 5-ClR ranged from 10 μM to 10 mM, representing a range of 0.6 to 600 K_m.

2.5.8: Lactone Opening Assay.

A colorimetic assay for the detection of functionalized carboxylic acids was used to monitor the hydrolysis of 5-ClRL to 5-ClRI. 10 mM synthetically prepared 5-ClRL was dissolved in 100 mM Tris-HCl pH 7.5 buffer and 3 ml was aliquoted into two identical tubes. Active or denatured (boiled for 10 minutes) SalM (0.008 mg ml^{-1}), both presoaked with 10 mM $MgCl_2$, was added to the 5-ClRL solution. Two 200 μl aliquots were removed from each tube at regular intervals and subjected to derivatization and colorimetric analysis as previously described.[35] The experiment was repeated with 0.5 mM NAD^+ and 0.5 mM NADH present in the buffer. Absorbance measurements were converted to 5-ClRL concentration by reference to a standard curve generated at the time of the assay. To determine the hydrolysis rate constants, a linear line was fit to the plot of the natural logarithm of lactone concentration vs. time using SigmaPlot 11.0.

2.5.9: NMR Based Assays.

Carbon detected NMR experiments were measured on a Varian VX500 spectrometer equipped with an XSENS Cold Probe. All assays were performed with the sample chamber set at a constant temperature of 30 °C. Carbon-free 60 mM sodium phosphate buffer at pH 7.5 was used instead of Tris-HCl. Final reaction volume was 250 μl in a 3 mm diameter NMR tube. Acetonitrile was added as an internal standard.

2.5.10: Uniformly ^{13}C Labeled Ribose.

A 3 mM solution of [U-^{13}C]ribose, 3.5 mM NAD^+, and 2 mM $MgCl_2$ in 200 μl of 62.5 mM sodium phosphate pH 7.5 buffer with approximately 30% deuterium oxide was placed in the NMR tube. To the reaction, 35 μg SalM was added (in a 50 μl volume of 50 mM sodium phosphate pH 7.5 buffer) for a final enzyme concentration of 0.140

mg ml^{-1}. 1D ^{13}C NMR spectra were measured using 256 scans with a 1 second T_1 relaxation time. A spectrum was taken before enzyme addition, and then following enzyme addition, spectra were recorded every 10–15 minutes for 4 hours. Additional spectra were taken 21 and 72 hours after enzyme addition during which the sample was exposed to ambient temperature.

2.5.11: Unlabeled 5-ClR DEPT NMR Assay.

4 mM of unlabeled 5-ClR, 3.5 mM NAD^+ and 2 mM $MgCl_2$ were dissolved into 200 μl of 62.5 mM pH 7.5 sodium phosphate buffer. To the reaction, 24 μg of SalM was added (in a 50 μl volume of 50 mM sodium phosphate pH 7.5 buffer) for a final enzyme concentration of 0.120 mg ml^{-1}. The final deuterium oxide concentration was approximately 50%. A 2048 scan DEPT135 spectrum with a T_1 of 1 second was recorded before enzyme addition, then repeatedly following enzyme addition for the first four spectra. Each acquisition required approximately 68 minutes. A final spectrum was started eight hours after enzyme addition.

2.6: Acknowledgements

We kindly thank William Fenical and Paul Jensen (Scripps Institution of Oceanography, La Jolla, CA) for *S. tropica* strains, Anthony Mrse (University of California San Diego, La Jolla, CA) for NMR spectroscopy assistance, and Yuan Liu and Xavier Mico Alvarez (Scripps Institution of Oceanography, La Jolla, CA) for assistance with chemical synthesis. This work was supported by the National Institutes of Health (CA127622 to B.S.M.).

Chapter 2, in part, is a reprint of the material as it appears in Characterization of 5-Chloro-5-Deoxy-D-Ribose-1-Dehydrogenase in Chloroethylmalonyl-Coenzyme A Biosynthesis: Substrate and Reaction Profiling (2010). Kale, Andrew J.; McGlinchey, Ryan P; and Moore, Bradley S., Journal of Biological Chemistry, volume 285, 33710-33717. The dissertation author was the primary investigator and author of this paper.

2.7: Appendix

Table A2.1. Optical density at 540 nm after treatment of lactone and inactivated or active SalM solution with hydroxylamine and ferric chloride. Absorbance was measured twice (samples A and B) at each time point for both inactive and active SalM. Absorbances were converted to concentrations in mM from the empirical formula: Concentration = (Absorbance + .02) / 0.1309, calculated by assaying known concentrations of bovine serum albumin.

Inactivated SalM					
Minutes	Sample A	Sample B	Ave. OD	mM	ln (mM)
0	1.3	1.33	1.32	10.20	2.32
20	1.26	1.19	1.23	9.51	2.25
40	1.14	1.08	1.11	8.63	2.16
60	1.04	1.13	1.09	8.44	2.13
90	0.99	0.94	0.97	7.52	2.02
120	0.89	0.85	0.87	6.80	1.92
180	0.74	0.69	0.72	5.61	1.73
Active SalM					
Minutes	Sample A	Sample B	Ave. OD	mM	ln (mM)
0	1.41	1.33	1.37	10.62	2.36
20	1.25	1.15	1.20	9.32	2.23
40	1.18	1.16	1.17	9.09	2.21
60	1.1	1.05	1.08	8.37	2.12
90	0.98	0.92	0.95	7.41	2.00
120	0.92	0.86	0.89	6.95	1.94
180	0.73	0.68	0.71	5.54	1.71

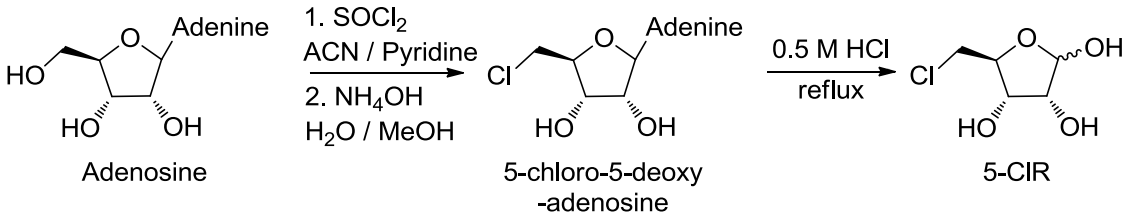

Scheme A2.1. Synthetic route for the SalM substrate 5-chloro-5-deoxyribose (5-ClR).

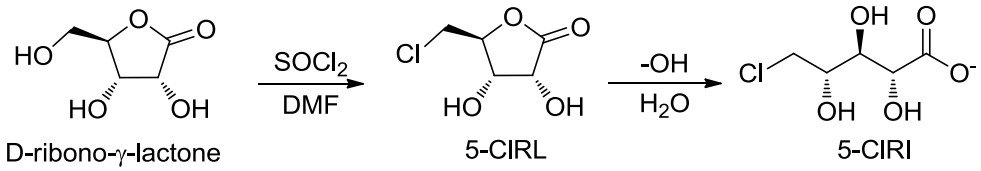

Scheme A2.2. Synthetic routes for potential SalM products 5-chloro-5-deoxyribono-γ-lactone (5-ClRL) and 5-chloro-5-deoxyribonate (5-ClRI).

2.8: References

1. Gulder, T. A. M., and Moore, B. S. (2010) Salinosporamide natural products: potent 20S proteasome inhibitors as promising cancer chemotherapeutics, *Angew. Chem. Int. Ed.* 49, 9346-9367.

2. Eustáquio, A. S., McGlinchey, R. P., Liu, Y., Hazzard, C., Beer, L. L., Florova, G., Alhamadsheh, M. M., Lechner, A., Kale, A. J., Kobayashi, Y., Reynolds, K. A., and Moore, B. S. (2009) Biosynthesis of the salinosporamide A polyketide synthase substrate chloroethylmalonyl-coenzyme A from S-adenosyl-L-methionine, *Proc. Natl. Acad. Sci. U. S. A.* 106, 12295-12300.

3. Huang, F. L., Haydock, S. F., Spiteller, D., Mironenko, T., Li, T. L., O'Hagan, D., Leadlay, P. F., and Spencer, J. B. (2006) The gene cluster for fluorometabolite biosynthesis in Streptomyces cattleya: A thioesterase confers resistance to fluoroacetyl-coenzyme A, *Chem. Biol.* 13, 475-484.

4. Eustáquio, A. S., Pojer, F., Noe, J. P., and Moore, B. S. (2008) Discovery and characterization of a marine bacterial SAM-dependent chlorinase, *Nat. Chem. Biol.* 4, 69-74.

5. Schiwara, H. W., Domschke, W., and Domagk, G. F. (1968) Sugar dehydrogenases from mammalian liver. I. Differentiation of various sugar dehydrogenases from pig liver by disc electrophoresis and ion exchange chromatography, *Hoppe-Seyler's Z. Physiol. Chem.* 349, 1575-1581.

6. Scher, B. M., and Horecker, B. L. (1966) Pentose metabolism in Candida. 3. The triphosphopyridine nucleotide-specific polyol dehydrogenase of *Candida utilis*, *Arch. Biochem. Biophys.* 116, 117-128.

7. Johnsen, U., and Schonheit, P. (2004) Novel xylose dehydrogenase in the halophilic Archaeon *Haloarcula marismortui*, *J. Bacteriol.* 186, 6198-6207.

8. Brouns, S. J. J., Walther, J., Snijders, A. P. L., de Werken, H., Willemen, H., Worm, P., de Vos, M. G. J., Andersson, A., Lundgren, M., Mazon, H. F. M., van den Heuvel, R. H. H., Nilsson, P., Salmon, L., de Vos, W. M., Wright, P. C., Bernander, R., and van der Oost, J. (2006) Identification of the missing links in prokaryotic pentose oxidation pathways - Evidence for enzyme recruitment, *J. Biol. Chem.* 281, 27378-27388.

9. Watanabe, S., Kodak, T., and Makino, K. (2006) Cloning, expression, and characterization of bacterial L-arabinose 1-dehydrogenase involved in an alternative pathway of L-arabinose metabolism, *J. Biol. Chem.* 281, 2612-2623.

10. Bonete, M. J., Pire, C., Llorca, F. I., and Camacho, M. L. (1996) Glucose dehydrogenase from the halophilic Archaeon *Haloferax mediterranei*: enzyme purification, characterisation and N-terminal sequence, *FEBS Lett.* 383, 227-229.

11. Milburn, C. C., Lamble, H. J., Theodossis, A., Bull, S. D., Hough, D. W., Danson, M. J., and Taylor, G. L. (2006) The structural basis of substrate promiscuity in glucose dehydrogenase from the hyperthermophilic archaeon *Sulfolobus solfataricus*, *J. Biol. Chem.* 281, 14796-14804.

12. Stephens, C., Christen, B., Fuchs, T., Sundaram, V., Watanabe, K., and Jenal, U. (2007) Genetic analysis of a novel pathway for D-xylose metabolism in *Caulobacter crescentus*, *J. Bacteriol.* 189, 2181-2185.

13. Kallberg, Y., Oppermann, U., Jornvall, H., and Persson, B. (2002) Short-chain dehydrogenases/reductases (SDRs) - Coenzyme-based functional assignments in completed genomes, *Eur. J. Biochem.* 269, 4409-4417.

14. Kavanagh, K., Jornvall, H., Persson, B., and Oppermann, U. (2008) The SDR superfamily: functional and structural diversity within a family of metabolic and regulatory enzymes, *Cell. Mol. Life Sci.* 65, 3895-3906.

15. Wierenga, R. K., Terpstra, P., and Hol, W. G. J. (1986) Prediction of the occurrence of the Adp-binding βαβ-fold in proteins, using an amino acid sequence fingerprint, *J. Mol. Biol.* 187, 101-107.

16. Graninger, M., Nidetzky, B., Heinrichs, D. E., Whitfield, C., and Messner, P. (1999) Characterization of dTDP-4-dehydrorhamnose 3,5-epimerase and dTDP-4-dehydrorhamnose reductase, required for dTDP-L-rhamnose biosynthesis in *Salmonella enterica* serovar typhimurium LT2, *J. Biol. Chem.* 274, 25069-25077.

17. Blankenfeldt, W., Kerr, I. D., Giraud, M. F., McMiken, H. J., Leonard, G., Whitfield, C., Messner, P., Graninger, M., and Naismith, J. H. (2002) Variation on a theme of SDR: dTDP-6-deoxy-L-lyxo-4-hexulose reductase (RmID) shows a new Mg^{2+}-dependent dimerization mode, *Structure* 10, 773-786.

18. Niefind, K., Muller, J., Riebel, B., Hummel, W., and Schomburg, D. (2003) The crystal structure of R-specific alcohol dehydrogenase from *Lactobacillus brevis* suggests the structural basis of its metal dependency, *J. Mol. Biol.* 327, 317-328.

19. Angyal, S. J., and Pickles, V. A. (1972) Equilibria between pyranoses and furanoses. 2. Aldoses, *Aust. J. Chem.* 25, 1695-1710.

20. Breitmaier, E., and Hollstein, U. (1976) Complete assignment of C-13 NMR-spectrum of muta-rotated D-ribose by integration and specific deuteration, *Org. Magn. Resonance* 8, 573-575.

21. Jacobsen, N. A. (2007) *NMR Spectroscopy Explained*, John Wiley & Sons, Inc., Hoboken, NJ.

22. Jermyn, M. A. (1960) Studies on the glucono-δ–lactonase of *Pseudomonas fluorescens*, *Biochim. Biophys. Acta* 37, 78-92.

23. Eustáquio, A. S., and Moore, B. S. (2008) Mutasynthesis of fluorosalinosporamide, a potent and reversible inhibitor of the proteasome, *Angew. Chem. Int. Ed.* 47, 3936-3938.

24. Baker, P. J., Britton, K. L., Fisher, M., Esclapez, J., Pire, C., Bonete, M. J., Ferrer, J., and Rice, D. W. (2009) Active site dynamics in the zinc-dependent medium chain alcohol dehydrogenase superfamily, *Proc. Natl. Acad. Sci. U. S. A.* 106, 779-784.

25. Angelov, A., Futterer, O., Valerius, O., Braus, G. H., and Liebl, W. (2005) Properties of the recombinant glucose/galactose dehydrogenase from the extreme thermoacidophile, *Picrophilus torridus*, *FEBS J.* 272, 1054-1062.

26. Lamble, H. J., Heyer, N. I., Bull, S. D., Hough, D. W., and Danson, M. J. (2003) Metabolic pathway promiscuity in the Archaeon *Sulfolobus solfataricus* revealed by studies on glucose dehydrogenase and 2-keto-3-deoxygluconate aldolase, *J. Biol. Chem.* 278, 34066-34072.

27. Tanaka, Y., Morikawa, K., Ohki, Y., Yao, M., Tsumoto, K., Watanabe, N., Ohta, T., and Tanaka, I. (2007) Structural and mutational analyses of Drp35 from *Staphylococcus aureus* - A possible mechanism for its lactonase activity, *J. Biol. Chem.* 282, 5770-5780.

28. Mathias, A. L., Rigo, L. U., Funayama, S., and Pedrosa, F. O. (1989) L-arabinose metabolism in *Herbaspirillum seropedicae*, *J. Bacteriol.* 171, 5206-5209.

29. Watanabe, S., Shimada, N., Tajima, K., Kodaki, T., and Makino, K. (2006) Identification and characterization of L-arabonate dehydratase, L-2-keto-3-deoxyarabonate dehydratase, and L-arabinolactonase involved in an alternative pathway of L-arabinose metabolism - novel evolutionary insight into sugar metabolism, *J. Biol. Chem.* 281, 33521-33536.

30. Udwary, D. W., Zeigler, L., Asolkar, R. N., Singan, V., Lapidus, A., Fenical, W., Jensen, P. R., and Moore, B. S. (2007) Genome sequencing reveals complex

secondary metabolome in the marine actinomycete *Salinispora tropica*, *Proc. Natl. Acad. Sci. U. S. A.* 104, 10376-10381.

31. Penn, K., Jenkins, C., Nett, M., Udwary, D. W., Gontang, E. A., McGlinchey, R. P., Foster, B., Lapidus, A., Podell, S., Allen, E. E., Moore, B. S., and Jensen, P. R. (2009) Genomic islands link secondary metabolism to functional adaptation in marine Actinobacteria, *ISME Journal* 3, 1193-1203.

32. Suzuki, Y. (1974) Hydrolysis of several purine nucleosides with strong hydrochloric acid or cation exchange resin, *Bull. Chem. Soc. Jpn.* 47, 2077-2078.

33. Bouchez, V., Stasik, I., Beaupere, D., and Uzan, R. (1997) Regioselective halogenation of pentono-1,4-lactones. Efficient synthesis of 5-chloro- and 5-bromo-5-deoxy derivatives, *Carb. Res.* 300, 139-142.

34. Jez, J. M., Ferrer, J. L., Bowman, M. E., Dixon, R. A., and Noel, J. P. (2000) Dissection of malonyl-coenzyme A decarboxylation from polyketide formation in the reaction mechanism of a plant polyketide synthase, *Biochemistry* 39, 890-902.

35. Hestrin, S. (1949) The reaction of acetylcholine and other carboxylic acid derivatives with hydroxylamine, and its analytical application, *J. Biol. Chem.* 180, 249-261.

Chapter 3:

Bacterial Self-Resistance to the Natural Proteasome Inhibitor Salinosporamide A

3.1: Abstract

Proteasome inhibitors have recently emerged as a therapeutic strategy in cancer chemotherapy but susceptibility to drug resistance limits their efficacy. The marine actinobacterium *Salinispora tropica* produces salinosporamide A (NPI-0052, marizomib), a potent proteasome inhibitor and promising clinical agent in the treatment of multiple myeloma. Actinobacteria also possess 20S proteasome machinery, raising the question of self-resistance. We identified a redundant proteasome β-subunit, SalI, encoded within the salinosporamide biosynthetic gene cluster and biochemically characterized the SalI proteasome complex. The SalI β-subunit has an altered substrate specificity profile, 30-fold resistance to salinosporamide A, and cross-resistance to the FDA-approved proteasome inhibitor bortezomib. An A49V mutation in SalI correlates to clinical bortezomib resistance from a human proteasome β5-subunit A49T mutation, suggesting that self-resistance to natural proteasome inhibitors may predict clinical outcomes.

3.2: Introduction

The 26S proteasome is a macromolecular enzymatic complex responsible for the regulated hydrolysis of cellular proteins that in turn mediates processes such as amino acid recycling, cell cycle control, cell differentiation, and apoptosis.[1] Ubiquitinated proteins are targeted by the 19S regulatory cap and transferred into the interior of the cylindrical 20S proteasome core particle for degradation by catalytic β-subunits having nucleophilic N-terminal threonine residues.[1] Eukaryotes harbor a two-fold symmetrical

$\alpha_{(1–7)}\beta_{(1–7)}\beta_{(1–7)}\alpha_{(1–7)}$ barrel-shaped 20S structure with three active β-subunits (β1, caspase-like (C-L); β2, trypsin-like (T-L); and β5, chymotrypsin-like (CT-L)) that display distinct proteolytic specificities.[2] Their catalytic inhibition with mechanism-based small molecules has exposed the proteasome as an important therapeutic target in cancer and inflammation.[3] Recently the dipeptide boronic acid bortezomib (**1**, Figure 3.1) was approved by the FDA for the treatment of relapsed multiple myeloma and mantle cell lymphoma as a first in class proteasome inhibitor (PI) that functions as a reversible inhibitor of the β5-subunit.[4,5] Acquired resistance to bortezomib, however, has already emerged and limits its pronounced clinical benefit that in part is due to point mutations in the proteasome β5-subunit.[6-9]

Salinosporamide A (**2**), a potent PI naturally synthesized by the marine bacterium *Salinispora tropica*, represents an alternative treatment option due to its distinct chemical structure and mechanism of action.[10] Its biosynthesis in an actinobacterium, which is unique amongst bacterial divisions to maintain a 20S proteasome,[1] with a simplified $\alpha_7\beta_7\beta_7\alpha_7$ structure, raises the question of the molecular basis behind natural proteasome resistance and whether this mechanism correlates to clinical drug resistance. Unlike the eukaryotic 26S proteasome which is essential for survival,[11] the 20S proteasome has been inactivated in several actinobacteria without loss of viability.[12,13] *Mycobacterium tuberculosis* is a notable exception that requires the proteasome for pathogenicity in response to host induced oxidative stress.[14] The recent discovery of the prokaryotic ubiquitin-like protein (PUP) has established that the actinobacterial proteasome regulates the controlled destruction of targeted proteins.[15-18]

Elucidating the specific proteins and pathways regulated by the 20S proteasome in actinobacteria remains an active area of investigation.

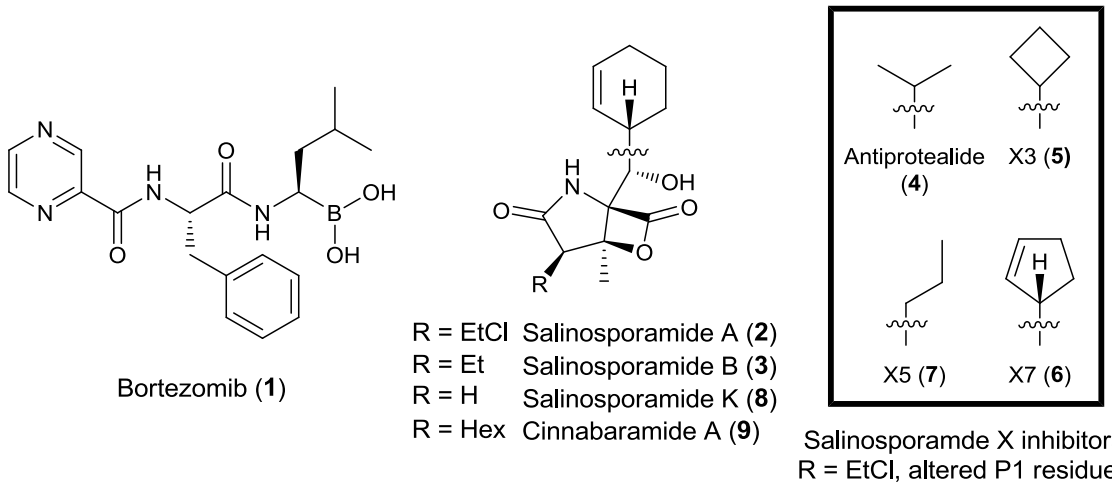

Figure 3.1. Chemical structures of small molecule proteasome inhibitors discussed in Chapter 3. The respective P1 residues (Leu in bortezomib; cyclohexenyl in salinosporamides A, B, K, and cinnabaramide A; and the boxed residues in the salinosporamide X series) interact with the S1 specificity pocket of the proteasome β-subunit upon binding. The displaceable chloride of salinosporamide A confers irreversible inhibition.

Salinosporamide A belongs to a growing family of potent natural PIs that also includes the actinomycete natural products lactacystin, cinnabaramide A, epoxomicin, and belactosin A.[10,19] However, despite the many examples of natural product PIs being produced by microbes that must maintain their own functional proteasomes, the biochemical basis for natural resistance has not been defined. We describe here the identification and characterization of a 20S proteasome target modification resistance mechanism to salinosporamide A in the producing organism *S. tropica.*

3.3: Results and Discussion

3.3.1: Identification of a Transcriptionally Active 20S Proteasome β-subunit in the Salinosporamide Biosynthetic Gene Cluster.

We recently sequenced the complete genome of *S. tropica* CNB-440 and functionally characterized the salinosporamide A gene locus.[20,21] Curiously, towards one end of the 41-kb *sal* gene cluster resides the gene *salI* (Strop_1015) encoding a proteasome β-subunit (Figure 3.2). Its physical location in a biosynthetic operon associated with a PI strongly suggested its involvement in resistance through target modification, a strategy more commonly associated with antibiotic resistance.[22] Further genomic analysis of *S. tropica* CNB-440 identified a typical actinobacterial 20S proteasome gene cluster (Strop_2241–2247) that includes adjacent genes encoding α and β proteasome subunits (Figure 3.2). We reasoned that the SalI β-subunit would additionally complex with the lone α-subunit during the biosynthesis of salinosporamide A to render a functional 20S proteasome with greater tolerance to the PI. To this end, we analyzed mRNA transcripts of *Strop_2245* (α-subunit), *Strop_2244* (β-subunit, referred henceforth as β_1), *salI*, and the salinosporamide biosynthesis gene *salL* as a reference to correlate SalI to inhibitor production. We observed active transcription of *salI* in parallel to the proteasome α and β subunits and *salL* (Figure 3.3), suggesting that SalI has the potential to form an active proteasome complex during salinosporamide A biosynthesis.

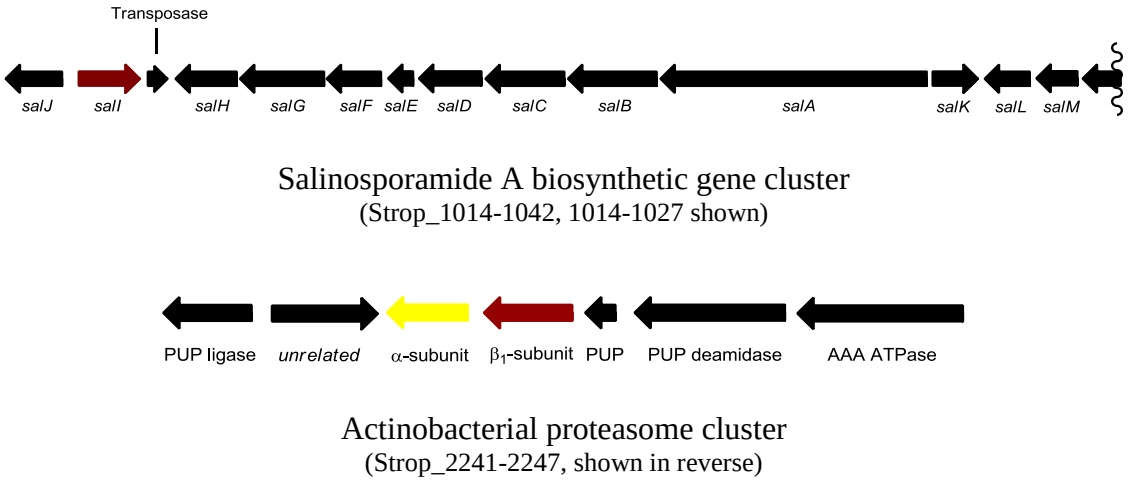

Figure 3.2. Loci of the proteasome β-subunit encoding genes of *S. tropica* CNB-440. Annotated β-subunits (red) are located both within the salinosporamide (SalI) and actinobacterial 20S proteasome (β_1) gene clusters.

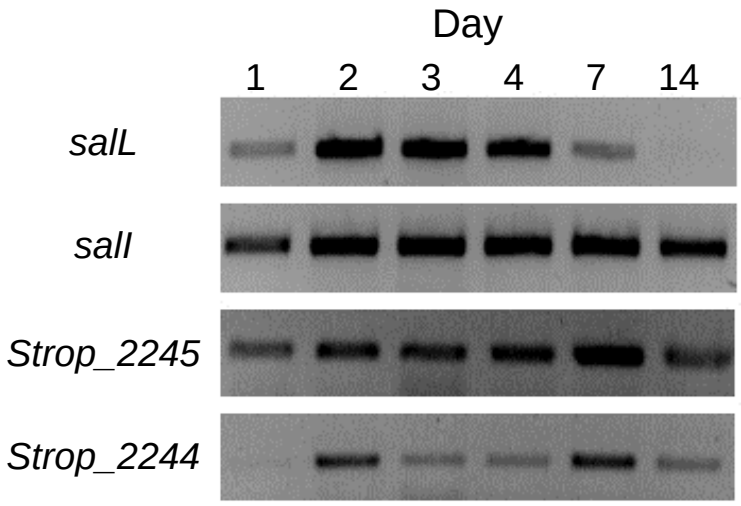

Figure 3.3. Proteasome transcriptional analysis in *S. tropica*. mRNA was isolated at multiple time points and transcripts of *salI*, *Strop_2245* (α-subunit), *Strop_2244* (β_1-subunit), and the salinosporamide chlorinase *salL* are shown. The *salI* gene is actively transcribed at all time points that salinosporamide A is being produced, as indicated by transcription of *salL*. Concurrent transcription of the α-subunit indicates that the α/SalI complex may form *in vivo* with salinosporamide production.

3.3.2: *In Vitro* Characterization of *S. tropica* Proteasome Complexes.

To generate homogeneous proteasome complexes for *in vitro* analysis, we heterologously expressed proteasome subunits in *Escherichia coli*, which lacks an endogenous 20S proteasome. Individually expressed β_1 and SalI remained insoluble until complexed with the α-subunit, suggesting a mutual dependence for correct folding. Coexpression of the readily soluble α-subunit as an N-terminal His_6-tagged protein (29.1 kDa) with untagged β_1 or SalI (23.4 and 24.6 kDa, respectively, after prosequence removal) and purification of the respective complexes by Ni^{2+} affinity chromatography and size-exclusion chromatography gave protein bands in excess of 669 kDa (Figure 3.4), which was consistent with fully assembled $\alpha_7(\beta_1)_7(\beta_1)_7\alpha_7$ (ca. 735 kDa) and $\alpha_7SalI_7SalI_7\alpha_7$ (ca. 752 kDa) proteasome complexes. Proteolytic activity of these bands was verified by the application of a fluorogenic peptide-7-amino-4-methylcoumarin (amc) substrate directly to the gel (Figure 3.4). We next explored the respective hydrolytic activities and substrate specificities of the purified proteasome complexes using an array of peptide-amc substrates (Table 3.1). The α/β_1 complex was most active against the T-L substrate Ac-RLR-amc with further activity against the CT-L substrate Suc-LLVY-amc and the general substrate Z-VKM-amc. For the α/SalI complex, T-L activity was abolished while that of CT-L was highly reduced. Instead, the α/SalI complex was 6-fold more active against Z-VKM-amc than with CT-L substrate Suc-LLVY-amc, which is often preferred by other actinobacterial proteasomes.[23-26] We thus observed a markedly different substrate specificity between

the two complexes in which the α/SalI complex was approximately 5-fold less active than the α/β_1 complex with the substrates evaluated.

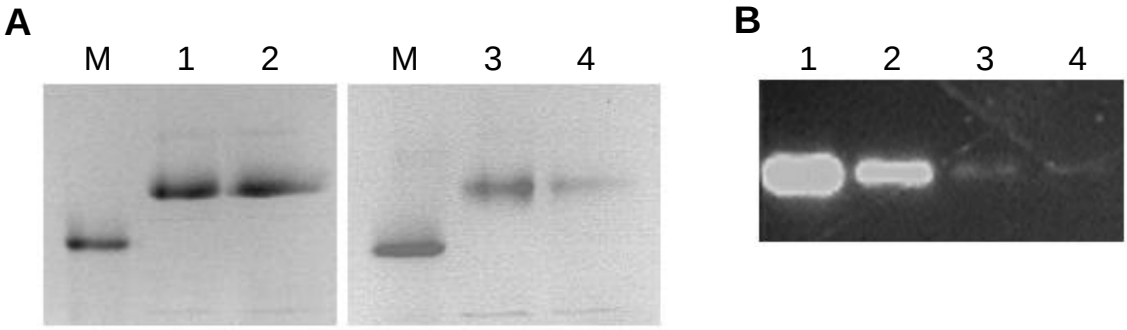

Figure 3.4. Native gel analysis of proteasome assembly and activity. (A) Native PAGE analysis of the assembled proteasome complexes. Lanes: M, Thyroglobulin (669 kDa); 1, α/β_1; 2, α/β_1 pre-incubated with 75 μM salinosporamide A; 3, α/SalI; and 4, α/SalI pre-incubated with 75 μM salinosporamide A. Major bands above the 669 kDa marker correspond to fully assembled proteasome. (B) Fully assembled proteasome bands, based on migration of and with the same lane assignments as in (A), were visualized in overlay assays using the fluorogenic substrate Suc-LLVY-amc.

Table 3.1. Hydrolysis rates of *S. tropica* proteasome complexes for all active substrates. No activity was observed with substrates Z-LLL-amc, MeOSuc-AAPV-amc, Z-LLE-amc, and Suc-APA-amc. Data shown is the mean ± standard deviation, N = 3.
Both α/β_1 A49V and α/β_1 M45F/A49V displayed detectable activity toward substrate Z-VKM-amc. However, these complexes were recovered in low yield and were prone to aggregation upon purification, therefore hydrolytic rates were not determined (ND).

Proteasome Complex	Hydrolysis rate (nmol hr^{-1} mg^{-1})		
	Suc-LLVY-amc	Ac-RLR-amc	Z-VKM-amc
α/β_1	56.0 ± 1.3	93.8 ± 5.0	51.6 ± 2.7
α/β_1 M45F	46.9 ± 10.7	89.4 ± 6.6	53.8 ± 1.9
α/β_1 A49V	Inactive	Inactive	ND
α/β_1 M45F/A49V	Inactive	Inactive	ND
α/SalI	3.4 ± 0.2	Inactive	19.4 ± 0.6
α/SalI F45M	33.1 ± 2.5	Inactive	78.4 ± 0.3
α/SalI V49A	Inactive	Inactive	Inactive
α/SalI F45M/V49A	Inactive	Inactive	Inactive

We next interrogated the α/β_1 and α/SalI complexes against salinosporamide A inhibition to explore their relevant tolerance. As hypothesized, we observed a 16–30 fold increase in IC_{50} with the α/SalI complex in comparison to the α/β_1 complex (Table 3.2). Both proteasome complexes exhibited time-dependent inhibition by salinosporamide A (Figure 3.5) and no recovery of proteolytic activity was observed after buffer exchange to remove salinosporamide A. The resistance of the α/SalI complex to inhibition was conserved with the reversibly-inhibiting deschloro analog salinosporamide B (**3**)[27] and the structurally distinct bortezomib, showing 7 and 13 fold increases in IC_{50} values, respectively (Table 3.3). The resistance to both salinosporamide A and bortezomib, combined with the marked shift in proteolytic specificities, indicated that β_1 and SalI have significant differences in substrate binding pocket dynamics.

Table 3.2. Salinosporamide A inhibition (IC_{50}) values for all wild-type and mutant complexes. Substrate represents amino acid residues preceding fluorescent amc tag (ex. LLVY = Suc-LLVY-amc). Data shown is the mean ± standard deviation, N = 3.

Proteasome complex	Substrate	IC_{50} (μM) salinosporamide A
α/β1	LLVY	3.1 ± 0.2
	RLR	1.7 ± 0.8
	VKM	1.2 ± 0.1
α/β1 M45F	VKM	1.2 ± 0.1
α/β1 A49V	VKM	13.6 ± 2.2
α/β1 M45F/A49V	VKM	15.3 ± 2.2
α/SalI	LLVY	52.0 ± 3.5
	RLR	Inactive
	VKM	36.8 ± 2.4
α/SalI F45M	VKM	45.5 ± 2.3
α/SalI V49A	VKM	Inactive
α/SalI F45M/V49A	VKM	Inactive

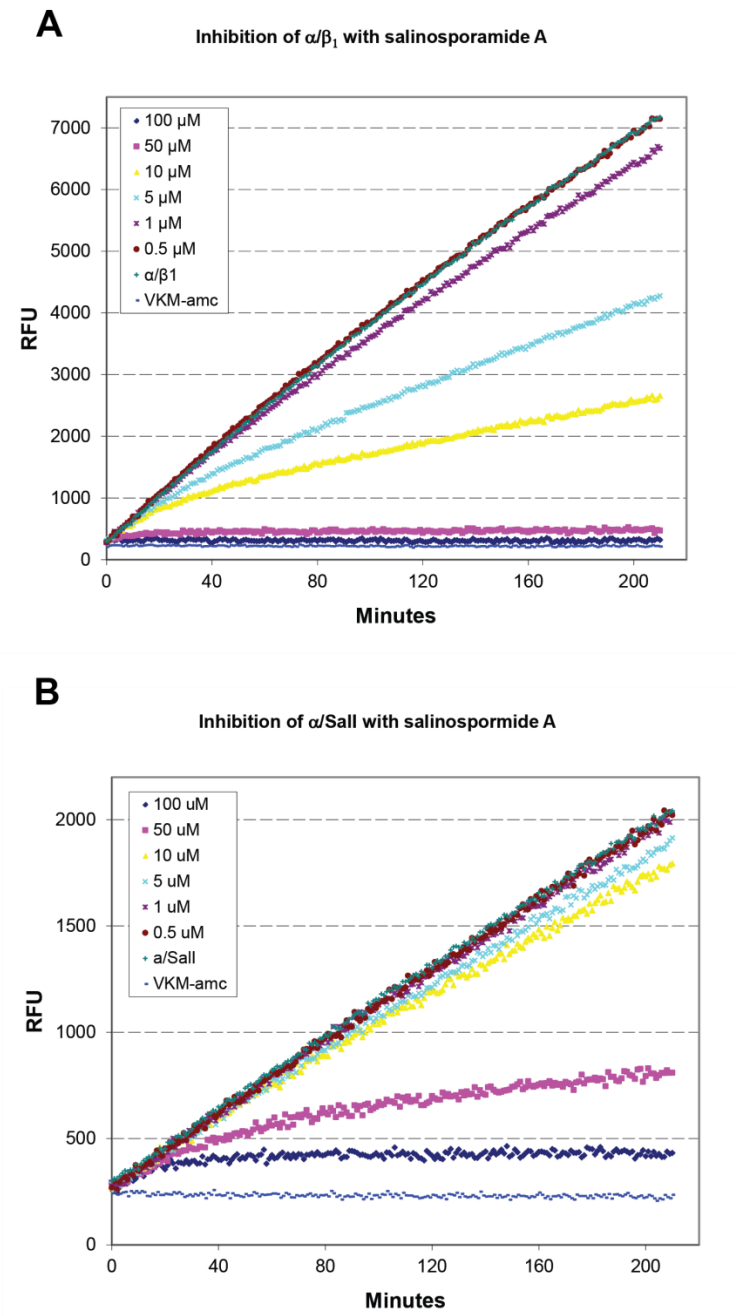

Figure 3.5. Time-dependence of salinosporamide A inhibition on the (A) α/β_1 and (B) α/SalI complexes. Various concentrations of salinosporamide A were premixed with fluorogenic Z-VKM-amc substrate. Proteasome complex was then added at 20 μg ml^{-1} and substrate hydrolysis was measured once per minute. RFU = Relative fluorescence units. Salinosporamide A is spontaneously hydrolyzed in aqueous buffer with an estimated half-life of 20–30 minutes at pH 8.0.[28]

Table 3.3. Inhibition (IC_{50}) values of wild-type α/β_1 and α/SalI proteasome complexes with various proteasome inhibitors. All assays were performed using the Z-VKM-amc substrate. Inhibitor insolubility prevented accurate IC_{50} determination at concentrations exceeding 250 μM. Data shown is the mean ± standard deviation, N = 3.

Inhibitor	α/β_1 IC_{50} (μM)	α/SalI IC_{50} (μM)
Salinosporamide A	1.2 ± 0.1	36.8 ± 2.4
Salinosporamide B	19.2 ± 3.5	138.7 ± 27.3
Bortezomib	3.3 ± 0.2	42.7 ± 3.4
Antiprotealide	103.6 ± 7.2	>250
Salinosporamide X3	>250	>250
Salinosporamide X5	>250	>250
Salinosporamide X7	3.6 ± 0.2	>250

3.3.3: Probing Proteasome Binding Pocket Residues with Mutational Analysis.

To gain insight into the molecular basis governing SalI's PI resistance, we scrutinized its amino acid residues lining the conserved S1 and S2 pockets since the compact nature of salinosporamide restricts its proteasome binding interactions to these sites. Crystallographic analysis of salinosporamide A bound to the β5-subunit of the *Saccharomyces cerevisiae* proteasome (PDB: 2FAK) previously revealed beneficial hydrophobic interactions between its cyclohexenyl side chain and several residues of the S1 binding pocket, most notably Met45, yet minimal contact with the S2 pocket.[27] Alignment of β_1, SalI, β5 from *S. cerevisiae* and *Homo sapiens,* and previously characterized actinobacterial proteasome β-subunits revealed that SalI possesses unique Phe45 and Val49 residues, both located within the S1 binding pocket (Figure 3.6). Position 45 forms the base of the S1 binding pocket and is known to confer CT-L, T-L, or C-L preference to the eukaryotic β-subunits, while position 49 resides at the entrance of the pocket (Figure 3.7).[2] We thus targeted both positions by site-directed mutagenesis

and generated mutants in which we exchanged their residues in order to investigate substrate specificity and salinosporamide resistance in both *S. tropica* β-subunits, β_1 and SalI.

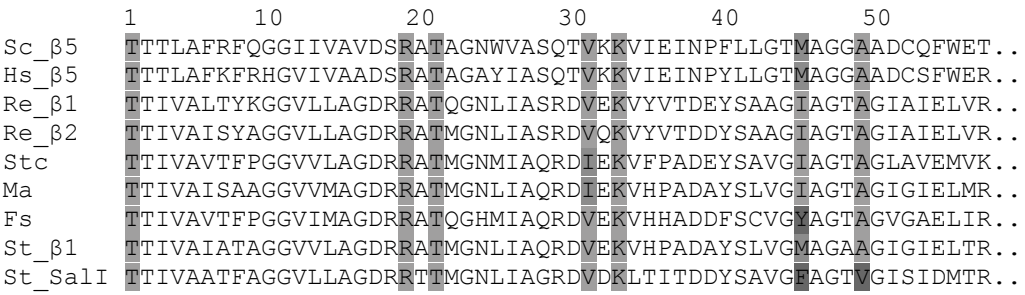

Figure 3.6. Comparison of actinobacterial and eukaryotic β-subunit S1 binding pocket residues. A partial sequence alignment of characterized actinomycete β-subunits and the CT-L β5-subunits of *Saccharomyces cerevisiae* (Sc) and *Homo sapiens* (Hs) is shown from Thr1 to position 57. The actinobacterial β-subunits of *Rhodococcus erythropolis* PR4 (Re), *Streptomyces coelicolor* A3(2) (Stc), *Micromonospora aurantiaca* ATCC 27029 (Ma), *Frankia* sp. ACN14a (Fs), and *Salinispora tropica* CNB-440 (St) are displayed. Residues previously shown to interact with salinosporamide A during binding to the β5-subunit of *S. cerevisiae* are highlighted. Darker shades of gray indicate deviation from the consensus sequence. A full alignment is shown in the appendix (Figure A3.1).

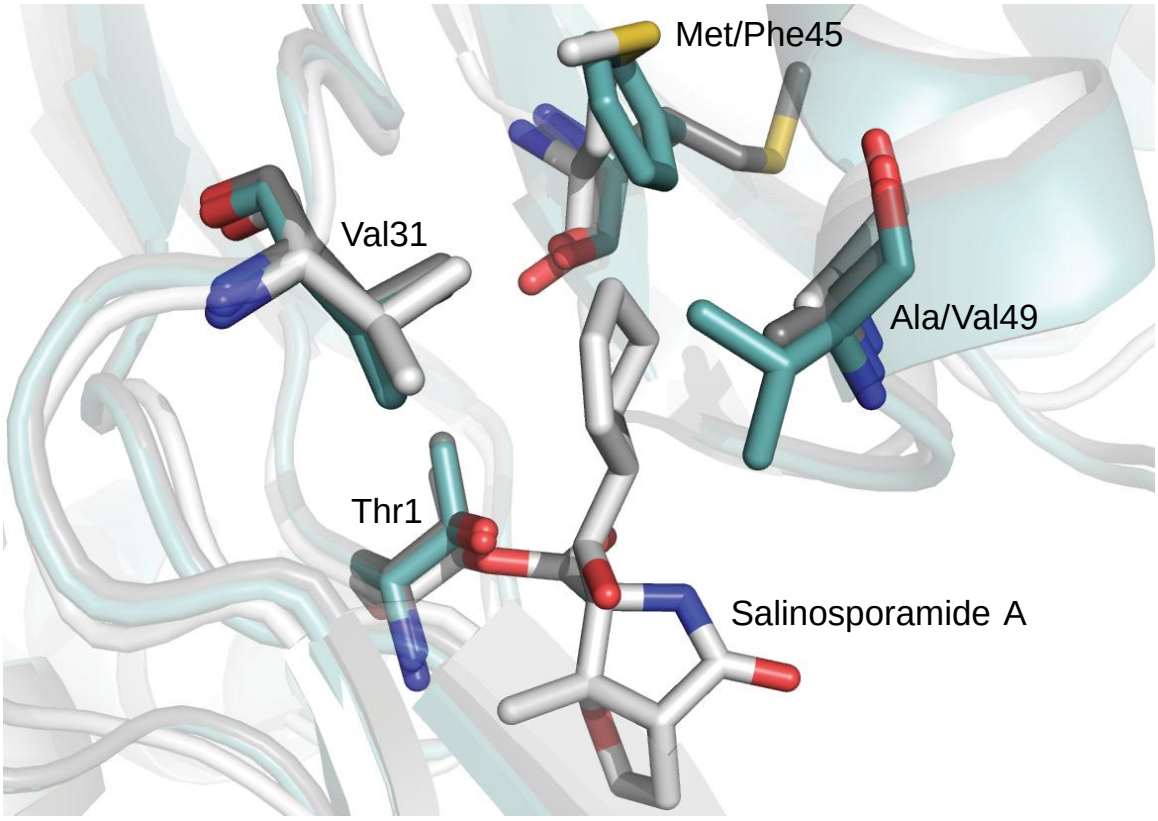

Figure 3.7. A structural depiction of salinosporamide A bound to the 20S proteasome. Residues forming the S1 binding pocket are shown. The *Saccharomyces cerevisiae* β5-subunit with salinosporamide A bound (white, PDB 2FAK chain K) is overlayed with β_1 (gray) and SalI (blue) of *S. tropica*, both homology modeled against the prokaryotic proteasome β-subunit of *Rhodococcus erythropolis* (PDB 1Q5Q chain H). The substitution of Phe45 and Val49 in SalI were predicted to alter substrate and inhibitor binding and therefore targeted for mutagenesis.

Mutagenesis of the β_1 Met45 residue, which is conserved in the *S. cerevisiae* and human β5-subunits where it contributes to their CT-L activities, to Phe as in SalI resulted in the α/β_1 M45F mutant that maintained its native proteolytic activity (Table 3.1) and sensitivity to salinosporamide A (Table 3.2). Conversely, the α/SalI F45M mutant had significantly greater hydrolytic activity for its substrates Suc-LLVY-amc and Z-VKM-amc at ~10 and 4 times, respectively, its native activity (Table 3.1). This

mutant did not engender new activity against the five previously tested inactive substrates, revealing that substrate specificity was not altered as originally envisaged, just its catalytic efficiency. Further, α/SalI F45M was slightly more resistant to salinosporamide A than the native α/SalI complex (Table 3.2), indicating that position 45 is not a major determinant in salinosporamide A resistance.

We rather hypothesized that position 49 contributes to salinosporamide resistance as the substitution of the larger Val residue in SalI for the conserved Ala residue that typifies β-subunits would constrict the S1 binding pocket and hinder inhibitor binding. An A49V mutation was previously identified in the *S. cerevisiae* β5-subunit that resulted in a shift of substrate specificity away from CT-L activity.[29] As extensively discussed in Chapter 1, similar A49V and A49T acquired mutations in human monocytic/macrophage, multiple myeloma, and lymphoblastic Jurkat T cell lines were recently shown to confer resistance to bortezomib and cross-resistance to other peptide-based PIs.[7-9] We thus first generated the α/β_1 A49V mutant. This mutant lost most of its hydrolytic activity while maintaining Z-VKM-amc activity, albeit at reduced levels (Table 3.1). When incubated with salinosporamide A, we observed greater than a ten-fold increase in its IC_{50} (Table 3.2). Unfortunately, our attempts to further correlate the role of Val49 in salinosporamide resistance with α/SalI V49A were unsuccessful since this mutant complex lost its hydrolytic activity. Denaturing PAGE revealed a 2–3 kDa increase in the SalI subunits containing the V49A mutation, indicating activity was lost due to improper prosequence cleavage (Figure 3.8). The α/β_1 M45F/A49V and α/SalI F45M/V49A double mutants behaved similarly to the

respective position 49 single mutants, indicating that this residue is significantly more influential to S1 binding pocket dynamics in both complexes.

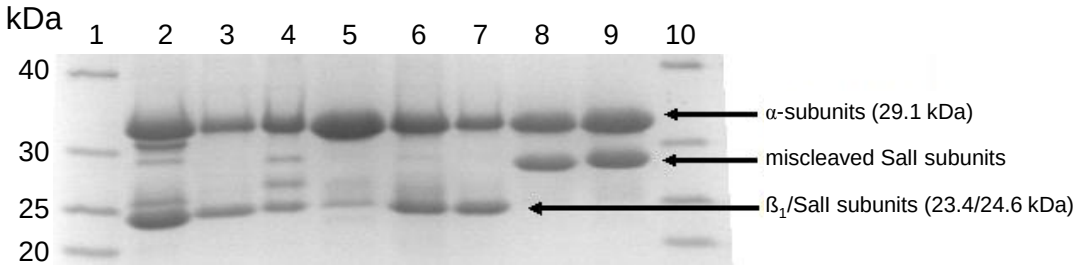

Figure 3.8. Denaturing 16% SDS PAGE analysis of the proteasome complexes. Lanes: 1,10, NativeMark™ ladder; 2, α/β_1; 3, α/β_1 M45F; 4, α/β_1 A49V; 5, α/β_1 M45F/A49V; 6, α/SalI; 7, α/SalI F45M; 8, α/SalI V49A; and 9, α/SalI F45M/V49A. The increased size of SalI in lanes 8 and 9 indicate improper prosequence cleavage due to the V49A mutation.

The mechanism of self-resistance to endogenously produced salinosporamide A in *S. tropica* appears to have independently evolved in human cancer cell lines with prolonged exposure to the drug. Intriguingly, acquired human resistance to a natural anticancer agent that mirrors the evolved natural resistance strategy was also recently described for the topoisomerase I inhibitor camptothecin. In this case, the camptothecin-containing medicinal plant carries a point mutation in the encoding topoisomerase I gene that is identical to one found in resistant human cell lines.[30] However, there is a subtle difference in the salinosporamide and camptothecin resistance examples since camptothecin is produced by an endophytic fungus associated with the plant,[31] and thus genes for biosynthesis and resistance are rather decoupled between the producer and the resistant host.

3.3.4: Targeting SalI for Inhibition with Modified P1 Residues.

Mutational analysis revealed the SalI A49V mutation to be the primary driver of salinosporamide A resistance. The observed cross-resistance to bortezomib, bearing a P1 leucine residue, and decreased activity with the CT-L substrate suggested that Val49 diminishes the potent inhibition of salinosporamide A via S1 binding pocket constriction. To probe this premise, we further interrogated the *S. tropica* 20S proteasome complexes with salinosporamide derivatives bearing modified C-5 residues corresponding to the P1 site. We thus assayed four salinosporamide X derivatives previously generated by mutasynthesis[32] in which the cyclohexenyl ring of salinosporamide A was replaced with smaller (antiprotealide (**4**), salinosporamides X3 (**5**) and X7 (**6**)) or more flexible (salinosporamide X5 (**7**)) aliphatic P1 residues. In each case, we measured a loss in proteasome inhibition in relation to salinosporamide A (Table 3.3), suggesting a more complicated picture in inhibitor binding and S1 pocket dynamics.

3.3.5: Survey of Secondary Proteasomal β-subunits in Actinomycetes.

Having validated the relationship between the endogenous *S. tropica* PI salinosporamide A and the resistance proteasome β-subunit SalI, we next probed other actinobacterial genomes for similar associations in order to query whether this is a common phenomenon for PI biosynthesis. Since salinosporamide A is structurally related to the PIs salinosporamide K (**8**) from "*Salinispora pacifica*" strain CNT-133A[33] and the cinnabaramides (**9**) from *Streptomyces* sp. JS360,[34] we first probed their biosynthetic loci. We cloned and partially sequenced the cinnabaramide biosynthetic

gene cluster and identified an associated *salI* homolog (46% sequence identity) whose product has the resistance Phe45/Val49 sequence signature (Table 3.4). The complete cinnabaramide biosynthetic cluster, including this 20S proteasome β-subunit (CinJ), was independently published.[35] As in the case with *S. tropica*, *S.* sp. JS360 also harbors a primary 20S proteasome gene cluster that includes a β-subunit containing residues Ile45 and Ala49, which is consistent with previously characterized actinobacterial β-subunits.[23-26] Sequence analysis of the recently sequenced "*S. pacifica*" salinosporamide K biosynthetic gene cluster, on the other hand, did not reveal an associated proteasome β-subunit, which may correlate with salinosporamide K's lower biosynthetic titer and diminished inhibitory activity.[33]

BLAST analysis of the *S. tropica* β_1-subunit against all available actinobacterial genomes uncovered several organisms with dual proteasome β-subunits. Comparison of the primary and secondary proteasome β-subunits of *Streptomyces avermitilis* MA-4680, *Thermomonospora curvata* DSM 43183, and *Streptomyces bingchenggensis* BCW-1 showed that Ala49 is switched to either Val or Leu in one of the two subunits (Table 3.4). In two cases, Val49 occurs in the freestanding secondary β-subunit, as is the case with *S. tropica*, while the primary β-subunit of *S. bingchenggensis* contains Leu49. Further sequence analysis of the gene neighborhoods of the secondary proteasome β-subunits revealed in the case of *S. bingchenggensis* a hybrid NRPS/PKS biosynthetic gene cluster (accession: ADI05330/locus tag: SBI_02209 and ADI05329/SBI_02208) located immediately adjacent to its secondary β-subunit (Figure 3.9). This gene cluster is predicted to encode the biosynthesis of a tripeptide natural

product with a modified C-terminal acetate extension (Figure 3.10). As many synthetic and natural PIs are short peptides with an electrophilic modification at the C-terminus,[19] we anticipate that this cluster encodes an orphan PI with a novel peptidic structure. This clear association of a secondary proteasome β-subunit with a natural product biosynthetic gene cluster may signal a new experimental paradigm for the discovery of natural PIs.

Table 3.4. Sequence comparison of secondary β-subunits in Actinomycetes. The two previously characterized β-subunits of *R. erythropolis* were omitted as both associate with α-subunits.[25] The full sequence alignment is provided in the appendix (Figure A3.1). The designation of 1º is based on β-subunit association with a proteasomal gene cluster containing an α-subunit and accessory proteins, whereas 2º β-subunits are found without other proteasomal encoding genes and often cluster with natural product biosynthesis genes. The % identity is calculated relative to SalI without the prosequence. E-values are relative to *S. tropica* β_1 without prosequence.

Organism	β-subunit	Accession	Motif 45–49	% identity	E-value
Salinispora tropica CNB-440	1°, β_1	YP_001159072	MAGAA	58	NA
	2°, SalI	YP_001157868	FAGTV	100	6.0E-68
Streptomyces sp. JS360	1°	JF970179	IAGTA	52	5.0E-75
	2°, CinJ	JF970180	FAGSV	46	3.0E-71
Streptomyces avermitilis MA-4680	1°	NP_827857	IAGTA	53	7.0E-77
	2°	NP_823988	FAGTV	51	6.0E-66
Thermomonospora curvata DSM 43183	1°	YP_003299915	IAGTA	56	2.0E-76
	2°	YP_003300043	MAGTV	50	3.0E-61
Streptomyces bingchenggensis BCW-1	1°	ADI11600	IAGTL	52	9.0E-75
	2°	ADI05332	IAGTA	52	9.0E-65

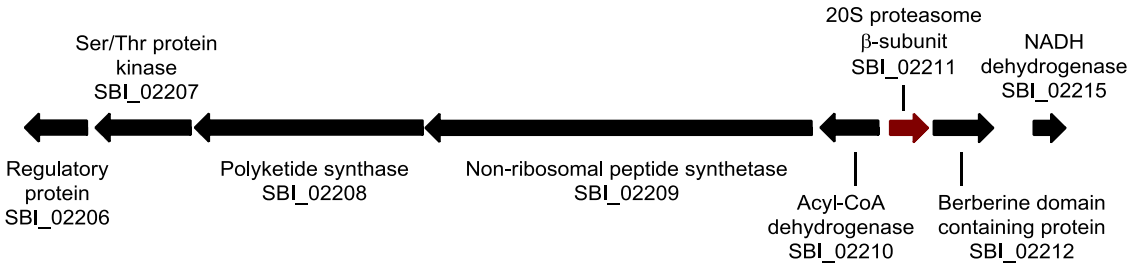

Figure 3.9. Gene neighborhood of the secondary 20S proteasome β-subunit of *Streptomyces bingchenggensis* BCW-1. The predicted proteasome β-subunit (Accession: ADI05332, shown in red) is immediately adjacent to a putative NRPS/PKS biosynthetic cluster. A 27.5 kb region which includes possible tailoring enzymes of this natural product is shown. A larger listing of genes flanking SBI_02211 is found in the appendix (Table A3.1).

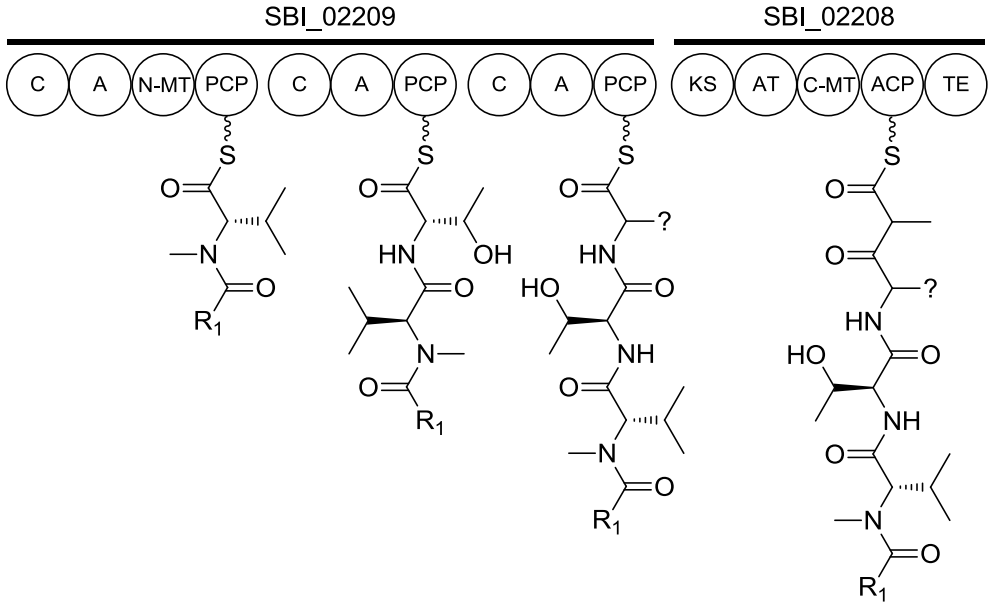

Figure 3.10. Predicted domain architecture of the NRPS/PKS encoding enzymes SBI_02208 and SBI_02209. The three adenylation domains of SBI_02209 were predicted to load valine, threonine, and a non-proteinogenic amino acid (?), respectively. The first, N-terminal C-domain is predicted to attach a fatty acyl or aromatic acyl group (R_1). The AT domain of SBI_02208 was predicted to load a malonyl-CoA extender unit.

The N-terminal C-domain of SBI_02209 suggests that the encoded tripeptide is primed with a non-proteinogenic acyl starter. A bioinformatics analysis of the amino acid sequence of this C-domain using the online NaPDoS (Natural Product Domain Seeker) tool revealed that it clades with other "starter" C-domains (Figure 3.11).[36] Natural products with "starter" C-domains typically initiate biosynthesis with a β-hydroylated fatty acyl unit or an acyl aromatic unit.[37] This C-domain clades most closely to that of bacillibactin biosynthesis from several species of *Bacillus*, which incorporates a 2,3-dihydroxybenzoate acyl group. This type of N-terminal modification supports our hypothesis of a cryptic PI gene cluster as the recently described PIs carmaphycin A/B and fellutamide B incorporate a fatty acyl chain, while synthetic PIs such as bortezomib, MLN2338, and CEP-18770 employ aromatic acyl extensions (see Figure 1.4 for structures).

The three adenylation domains of SBI_02209 were predicted to load valine (E-value = 0.100, as compared to tyrocidine, surfactin, lichenysin, and gramicidin), threonine (E-value = 0.006, as compared to coelichelin, pyoverdin, and fengycin) and a non-ribosomal amino acid of unknown structure using the "PKS/NRPS Analysis Web-site".[38] The AT domain of SBI_02208 was predicted to load a malonyl-CoA extender unit using the online antiSMASH tool, which also supported the prediction of amino acids loaded by each adenylation domain.[39]

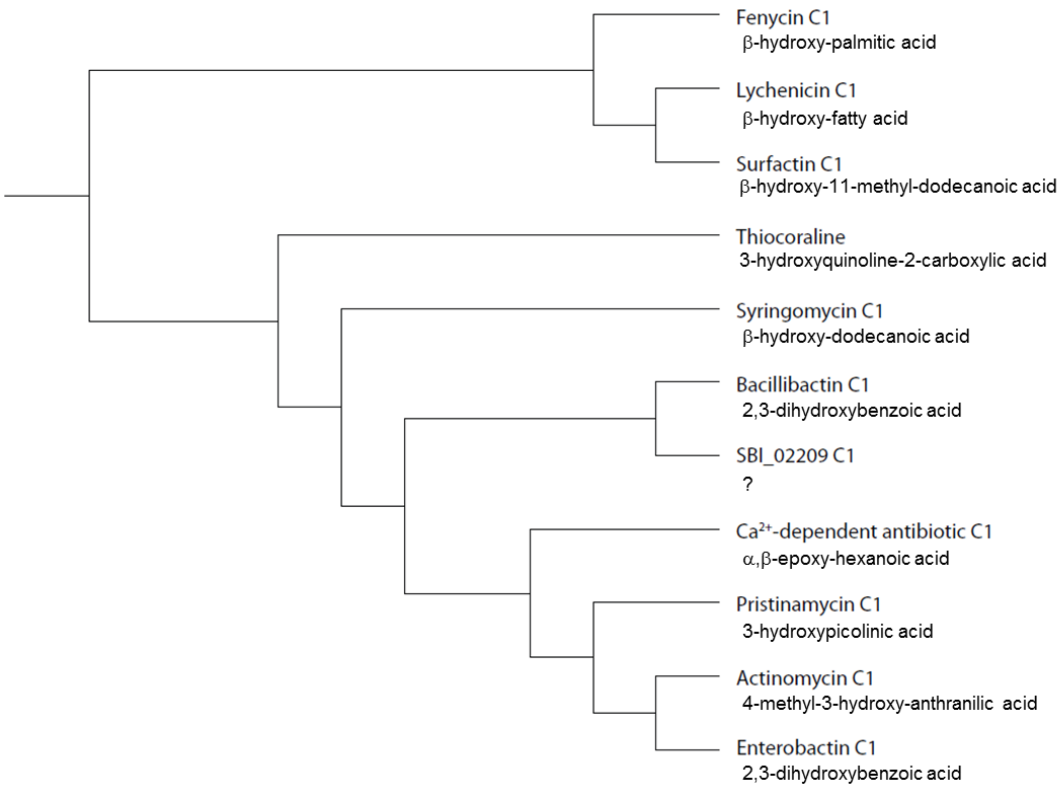

Figure 3.11. Phylogenetic tree of NRPS "starter" C-domains. The N-terminal C-domain of SBI_02209 clades with other "starter" C-domains which incorporate various acyl groups into characterized natural products.[36] The incorporated acyl group is listed below the natural product. SBI_02209 most closely clades with the bacillibactin C1 "starter" domain, indicating that this potential PI may be initiated with 2,3-dihydrobenzoic acid.

Our attempts to obtain the *S. bingchenggensis* BCW-1 strain from Chinese culture collections were unsuccessful. As such, we have no concrete evidence that this organism produces a PI of any structure. As the biosynthetic pathways of many PIs such as epoxomicin and eponemycin have yet to be elucidated, they cannot serve as a reference point for homology. If we were able to obtain the organism, I would begin with bioassay guided fractionation to locate a cytotoxic compound and then follow up with 20S proteasome inhibition assays to verify the cellular target. If a PI were

discovered, the chemical structure would be solved by high resolution mass spectroscopy and standard 1D and 2D NMR spectroscopy. Investigation into the biosynthetic origin of the PI's warhead and non-proteinogenic amino acid would begin with stable isotope labeling of possible precursors such as acetate and S-adenosyl-L-methionine. To verify that this gene cluster does hold the biosynthetic blueprints for the PI, a gene inactivation of the NRPS/PKS genes would be utilized to abolish production.

The following proposal for the structure and biosynthesis of this PI is a purely speculative bioinformatics exercise. If this natural product is indeed a PI, then the C-terminal acetate would require modification to generate an electrophilic warhead such as an aldehyde, β-lactone, or α,β-epoxyketone. Possible mechanisms to generate such functional groups are explored in Figure 3.12. Reductive cleavage of the PCP bound **10** to yield the β-keto aldehyde **11** which could then tautomerize to **12** followed by an unprecedented epoxide formation to yield an α,β-epoxyketone epoxomicin derivative **13**. This route, however, appears unlikely as the annotated thioesterase domain lacks an electron accepting cofactor binding site. Alternatively, non-reductive hydrolysis of **10** to the β-keto acid **14** could be followed by spontaneous decarboxylation to yield an electrophilic ethylketone (**15**). Subsequent oxidation of **15** to **16** would generate a Michael acceptor to potentially act as an irreversible inhibitor. Three annotated oxidoreductase enzymes are present in this gene neighborhood, including an acyl-CoA dehydrogenase, an NADH dependent dehydrogenase, and an FAD dependent berberine domain containing protein. An alternative fate of **14** may be oxidation of the α-methyl group to **17**. Intramolecular cyclization would form a β-lactone warhead (**19**) as seen in

the salinosporamides, cinnabaramides, and lactacystin. This process may be catalyzed by the berberine domain containing protein which was originally characterized to catalyze the oxidation of the exocyclic N-methyl group of (*S*)-reticuline which then serves and an electrophile for a concerted intramolecular cyclization reaction to (*S*)-scoulerine, en route to berberine.[40,41] The berberine-bridge enzyme may also participate in a redox reaction to facilitate epoxide or strained ring formation analogous to the hypothesized role of the 53% identical Azic01 in aziridine formation of azicemicin A.[42] In this case, aziridine formation results in dehydration as opposed to saturation of a double bond. Caution should be used in this assumption as several other berberine domain-containing proteins have been characterized and shown to have diverse functions such as keto/alchohol conversions and dehydrogenations.[43-45] Reduction of **19** to the hemiacetal (**20**) followed by chain opening (**21**), tautomerization (**22**) and epoxide formation may yield **23** with the eponemycin/epopomycin-like warhead.

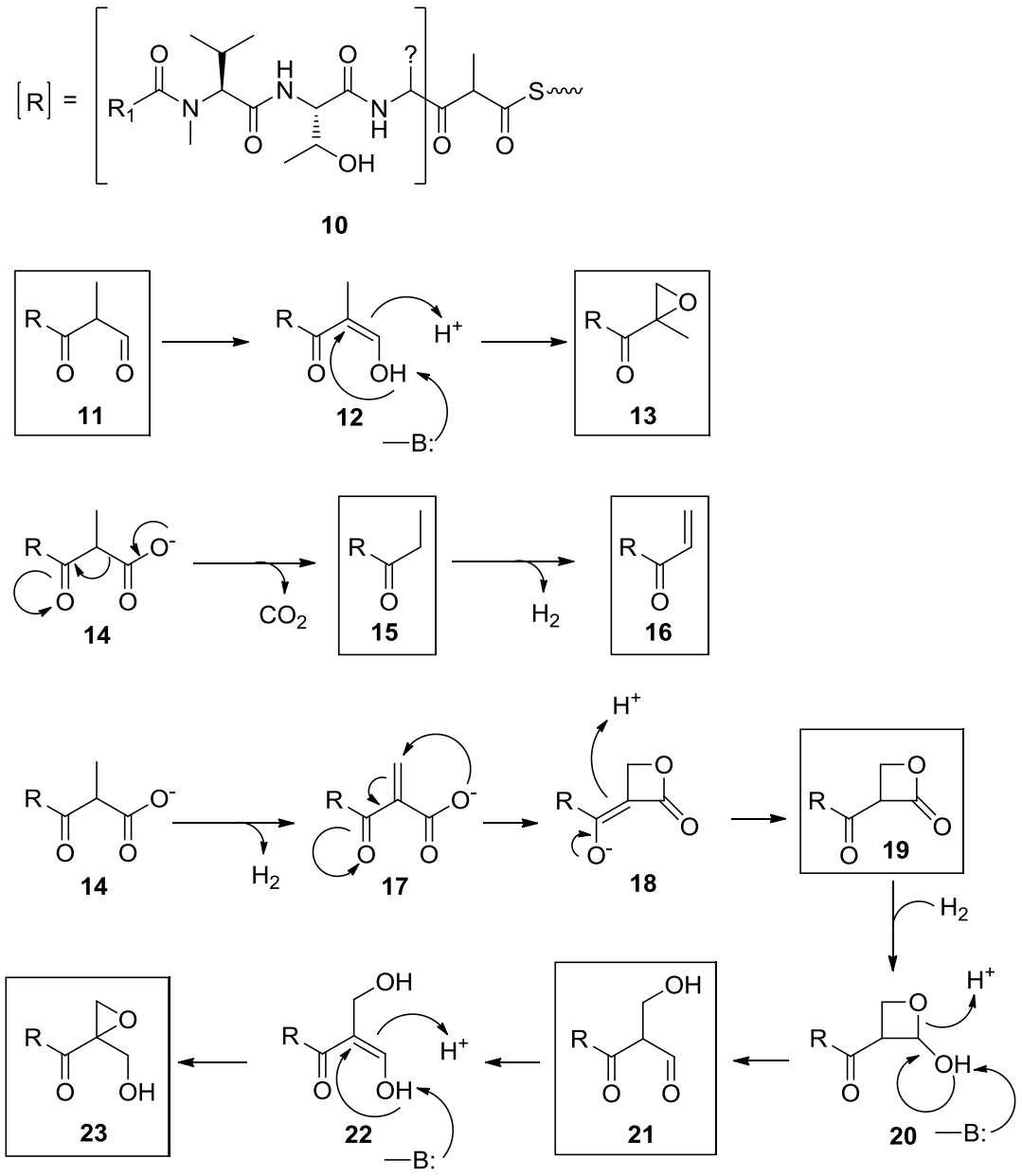

Figure 3.12. Possible mechanisms to generate electrophilic modifications on the C-terminus of the SBI_02208-9 encoded NRPS/PKS natural product of *S. bingchenggensis* BCW-1. Potential electrophilic endpoints are enclosed in boxes.

3.3.6: Summary.

The recruitment of a pathway specific proteasome β-subunit to assemble with the primary α-subunit to form a 20S proteasome complex (α/SalI) that is both hydrolytically active and relatively resistant to PIs is unprecedented and defines a new mechanism of natural product resistance. This evolved resistance mechanism in a PI-producing microbe is strikingly similar to the analogous target modification paradigm recently reported for bortezomib treatment in human cancer cell lines, thereby suggesting that natural PI chemotherapy, which includes salinosporamide A, may ultimately be similarly susceptible to acquired resistance by proteasome modification.

3.4: Methods

3.4.1: Materials.

Salinosporamides A and B were purified from cultures of *S. tropica* CNB-440.[46] Proteasome inhibitors of the salinosporamide X series were produced and purified from a genetically modified *S. tropica* strain as previously described.[32,47] All chemicals purchased were of the highest quality. Proteasome inhibitor Velcade® (Bortezomib) was purchased from LC Laboratories and the seven 7-amino-4-methylcoumarin (amc) tagged peptide substrates were purchased as follows: substrates Z-Val-Lys-Met-amc, Z-Leu-Leu-Leu-amc, Suc-Leu-Leu-Val-Tyr-amc, MeOSuc-Ala-Ala-Pro-Val-amc, Ac-Arg-Leu-Arg-amc, and Z-Leu-Leu-Glu-amc from Enzo Life Sciences and substrate Suc-Ala-Pro-Ala-amc from Peptides International, Inc.

3.4.2: mRNA Transcript Analysis.

Total RNA was extracted from *S. tropica* CNB-440 and converted to cDNA as reported previously.[21] PCR was run for 25 cycles using Taq polymerase (New England Biolabs) and 500 ng of cDNA in 10 μL reactions. Primers used were: *salL*, forward 5` TCGTGGACATAACCCATGAC 3` and reverse 5` AGGACCTCGTGACACTCGAC 3`; *salI*, forward 5` TAGTCGTCCGTGATCGTGAG 3` and reverse 5` GCCGTCCACGTTCTTAACAT 3`; Strop_2244, forward 5` CTGGAGCACTACGAGAAGAC 3` and reverse 5` GTCACGTCGAAGCTGAAG 3`; and Strop_2245, forward 5` CCTGAACGGTCTGAGCTAC 3` and reverse 5` GGTACAGTTCGTCGTCCTC 3`. PCR products were approximately 250 bp in size.

3.4.3: Plasmid Construction.

Proteasome α (Strop_2245, accession: YP_001159073) and β_1 (Strop_2244, accession: YP_001159072) or SalI (Strop_1015, accession: YP_001157868) subunits were sequentially cloned from genomic DNA of *S. tropica* CNB-440 into the ampicillin resistant pETDuet-1 coexpression vector (EMD Chemicals) to generate α/β_1 pETDuet and α/SalI pETDuet. The α-subunit contained an N-terminal His_6 tag while the β_1 and SalI subunits were untagged. An additional β_1-subunit was cloned into the kanamycin resistant pHIS8 expression vector.[48] PCR reactions used *Pfu* Turbo DNA polymerase and were sequenced by Seqxcel, Inc.

The β_1-subunit was amplified for the pHIS8 vector with the primers: forward 5' CCCATGGCGGATCC**GTG**GCAGCGGCTTTCGACC 3' and reverse 5' CCCATGGCGAATTC**TCA**GCCGCCCGGATTCTCC 3'. The α-subunit was

amplified for MCS1 of pETDuet-1 with the primers: forward 5' CACAGCCAGGATCCG**GTG**GCCATGCAGTTCTACGCC 3' and reverse 5' CCCATGGCGAATTC**CTA**GGGGGCCTCGGAATCGG 3'. β_1 was amplified for MCS2 of pETDuet-1 with the primers: forward 5' GAGATATACAT**ATG**GCAGCGGCTTTCGACCCATC 3'

and reverse 5' CCCATGGCGATATC**TCA**GCCGCCCGGATTCTCC 3'.

SalI was amplified for MCS2 of pETDuet-1 with the primers: forward 5' GAGATATACAT**ATG**AATCGGGGTCTGCCGTCCAC 3' and reverse 5' CCCATGGCGATATC**TCA**GGACGCGGTAAAGCTTCG 3'. The introduced BamHI, EcoRI, NdeI and EcoRV sites are underlined. The start and stop codons are shown in bold.

3.4.4: Site-Directed Mutagenesis.

Site-directed mutagenesis was performed using the Stratagene Quikchange kit (Agilent Technologies). Single point mutations were performed using the α/β_1 pETDuet and α/SalI pETDuet constructs as templates to generate α/β_1 M45F pETDuet, α/β_1 A49V pETDuet, α/SalI F45M pETDuet, and α/SalI V49A pETDuet. Positions 45 and 49 refer to the amino acid position of the β_1 or SalI subunit from Thr1 after prosequence cleavage. Double mutations were performed sequentially. The α/β_1 M45F pETDuet plasmid was used as a template to generate the α/β_1 M45F/A49V double mutant while the α/SalI F45M pETDuet plasmid was similarly used to generate the α/SalI F45M/V49A double mutant. Both subunits of the mutant vectors were resequenced for verification following mutagenesis.

Primers sequences used were as follows with mutation sites underlined: α/β_1 M45F forward 5' CTCCCTGGTGGGCTTCGCGGGTGCCGCC 3' and reverse 5' GGCGGCACCCGCGAAGCCCACCAGGGAG 3'; α/β_1 A49V forward 5' CATGGCGGGTGCCGTCGGAATCGGGATC 3' and reverse 5' GATCCCGATTCCGACGGCACCCGCCATG 3'; α/β_1 M45F/V49A (from α/β_1 M45F) forward 5' CTTCGCGGGTGCCGTCGGAATCGGGATC 3' reverse 5' GATCCCGATTCCGACGGCACCCGCGAAG 3'; α/SalI F45M forward 5' CTATTCGGCGGTCGGTATGGCCGGCACGGTGGGC 3' and reverse 5' GCCCACCGTGCCGGCCATACCGACCGCCGAATAG 3'; α/SalI V49A forward 5' GTTTCGCCGGCACGGCAGGCATCTCCATTGAC 3' and reverse 5' GTCAATGGAGATGCCTGCCGTGCCGGCGAAAC 3'; α/SalI F45M/V49A (from α/SalI F45M) forward 5' GTATGGCCGGCACGGCAGGCATCTCCATTGAC 3' and reverse 5' GTCAATGGAGATGCCTGCCGTGCCGGCCATAC 3'.

3.4.5: Protein Expression.

All expression vectors were transformed into *Escherichia coli* BL21(DE3). To increase titers of the α/β_1 wild-type complex, a second β_1 expression plasmid, β_1 pHIS8, was transformed concurrently with α/β_1 pETDuet. A 10 ml culture in LB broth containing 100 μg ml^{-1} ampicillin was grown overnight at 37 °C. This was used to inoculate a 1 L culture of ZY media with autoinduction containing 100 μg ml^{-1} ampicillin.[49] In the case of the wild-type α/β_1 proteasome expression, 50 μg ml^{-1} kanamycin was also added to starter and expression cultures. Expression cultures were grown on an orbital shaker for 20 h at 28 °C.

3.4.6: Protein Purification.

All protein purification steps took place at 4 °C. Protein purification buffers contained 300 mM NaCl, 50 mM sodium phosphate adjusted to pH 8.0, and increasing concentrations of imidazole. Buffers A (lysis), B (wash), and C (elution) contained 10, 20, and 250 mM imidazole, respectively. Cells were pelleted at 6,300 g for 15 min, resuspended in buffer A and lysed with six 30 sec bursts of probe sonication with resting periods of 30 sec. The lysate was centrifuged for 45 min at 20,000 g. Soluble protein was collected and equilibrated with Ni-NTA resin for 1 h before it was purified by Ni-NTA affinity chromatography, washed with several volumes of buffer B and eluting with 10 ml of buffer C. Washed and eluted protein was concentrated with a Vivaspin 100 kDa cut-off spin concentrator (GE biosciences) and resuspended in 100 mM Tris-HCl at pH 8.0. Concentrated protein was further purified by size exclusion chromatography on a HiLoad 16/60 Superdex 200 column (GE biosciences) with a 100 mM Tris-HCl pH 8.0 mobile phase and reconcentrated with a vivaspin 100 kDa cutoff protein concentrator.

3.4.7: Native Gel Analysis and Fluorescent Overlay Assay.

10 μg α/β_1 or 10 μg α/SalI were loaded onto an Invitrogen (4–16%) NativePAGE gel (Life Technologies). The gel was run at 150 V at 4 °C. For direct band visualization, the gels were washed and stained with Coomassie Brilliant Blue. For fluorescent visualization assays, the unstained native gel was briefly washed with H_2O then submerged in 25 μM Suc-LLVY-amc containing 50 mM Tris-HCl pH 8.0 buffer solution and shaken at room temperature for 60 minutes in darkness. The gel was

transilluminated at 360 nm using a Gel Logic 2200 gel imager (Carestream). For salinosporamide inhibition, proteasome was incubated with 75 μM salinosporamide A for 20 min prior to loading of the gel.

3.4.8: Denaturing Gel Analysis.

Protein samples were prepared for denaturing PAGE by boiling for 5 min prior to loading 5–15 μg proteasome onto the gel. Samples were loaded onto an Invitrogen NuPAGE 16% Tris-glycine SDS gel and run at 125 V for 3 h. Gels were washed and stained with Coomassie brilliant blue.

3.4.9: Proteasome Assays.

All proteasome assays were performed at a final volume of 50 μL in Greiner half-well microplates at 30 °C in 50 mM Tris-HCl pH 8.0, unless otherwise specified. Fluorescence was measured on a Spectramax M2 plate reader (Molecular Devices) with an excitation wavelength of 355 nm and an emission wavelength of 460 nm.

3.4.10: Rates of Hydrolysis.

Purified proteasome complexes were assayed at three concentrations, each in triplicate. Enzyme concentrations assayed varied by proteasome complex from 5–60 μg ml^{-1} depending on activity. Substrate was added to 40 μM. Change in fluorescence was monitored continuously and the slope of the steady state portion of the curve was used to calculate the hydrolysis rate at that enzyme concentration. The average hydrolysis rate at each enzyme concentration was then plotted and a line was fit to obtain the hydrolysis rate per enzyme concentration using SigmaPlot 11.0 (Systat Software, Inc.).

Relative fluorescence units were converted to μM by comparison to a standard curve of 7-amino-4-methylcoumarin in 50 mM Tris-HCl pH 8.0.

3.4.11: Proteasome Inhibition.

Proteasome complexes were incubated in serial dilutions of the proteasome inhibitors for 15 min at 30 °C. Enzyme concentration was adjusted between 1–3 μg per reaction (20–60 μg ml^{-1}) to ensure adequate activity for measurement of inhibition. Amounts of proteasome added per reaction were: 1.2 μg α/β_1, 1.3 μg α/β_1 F45M, 1.0 μg α/β_1 A49V, 3.0 μg α/β_1 M45F/V49A, 1.7 μg α/SalI, and 2.9 μg α/SalI F45M. The α/SalI V49A and α/SalI F45M/V49A mutants were not tested due to lack of hydrolytic activity. Fluorogenic substrate was then added to 40 μM and the reaction allowed to proceed for 30 min in darkness before fluorescence was measured. Maximum activity was set as proteasome in the absence of inhibitor and minimum activity was set as fluorogenic substrate in the absence of proteasome. Measurements were performed in triplicate and averaged. IC_{50} values were calculated from 4-parameter logistic curve fittings using SigmaPlot 11.0 (Systat Software, Inc.).

3.4.12: Time-Dependence of Inhibition.

Dilutions of salinosporamide A or B ranging from 0.5–100 μM and 40 μM Z-VKM-amc substrate (final concentrations) were warmed to 30 ºC in a 96-well plate. Pre-warmed α/β_1 or α/SalI was then added at 20 μg ml^{-1} (27 nM, 14 active sites) final concentration and fluorescence was measured every minute for 3.5 h at a constant temperature of 30 ºC.

3.4.13: Irreversibility of Inhibition.

To assess the reversibility of salinosporamide A inhibition on the α/β_1 and α/SalI complexes, 300 μl of 20 μg ml^{-1} enzyme in 50 mM Tris-HCl pH 8.0 buffer was incubated with 250 μM salinosporamide A or an equivalent amount of DMSO for 1.5 h at 30 ºC. Samples were buffer exchanged three times on Amicon Ultra 0.5ml 30 kDa cutoff centrifugal filters (Millipore) to remove inhibitor and added to a microplate containing 40 μM Z-VKM-amc substrate. Fluorescence was monitored at 30 ºC every minute for 3 h.

3.4.14: Cinnabaramide Biosynthetic Gene Cluster Cloning.

DNA isolation and manipulations in *E. coli* and *Streptomyces* sp. JS360 were carried out according to standard methods.[50,51] PCR amplifications were carried out using Taq DNA polymerase (Fermentas). Fosmid sequencing was conducted by GenoTech Corp. A genomic fosmid library of *S.* sp. JS360 was constructed in pCC2 (Epicentre) according to manufacturer's protocol. This library was screened by colony PCR with degenerate ketosynthase primers based on five ketosynthase sequences: the tetronomycin synthase TetA from *Streptomyces* sp. NRRL 11266 (BAE93722), the tylactone synthase TylG from *Streptomyces fradiae* (O33954), the jamaicamide synthase JamE from *Lyngbya majuscula* (AAS98777), and the salinosporamide A and K synthase SalA and Sp_SalA from *Salinospora tropica* (ABP73645) and *Salinospora pacifica* (ADZ28493), respectively. The primers were FP_KSdeg 5` TGGGARGCDCTGGARGABGCBGGC 3`, with a degeneracy of 108, and RP_ KSdeg 5` GCCGTYGGCDCGGGCGTCGAAGG 3`, with a degeneracy of 6. The *cinJ* gene sequence was obtained through gene walking from the 5'end of the *cinA* polyketide

synthase. The cinnabaramide associated 20S proteasome β-subunit was deposited in GenBank with the accession number JF970180.

3.4.15: *Streptomyces* sp. JS360 Proteasome Gene Cloning.

The α-subunit was cloned from *S.* sp JS360 genomic DNA using the forward 5`GTGTCGACGCCGTTCTATG 3' and reverse 5' GCTTGAACTTGCGCTGCTG 3' primers. Oligonucleotides were designed based on an alignment of α-subunit genes from *Streptomyces scabiei* 87.22, *Streptomyces avermitilis* MA-4680, *Streptomyces coelicolor* A3(2), *Streptomyces lividans* TK24, *Streptomyces griseus* NBRC 13350, and *Streptomyces ghanaensis* ATCC 14672. Specific primers were used subsequently to identify an appropriate fosmid, which was further used as template to obtain the primary proteasome β-subunit sequence through gene walking from the 5' end of the α-subunit. The primary 20S proteasome α and β subunit of *S.* sp. JS360 were deposited in GenBank with the accession number JF970179.

3.5: Acknowledgements

We wish to thank Tobias Gulder (Scripps Institution of Oceanography, La Jolla, CA) and Anthony Mrse (University of California San Diego, La Jolla, CA) for NMR assistance and Nadine Ziemert (Scripps Institution of Oceanography, La Jolla, CA) for assistance with C-domain analysis of SBI_02209 from *S. bingchenggensis* BCW-1. This work was supported by a grant from the NIH (CA127622) to Bradley S. Moore and the Albert and Anneliese Konanz Foundation, Mannheim, a graduate fellowship to Anna Lechner.

Chapter 3, in part, is a reprint of the material as it appears in Bacterial Self-resistance to the Natural Proteasome Inhibitor Salinosporamide A (2011). Kale, Andrew J.; McGlinchey, Ryan P.; Lechner, Anna; and Moore, Bradley S., ACS Chemical Biology, volume 6, 1257-1267. The dissertation author was the primary investigator and author of this paper.

3.6: Appendix

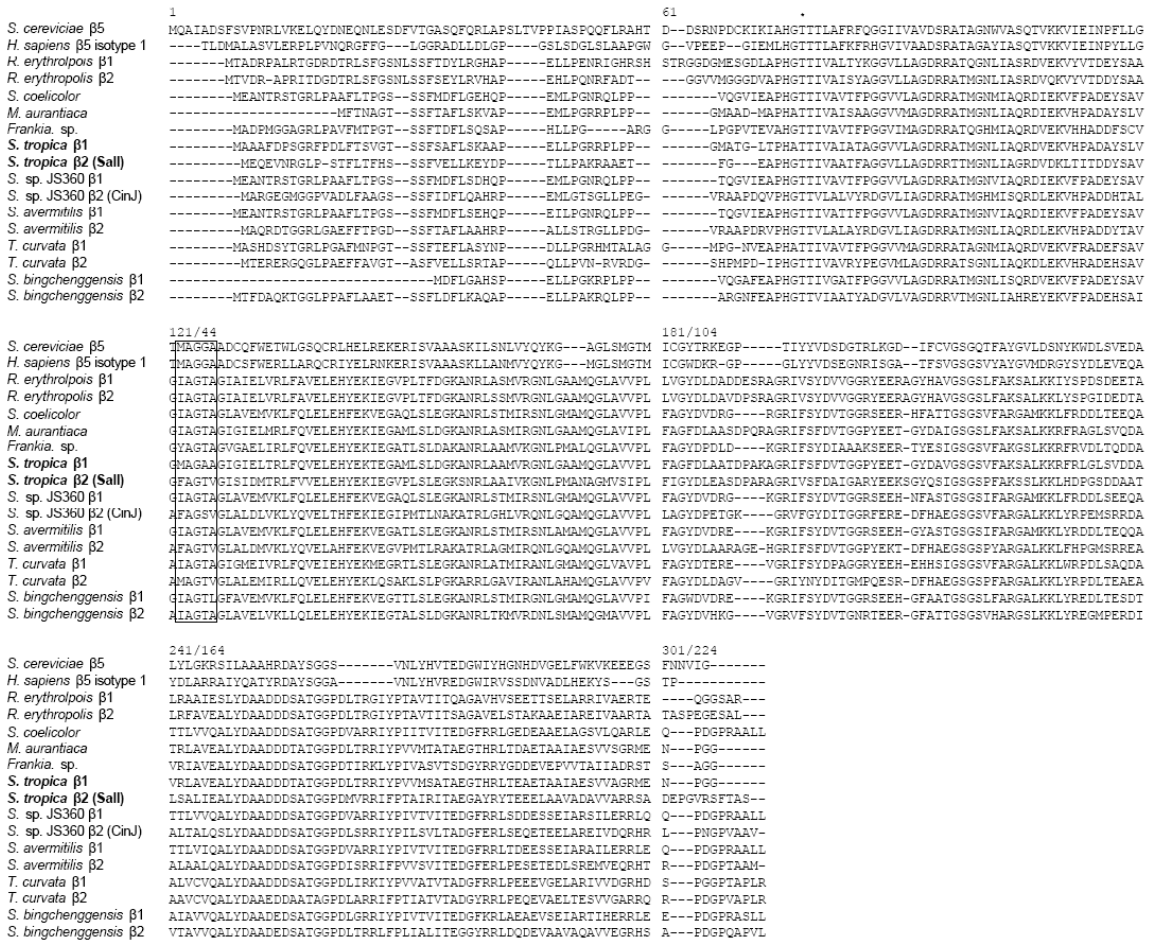

Figure A3.1. Alignment of actinobacterial 20S proteasome β-subunits, including prosequences, with the CT-L β5-subunits of *Saccharomyces cerevisiae* and *Homo sapiens*. Previously characterized β-subunit sequences from actinomycetes as well as organisms closely related to *S. tropica* (see Figure 3.6) are listed above those from *S. tropica.* The sequences listed below those from *S. tropica* are from organisms containing a secondary β-subunit (Table 3.4). Thr1 is denoted by "*" above the alignment. Amino acid positions (from start of pro-sequence/from Thr1) are indicated at the start of each 60 residue block. Residues 45–49, found within the S1 binding pocket, are enclosed inside a box. Sequences obtained from the following organisms: *Saccharomyces cerevisiae* β5-subunit, *Homo sapiens* β5-subunit, *Rhodococcus erythropolis* PR4, *Streptomyces coelicolor* A3(2), *Micromonospora aurantiaca* ATCC 27029, *Frankia* sp. ACN14a, *Salinispora tropica* CNB-440, *Streptomyces* sp. JS360, *Streptomyces avermitilis* MA-4680, *Thermomonospora curvata* DSM 43183, *Streptomyces binchenggensis* BCW-1.

Table A3.1. Annotations of genes flanking the secondary 20S proteasome β-subunit of *S. bingchenggensis* BCW-1. The complete genome is published[52] and annotations were provided from the Joint Genome Institute's Integrated Microbial Genomes server.

Locus tag	Accession number	Gene annotation	Direction of Transcription	% GC
SBI_02194	ADI05315	KORA protein	-	66
SBI_02195	ADI05316	putative SAM-dependent methyltransferase	+	67
SBI_02196	ADI05317	hypothetical protein	+	75
SBI_02197	ADI05318	secreted protein	-	70
SBI_02198	ADI05319	beta-galactosidase	-	72
SBI_02199	ADI05320	solute-binding lipoprotein	-	66
SBI_02200	ADI05321	binding-protein dependent transport protein	-	68
SBI_02201	ADI05322	ABC transporter permease protein	-	65
SBI_02202	ADI05323	LacI family transcriptional regulator	+	73
SBI_02203	ADI05324	secreted protein	-	72
SBI_02204	ADI05325	hypothetical protein	-	70
SBI_02205	ADI05326	melibiase	-	69
SBI_02206	ADI05327	transcriptional regulator	-	74
SBI_02207	ADI05328	serine/threonine protein kinase	-	71
SBI_02208	ADI05329	Beta-ketoacyl synthase	-	75
SBI_02209	ADI05330	non-ribosomal peptide synthetase	-	73
SBI_02210	ADI05331	acyl-CoA dehydrogenase FadE10	-	69
SBI_02211	ADI05332	**20S proteasome β-subunit**	**+**	**69**
SBI_02212	ADI05333	Berberine/berberine domain-containing protein	+	71
SBI_02213	ADI05334	hypothetical protein	-	71
SBI_02214	ADI05335	hypothetical protein	-	69
SBI_02215	ADI05336	NADH dehydrogenase subunit	+	69
SBI_02216	ADI05337	integral membrane protein	+	72
SBI_02217	ADI05338	putative two-component sensor kinase	+	74
SBI_02218	ADI05339	FHA domain containing protein	+	74
SBI_02219	ADI05340	hypothetical protein	+	64
SBI_02220	ADI05341	putative serine-threonine protein kinase	+	72
SBI_02221	ADI05342	regulatory protein	-	73
SBI_02222	ADI05343	AraC family transcriptional regulator	-	72
SBI_02223	ADI05344	RHS/YD repeat-containing protein	+	69
SBI_02224	ADI05345	RHS/YD repeat-containing protein	+	70
SBI_02225	ADI05346	hypothetical protein	+	68
SBI_02226	ADI05347	D-alanyl-D-alaninecarboxypeptidase	-	72
SBI_02227	ADI05348	hypothetical protein	-	75
SBI_02228	ADI05349	lantibiotic biosynthesis protein	-	74
SBI_02229	ADI05350	Lantibiotic dehydratase domain protein	-	74

3.7: References

1. Murata, S., Yashiroda, H., and Tanaka, K. (2009) Molecular mechanisms of proteasome assembly, Nat. Rev. Mol. Cell Biol. 10, 104-115.

2. Groll, M., Ditzel, L., Lowe, J., Stock, D., Bochtler, M., Bartunik, H. D., and Huber, R. (1997) Structure of 20S proteasome from yeast at 2.4 angstrom resolution, Nature 386, 463-471.

3. Borissenko, L., and Groll, M. (2007) 20S proteasome and its inhibitors: crystallographic knowledge for drug development, Chem. Rev. 107, 687-717.

4. Bross, P. F., Kane, R., Farrell, A. T., Abraham, S., Benson, K., Brower, M. E., Bradley, S., Gobburu, J. V., Goheer, A., Lee, S. L., Leighton, J., Liang, C. Y., Lostritto, R. T., McGuinn, W. D., Morse, D. E., Rahman, A., Rosario, L. A., Verbois, S. L., Williams, G., Wang, Y. C., and Pazdur, R. (2004) Approval summary for bortezomib for injection in the treatment of multiple myeloma, Clin. Cancer. Res. 10, 3954-3964.

5. Groll, M., Berkers, C. R., Ploegh, H. L., and Ovaa, H. (2006) Crystal structure of the boronic acid-based proteasome inhibitor bortezomib in complex with the yeast 20S proteasome, Structure 14, 451-456.

6. Chauhan, D., Li, G. L., Shringarpure, R., Podar, K., Ohtake, Y., Hideshima, T., and Anderson, K. C. (2003) Blockade of Hsp27 overcomes bortezomib/proteasome inhibitor PS-341 resistance in lymphoma cells, Cancer Res. 63, 6174-6177.

7. Oerlemans, R., Franke, N. E., Assaraf, Y. G., Cloos, J., van Zantwijk, I., Berkers, C. R., Scheffer, G. L., Debipersad, K., Vojtekova, K., Lemos, C., van der Heijden, J. W., Ylstra, B., Peters, G. J., Kaspers, G. L., Dijkmans, B. A. C., Scheper, R. J., and Jansen, G. (2008) Molecular basis of bortezomib resistance: proteasome subunit b5 (*PSMB5*) gene mutation and overexpression of PSMB5 protein, Blood 112, 2489-2499.

8. Lü, S. Q., Yang, J. M., Song, X. M., Gong, S. L., Zhou, H., Guo, L. P., Song, N. X., Bao, X. C., Chen, P. P., and Wang, J. M. (2008) Point mutation of the proteasome b5 subunit gene is an important mechanism of bortezomib resistance in bortezomib-selected variants of Jurkat T cell lymphoblastic lymphoma/leukemia line, J. Pharmacol. Exp. Ther. 326, 423-431.

9. Ri, M., Iida, S., Nakashima, T., Miyazaki, H., Mori, F., Ito, A., Inagaki, A., Kusumoto, S., Ishida, T., Komatsu, H., Shiotsu, Y., and Ueda, R. (2010) Bortezomib-resistant myeloma cell lines: a role for mutated *PSMB5* in

preventing the accumulation of unfolded proteins and fatal ER stress, Leukemia 24, 1506-1512.

10. Gulder, T. A. M., and Moore, B. S. (2010) Salinosporamide natural products: potent 20S proteasome inhibitors as promising cancer chemotherapeutics, Angew. Chem. Int. Ed. 49, 9346-9367.

11. Hochstrasser, M. (1995) Ubiquitin, proteasomes, and the regulation of intracellular protein degradation, Curr. Opin. Cell Biol. 7, 215-223.

12. Knipfer, N., and Shrader, T. E. (1997) Inactivation of the 20S proteasome in *Mycobacterium smegmatis*, Mol. Microbiol. 25, 375-383.

13. Hong, B., Wang, L. F., Lammertyn, E., Geukens, N., Van Mellaert, L., Li, Y., and Anne, J. (2005) Inactivation of the 20S proteasome in *Streptomyces lividans* and its influence on the production of heterologous proteins, Microbiology 151, 3137-3145.

14. Darwin, K. H., Ehrt, S., Gutierrez-Ramos, J. C., Weich, N., and Nathan, C. F. (2003) The proteasome of *Mycobacterium tuberculosis* is required for resistance to nitric oxide, Science 302, 1963-1966.

15. Pearce, M. J., Mintseris, J., Ferreyra, J., Gygi, S. P., and Darwin, K. H. (2008) Ubiquitin-like protein involved in the proteasome pathway of *Mycobacterium tuberculosis*, Science 322, 1104-1107.

16. Festa, R. A., McAllister, F., Pearce, M. J., Mintseris, J., Burns, K. E., Gygi, S. P., and Darwin, K. H. (2010) Prokayrotic ubiquitin-like protein (Pup) proteome of *Mycobacterium tuberculosis*, Plos One 5, e8589.

17. Watrous, J., Burns, K., Liu, W. T., Patel, A., Hook, V., Bafna, V., Barry, C. E., Bark, S., and Dorrestein, P. C. (2010) Expansion of the mycobacterial "PUPylome", Mol. Biosyst. 6, 376-385.

18. Poulsen, C., Akhter, Y., Jeon, A. H.-W., Schmitt-Ulms, G., Meyer, H. E., Stefanski, A., Stuhler, K., Wilmanns, M., and Song, Y.-H. (2010) Proteome-wide identification of mycobacterial pupylation targets, Mol Syst Biol 6, 386.

19. Moore, B. S., Eustáquio, A. S., and McGlinchey, R. P. (2008) Advances in and applications of proteasome inhibitors, Curr. Opin. Chem. Biol. 12, 434-440.

20. Udwary, D. W., Zeigler, L., Asolkar, R. N., Singan, V., Lapidus, A., Fenical, W., Jensen, P. R., and Moore, B. S. (2007) Genome sequencing reveals complex secondary metabolome in the marine actinomycete *Salinispora tropica*, Proc. Natl. Acad. Sci. U. S. A. 104, 10376-10381.

21. Eustáquio, A. S., McGlinchey, R. P., Liu, Y., Hazzard, C., Beer, L. L., Florova, G., Alhamadsheh, M. M., Lechner, A., Kale, A. J., Kobayashi, Y., Reynolds, K. A., and Moore, B. S. (2009) Biosynthesis of the salinosporamide A polyketide synthase substrate chloroethylmalonyl-coenzyme A from S-adenosyl-L-methionine, Proc. Natl. Acad. Sci. U. S. A. 106, 12295-12300.

22. Hopwood, D. A. (2007) How do antibiotic-producing bacteria ensure their self-resistance before antibiotic biosynthesis incapacitates them?, Mol. Microbiol. 63, 937-940.

23. Pouch, M. N., Cournoyer, B., and Baumeister, W. (2000) Characterization of the 20S proteasome from the actinomycete *Frankia*, Mol. Microbiol. 35, 368-377.

24. Nagy, I., Tamura, T., Vanderleyden, J., Baumeister, W., and De Mot, R. (1998) The 20S proteasome of *Streptomyces coelicolor*, J. Bacteriol. 180, 5448-5453.

25. Tamura, T., Nagy, I., Lupas, A., Lottspeich, F., Cejka, Z., Schoofs, G., Tanaka, K., Demot, R., and Baumeister, W. (1995) The characterization of a eubacterial proteasome: the 20S complex of *Rhodococcus*, Curr. Biol. 5, 766-774.

26. Zuhl, F., Tamura, T., Dolenc, I., Cejka, Z., Nagy, I., DeMot, R., and Baumeister, W. (1997) Subunit topology of the *Rhodococcus* proteasome, FEBS Lett. 400, 83-90.

27. Groll, M., Huber, R., and Potts, B. C. M. (2006) Crystal structures of salinosporamide A (NPI-0052) and B (NPI-0047) in complex with the 20S proteasome reveal important consequences of b-lactone ring opening and a mechanism for irreversible binding, J. Am. Chem. Soc. 128, 5136-5141.

28. Denora, N., Potts, B. C. M., and Stella, V. J. (2007) A mechanistic and kinetic study of the b-lactone hydrolysis of salinosporamide A (NPI-0052), a novel proteasome inhibitor, J. Pharm. Sci. 96, 2037-2047.

29. Richter-Ruoff, B., Heinemeyer, W., and Wolf, D. H. (1992) The proteasome/multicatalytic-multifunctional proteinase. *In vivo* function in the ubiquitin-dependent *N*-end rule pathway of protein degradation in eukaryotes, FEBS Lett. 302, 192-196.

30. Sirikantaramas, S., Yamazaki, M., and Saito, K. (2008) Mutations in topoisomerase I as a self-resistance mechanism coevolved with the production of the anticancer alkaloid camptothecin in plants, Proc. Natl. Acad. Sci. U. S. A. 105, 6782-6786.

31. Puri, S. C., Verma, V., Amna, T., Qazi, G. N., and Spiteller, M. (2005) An endophytic fungus from *Nothapodytes foetida* that produces camptothecin, J. Nat. Prod. 68, 1717-1719.

32. Nett, M., Guider, T. A. M., Kale, A. J., Hughes, C. C., and Moore, B. S. (2009) Function-oriented biosynthesis of b-lactone proteasome inhibitors in *Salinispora tropica*, J. Med. Chem. 52, 6163-6167.

33. Eustáquio, A. S., Nam, S. J., Penn, K., Lechner, A., Wilson, M. C., Fenical, W., Jensen, P. R., and Moore, B. S. (2011) The discovery of salinosporamide K from the marine bacterium "*Salinispora pacifica*" by genome mining gives insight into pathway evolution, ChemBioChem 12, 61-64.

34. Stadler, M., Bitzer, J., Mayer-Bartschmid, A., Muller, H., Benet-Buchholz, J., Gantner, F., Tichy, H. V., Reinemer, P., and Bacon, K. B. (2007) Cinnabaramides A-G: analogues of lactacystin and salinosporamide from a terrestrial streptomycete, J. Nat. Prod. 70, 246-252.

35. Rachid, S., Huo, L. J., Herrmann, J., Stadler, M., Kopcke, B., Bitzer, J., and Muller, R. (2011) Mining the cinnabaramide biosynthetic pathway to generate novel proteasome inhibitors, ChemBioChem 12, 922-931.

36. Ziemert, N., Podell, S., Penn, K., Badger, J. H., Allen, E., and Jensen, P. R. (2012) The natural product domain seeker NaPDoS: a phylogeny based bioinformatic tool to classify secondary metabolite gene diversity, Plos One 7, e34064.

37. Rausch, C., Hoof, I., Weber, T., Wohlleben, W., and Huson, D. H. (2007) Phylogenetic analysis of condensation domains in NRPS sheds light on their functional evolution, BMC Evol. Biol. 7, 78.

38. Bachmann, B. O., and Ravel, J. (2009) Methods for in silico prediction of microbial polyketide and ninribosomal peptide biosynthetic pathways from DNA sequence data, In *Complex Enzymes in Microbial Natural Product Biosynthesis, Part A: Overview Articles and Peptides* (Hopwood, D. A., Ed.), pp 181-217.

39. Medema, M. H., Blin, K., Cimermancic, P., de Jager, V., Zakrzewski, P., Fischbach, M. A., Weber, T., Takano, E., and Breitling, R. (2011) antiSMASH: rapid identification, annotation and analysis of secondary metabolite biosynthesis gene clusters in bacterial and fungal genome sequences, Nucleic Acids Res. 39, W339-W346.

40. Kutchan, T. M., and Dittrich, H. (1995) Characterization and mechanism of the berberine bridge enzyme, a covalently flavinylated oxidase of

benzophenanthridine alkaloid biosynthesis in plants, J. Biol. Chem. 270, 24475-24481.

41. Winkler, A., Lyskowski, A., Riedl, S., Puhl, M., Kutchan, T. M., Macheroux, P., and Gruber, K. (2008) A concerted mechanism for berberine bridge enzyme, Nat. Chem. Biol. 4, 739-741.

42. Ogasawara, Y., and Liu, H.-w. (2009) Biosynthetic studies of aziridine formation in azicemicins, J. Am. Chem. Soc. 131, 18066-18068.

43. Gullon, S., Olano, C., Abdelfattah, M. S., Brana, A. F., Rohr, J., Mendez, C., and Salas, J. A. (2006) Isolation, characterization, and heterologous expression of the biosynthesis gene cluster for the antitumor anthracycline steffimycin, Appl. Environ. Microbiol. 72, 4172-4183.

44. Kim, H. J., Pongdee, R., Wu, Q. Q., Hong, L., and Liu, H. W. (2007) The biosynthesis of spinosyn in *Saccharopolyspora spinosa*: synthesis of the cross-bridging precursor and identification of the function of SpnJ, J. Am. Chem. Soc. 129, 14582-14584.

45. Alexeev, I., Sultana, A., Mantsala, P., Niemi, J., and Schneider, G. (2007) Aclacinomycin oxidoreductase (AknOx) from the biosynthetic pathway of the antibiotic aclacinomycin is an unusual flavoenzyme with a dual active site, Proc. Natl. Acad. Sci. U. S. A. 104, 6170-6175.

46. Feling, R. H., Buchanan, G. O., Mincer, T. J., Kauffman, C. A., Jensen, P. R., and Fenical, W. (2003) Salinosporamide A: a highly cytotoxic proteasome inhibitor from a novel microbial source, a marine bacterium of the new genus *Salinospora*, Angew. Chem. Int. Ed. 42, 355-358.

47. McGlinchey, R. P., Nett, M., Eustáquio, A. S., Asolkar, R. N., Fenical, W., and Moore, B. S. (2008) Engineered biosynthesis of antiprotealide and other unnatural salinosporamide proteasome inhibitors, J. Am. Chem. Soc. 130, 7822-7823.

48. Jez, J. M., Ferrer, J. L., Bowman, M. E., Dixon, R. A., and Noel, J. P. (2000) Dissection of malonyl-coenzyme A decarboxylation from polyketide formation in the reaction mechanism of a plant polyketide synthase, Biochemistry 39, 890-902.

49. Studier, F. W. (2005) Protein production by auto-induction in high-density shaking cultures, Protein Expr. Purif. 41, 207-234.

50. Sambrook, J., and Russell, D. (2001) *Molecular Cloning: A Laboratory Manual*, 3 ed., Cold Spring Harbor Laboratory Press, Cold Spring Harbor, NY.

51. Kieser, T., Bibb, M. J., Buttner, M. J., Chater, K. F., and Hopwood, D. A. (2000) *Practical Streptomyces Genetics*, John Innes Centre, Norwich, United Kingdom.

52. Wang, X. J., Yan, Y. J., Zhang, B., An, J., Wang, J. J., Tian, J., Jiang, L., Chen, Y. H., Huang, S. X., Yin, M., Zhang, J., Gao, A. L., Liu, C. X., Zhu, Z. X., and Xiang, W. S. (2010) Genome sequence of the milbemycin-producing bacterium *Streptomyces bingchenggensis*, J. Bacteriol. 192, 4526-4527.

Chapter 4:

Conclusions and Future Directions

4.1: Conclusions

There will always be a need for new and improved drugs. While terrestrial plants and microorganisms have been exploited as sources of medicinal natural products for hundreds of years, the marine environment is only now beginning to be appreciated for its microbial diversity and natural product output. The recent discoveries of the new marine obligate actinobacterial genus *Salinispora*[1,2] and the proteasome inhibitor salinosporamide A,[3] which is currently in clinical trials for the treatment of multiple myeloma,[4] highlight the importance of continued exploration of the marine environment.

Beyond the search for new bioactive molecules, we must strive to understand how such sophisticated molecules are produced by seemingly primitive organisms. As we expand our knowledge of natural product biosynthesis, the information gained may help us to significantly increase natural product production, generate mutasynthetic derivatives, and bioengineer completely novel natural product pathways. With the advent of the genomic and metagenomic era, we will additionally utilize these biosynthetic clues to locate potential natural products *in silico*.

Another critical component for research in the field of natural products is to develop a deeper understanding of the biological activity of these compounds when used as pharmaceutical agents. By understanding how these chemicals alter disease biochemistry, we will gain fundamental knowledge of disease biology and pathogenicity. Medicinal treatments have a tendency to lose effectiveness over time, as classically illustrated by the emergence of antibiotic resistance.[5] By understanding

mechanisms of resistance to treatment, we will be better positioned to focus drug development on agents that will not be similarly susceptible.

In Chapter 2 of this dissertation, I reported the characterization of the oxidation of 5-ClR to 5-ClRL by the short-chain dehydrogenase/reductase enzyme SalM.[6] SalM participates in the biosynthesis of chloroethylmalonyl-CoA, a novel halogenated PKS extender unit, which specifically confers salinosporamide A with nM *in vivo* potency as an irreversible proteasome inhibitor. Using heterologous protein expression in *Escherichia coli*, I characterized SalM *in vitro* for its substrate specificity, kinetics, and reaction profile. Unlike most SDR enzymes, SalM had a strong dependence on the divalent metal cations Mg^{2+}, Ca^{2+}, or Mn^{2+}. I developed a sensitive, real-time ^{13}C NMR assay to visualize the oxidation of 5-ClR to 5-ClRL which is immediately followed by spontaneous hydrolysis to 5-ClRI. In addition to 5-ClR, SalM also oxidized D-erythrose and D-ribose, making SalM the first reported stereospecific non-phosphorylated ribose-1-dehydrogenase.

An understanding of salinosporamide biosynthesis has allowed us to generate new salinosporamide analogs by mutasynthesis[7,8] and increase production titers.[9] This studied revealed that a probable reliance on spontaneous lactone hydrolysis may present an additional opportunity to increase salinosporamide titers by the introduction of a lactonase encoding gene. Additionally, the ^{13}C NMR assay that I developed may be utilized in the future as a powerful analytical tool for enzymatic reactions with transient intermediates or unstable products because it eliminates the need for fully deuterated solvents, solvent suppression techniques, or isotopic labeling.

In Chapter 3 of this dissertation, I discuss the characterization of the secondary 20S proteasome β-subunit, SalI, which is encoded within the biosynthetic gene cluster for the potent PI salinosporamide A.[10] However, as actinobacteria also possess 20S proteasome machinery, it raised the question how the producing organism prevents self-inhibition. For a prospective drug, it is important to understand any evolved resistance mechanisms as they may ultimately limit effectiveness in humans. Using heterologous expression in *E. coli,* I biochemically characterized the housekeeping α/β_1 and the α/SalI proteasome complexes. The SalI subunit displayed an altered substrate specificity profile, significant resistance to salinosporamide A, and cross-resistance to the FDA-approved proteasome inhibitor bortezomib. We compared the amino acid sequences of the two β-subunits and identified potential causative mutations that were then investigated by site-directed mutagenesis. Intriguingly, the A49V mutation in SalI appears to be partially responsible for resistance in *S. tropica* and correlates to several reports of bortezomib resistant cell lines resulting from human proteasome β5-subunit A49V and A49T mutations (see Table A1.1),[11-16] suggesting that acquired resistance to natural proteasome inhibitors may predict clinical outcomes.

In Chapter 1 of this dissertation, I reviewed the molecular mechanisms of proteasome inhibitor resistance in human cell lines. The emergence of PIs over the past ten years has been a major breakthrough in the treatment of hematological malignancies.[17] However, both intrinsic and acquired PI resistances remain major obstacles.[18] Recent investigations into acquired bortezomib resistance in various cancer cell lines revealed upregulation of the proteasome at the mRNA and protein levels as

well as mutations of the β5-subunit (see Table A1.1).[11-16,19-22] The development of mutations in cell lines was observed in as little as a few months at clinically relevant concentrations of bortezomib. These mutations in the S1 binding pocket appear to form *de novo* and may also modulate proteolytic specificity. Therefore, analysis of proteasome activity with the fluorogenic LLVY-amc substrate may under represent proteolytic activity. However, caution should be used as no β-subunit mutations have yet been confirmed in patients.

While it is important to continue developing β-subunit inhibitors such as salinosporamide A, it is clear that the development of PIs must expand beyond β5-subunit inhibitors. Inhibitors of proteasome assembly and allosteric effectors will not be susceptible to resistance by β-subunit S1 pocket mutation. The development of Ub pathway enzyme inhibitors will achieve the same effect as PIs, the disregulation of cellular protein destruction, with an alternative target.[23] The development of E3 inhibitors will be especially useful as they may pinpoint treatment to specific oncogenic proteins.

4.2: Future Directions

My *in vitro* characterization of a secondary 20S proteasome β-subunit SalI, discussed in Chapter 3, encoded within the salinosporamide biosynthetic gene cluster demonstrated reduced susceptibility to inhibition by salinosporamide A, suggesting that it acts as a self-resistance mechanism. However, the actual biological role of the proteasome in *S. tropica* remains undefined. Protein degradation in eukaryotes utilizes

the well characterized Ubiquitin-Proteasome System where lysine residues on proteins marked for degradation are covalently modified with the small Ubiquitin peptide.[24] An analogous posttranslational modification has recently been uncovered in the actinobacteria where the Prokaryotic Ubiquitin-like Protein (PUP) is covalently linked to substrate lysine residues followed by 20S proteasome degradation.[25,26]

In my *in vitro* characterization of 20S proteasomes of *S. tropica*, I only investigated complexes of homogeneous β-subunit composition. However, I cannot rule out the possibility of mixed assemblages *in vivo.* Possible subunit topologies include the union of an α/β_1 half-proteasome and an α/SalI half-proteasome to form an $\alpha_7(\beta_1)_7(\text{SalI})_7\alpha_7$ complex or random intermixing of β-subunit types in one or both heptameric ring. In the case of *Rhodococcus erythropolis*, where two α-subunit and two β-subunit types are encoded, either α-subunit was equally capable of complexing with the lone β-subunit to form a heterogeneous ring of α-subunits.[27] In the event of a mixed assemblage in *S. tropica*, it is unknown if proteolytic activity and salinosporamide resistance would conform to the weighted average of the individual β-subunit activities. It is currently unknown if the lone α-subunit has a preference for one β-subunit type over the other. As β_1 and SalI differ in mass by 1 kDa, heterologous coexpression of the α-subunit and both β-subunits, followed by high resolution native gel electrophoresis could reveal the viable topologies.

Proteasome subunit regulation also remains to be elucidated. If SalI is related to salinosporamide resistance, I would expect to see upregulation concomitant with salinosporamide production. Given the assumption that the α/β_1 proteasome is

advantageous in the absence of salinosporamide A, I could also envision β_1-subunit expression being negatively correlated with SalI expression as they would compete with each other for α-subunits. Quantitative qRT-PCR could be employed in a time-course experiment to assess β-subunit transcription.

In an effort to verify the self-resistance functionality of SalI, I proposed to propose to isolate the 20S proteasome from wild-type *S. tropica* for trypsin digestion followed by protein mass spectrometric analysis. The purpose of this is to identify if both β_1 and SalI are incorporated into assembled 20 proteasome complexes and to identify any temporal or salinosporamide production dependence of SalI incorporation. Furthermore, I hope to observe covalent modification of the Thr1 residue of the β-subunits with salinosporamide A, indicating self-inhibition. If SalI is indeed acting as a self-resistance mechanism, I would expect to see preferential binding of salinosporamide A to the β_1-subunit.

In a parallel project, I propose to elucidate the role of 20S proteasome degradation in *S. tropica*. As proteins destined for proteasome degradation are covalently modified with the PUP tag (PUPylated), I have integrated a His_6-tagged PUP encoding gene into *S. tropica* and *S. arenicola*, the latter of which does not produce salinosporamides nor possess a secondary proteasome β-subunit, using the pSET152 integrating vector.[9] The goal of this experiment would be to capture His_6-PUPylated proteins by Ni^{2+} affinity chromatography followed by trypsin digest and mass spectrometric analysis. This methodology has been previously utilized to elucidate the "PUPylome" of both *Mycobacterium smegmatis* and *Mycobacterium tuberculosis.*[28-30]

The biosynthetic polyketide synthase proteins of mycolic acid biosynthesis have been shown to be PUPylated in the *Mycobacteria*.[29] However, no studies have explored PUPylation in actinobacteria outside of the *Mycobacteria* such as in the prolific natural product-producing *Streptomyces*. As the *Salinispora* are also prolific secondary metabolite produces and *S. tropica* has the possible resistance mechanism, it would provide a unique opportunity to investigate the role of PUPylation in natural products biosynthesis.

For the pursuit of science to be worthwhile, scientific knowledge must be applied to the improvement of human existence. The work presented in this dissertation represents my efforts to merge the diverse disciplines of marine microbiology, biochemistry, and pharmacology with the goal of generating effective medical treatments from marine-derived compounds. I trust that my contribution to the field of proteasome inhibitor biosynthesis and resistance may ultimately lead to more effective treatment strategies for cancer, ease suffering and save lives.

4.3: Acknowledgements

Chapter 4, in part, was submitted as Uncovering the Molecular Mechanisms of Proteasome Inhibitor Resistance (2012). Kale, Andrew J. and Moore, Bradley S., Journal of Medicinal Chemistry. The dissertation author was the primary author of this submission.

4.4: References

1. Jensen, P. R., Dwight, R., and Fenical, W. (1991) Distribution of actinomycetes in near-shore tropical marine sediments, Appl. Environ. Microbiol. 57, 1102-1108.

2. Mincer, T. J., Jensen, P. R., Kauffman, C. A., and Fenical, W. (2002) Widespread and persistent populations of a major new marine actinomycete taxon in ocean sediments, Appl. Environ. Microbiol. 68, 5005-5011.

3. Feling, R. H., Buchanan, G. O., Mincer, T. J., Kauffman, C. A., Jensen, P. R., and Fenical, W. (2003) Salinosporamide A: a highly cytotoxic proteasome inhibitor from a novel microbial source, a marine bacterium of the new genus *Salinospora*, Angew. Chem. Int. Ed. 42, 355-358.

4. Gulder, T. A. M., and Moore, B. S. (2010) Salinosporamide natural products: potent 20S proteasome inhibitors as promising cancer chemotherapeutics, Angew. Chem. Int. Ed. 49, 9346-9367.

5. Mazel, D., and Davies, J. (1999) Antibiotic resistance in microbes, Cell. Mol. Life Sci. 56, 742-754.

6. Kale, A. J., McGlinchey, R. P., and Moore, B. S. (2010) Characterization of 5-chloro-5-deoxy-D-ribose 1-dehydrogenase in chloroethylmalonyl coenzyme A biosynthesis: substrate and reaction profiling, J. Biol. Chem. 285, 33710-33717.

7. McGlinchey, R. P., Nett, M., Eustáquio, A. S., Asolkar, R. N., Fenical, W., and Moore, B. S. (2008) Engineered biosynthesis of antiprotealide and other unnatural salinosporamide proteasome inhibitors, J. Am. Chem. Soc. 130, 7822-7823.

8. Nett, M., Guider, T. A. M., Kale, A. J., Hughes, C. C., and Moore, B. S. (2009) Function-oriented biosynthesis of β-lactone proteasome inhibitors in *Salinispora tropica*, J. Med. Chem. 52, 6163-6167.

9. Lechner, A., Eustaquio, A. S., Gulder, T. A. M., Hafner, M., and Moore, B. S. (2011) Selective overproduction of the proteasome inhibitor salinosporamide A via precursor pathway regulation, Chem. Biol. 18, 1527-1536.

10. Kale, A. J., McGlinchey, R. P., Lechner, A., and Moore, B. S. (2011) Bacterial self-resistance to the natural proteasome inhibitor salinosporamide A, ACS Chem. Biol. 6, 1257-1264.

11. Oerlemans, R., Franke, N. E., Assaraf, Y. G., Cloos, J., van Zantwijk, I., Berkers, C. R., Scheffer, G. L., Debipersad, K., Vojtekova, K., Lemos, C., van

der Heijden, J. W., Ylstra, B., Peters, G. J., Kaspers, G. L., Dijkmans, B. A. C., Scheper, R. J., and Jansen, G. (2008) Molecular basis of bortezomib resistance: proteasome subunit β5 (*PSMB5*) gene mutation and overexpression of PSMB5 protein, Blood 112, 2489-2499.

12. Lü, S. Q., Yang, J. M., Chen, Z. L., Gong, S. L., Zhou, H., Xu, X. Q., and Wang, J. M. (2009) Different mutants of PSMB5 confer varying bortezomib resistance in T lymphoblastic lymphoma/leukemia cells derived from the Jurkat cell line, Exp. Hematol. 37, 831-837.

13. Lü, S. Q., Yang, J. M., Song, X. M., Gong, S. L., Zhou, H., Guo, L. P., Song, N. X., Bao, X. C., Chen, P. P., and Wang, J. M. (2008) Point mutation of the proteasome β5 subunit gene is an important mechanism of bortezomib resistance in bortezomib-selected variants of Jurkat T cell lymphoblastic lymphoma/leukemia line, J. Pharmacol. Exp. Ther. 326, 423-431.

14. Ri, M., Iida, S., Nakashima, T., Miyazaki, H., Mori, F., Ito, A., Inagaki, A., Kusumoto, S., Ishida, T., Komatsu, H., Shiotsu, Y., and Ueda, R. (2010) Bortezomib-resistant myeloma cell lines: a role for mutated *PSMB5* in preventing the accumulation of unfolded proteins and fatal ER stress, Leukemia 24, 1506-1512.

15. Franke, N. E., Niewerth, D., Assaraf, Y. G., van Meerloo, J., Vojtekova, K., van Zantwijk, C. H., Zweegman, S., Chan, E. T., Kirk, C. J., Geerke, D. P., Schimmer, A. D., Kaspers, G. J. L., Jansen, G., and Cloos, J. (2011) Impaired bortezomib binding to mutant β5 subunit of the proteasome is the underlying basis for bortezomib resistance in leukemia cells, Leukemia 26, 757-768.

16. de Wilt, L. H. A. M., Jansen, G., Assaraf, Y. G., van Meerloo, J., Cloos, J., Schimmer, A. D., Chan, E. T., Kirk, C. J., Peters, G. J., and Kruyt, F. A. E. (2012) Proteasome-based mechanisms of intrinsic and acquired bortezomib resistance in non-small cell lung cancer, Biochem. Pharmacol. 83, 207-217.

17. Moore, B. S., Eustáquio, A. S., and McGlinchey, R. P. (2008) Advances in and applications of proteasome inhibitors, Curr. Opin. Chem. Biol. 12, 434-440.

18. Ruschak, A. M., Slassi, M., Kay, L. E., and Schimmer, A. D. (2011) Novel proteasome inhibitors to overcome bortezomib resistance, J. Natl. Cancer Inst. 103, 1007-1017.

19. Balsas, P., Galan-Malo, P., Marzo, I., and Naval, J. (2012) Bortezomib resistance in a myeloma cell line is associated to PSMβ5 overexpression and polyploidy, Leukemia Res. 36, 212-218.

20. Fuchs, D., Berges, C., Opelz, G., Daniel, V., and Naujokat, C. (2008) Increased expression and altered subunit composition of proteasomes induced by continuous proteasome inhibition establish apoptosis resistance and hyperproliferation of Burkitt lymphoma cells, J. Cell. Biochem. 103, 270-283.

21. Pérez-Galán, P., Mora-Jensen, H., Weniger, M. A., Shaffer, A. L., Rizzatti, E. G., Chapman, C. M., Mo, C. C., Stennett, L. S., Rader, C., Liu, P. C., Raghavachari, N., Stetler-Stevenson, M., Yuan, C., Pittaluga, S., Maric, I., Dunleavy, K. M., Wilson, W. H., Staudt, L. M., and Wiestner, A. (2011) Bortezomib resistance in mantle cell lymphoma is associated with plasmacytic differentiation, Blood 117, 542-552.

22. Rückrich, T., Kraus, M., Gogel, J., Beck, A., Ovaa, H., Verdoes, M., Overkleeft, H. S., Kalbacher, H., and Driessen, C. (2009) Characterization of the ubiquitin-proteasome system in bortezomib-adapted cells, Leukemia 23, 1098-1105.

23. Edelmann, M. J., Nicholson, B., and Kessler, B. M. (2011) Pharmacological targets in the ubiquitin system offer new ways of treating cancer, neurodegenerative disorders and infectious diseases, Expert Rev. Mol. Med. 13, e35.

24. Finley, D. (2009) Recognition and processing of ubiquitin-protein conjugates by the proteasome, Annu. Rev. Biochem. 78, 477-513.

25. Pearce, M. J., Mintseris, J., Ferreyra, J., Gygi, S. P., and Darwin, K. H. (2008) Ubiquitin-like protein involved in the proteasome pathway of *Mycobacterium tuberculosis*, Science 322, 1104-1107.

26. Burns, K. E., Liu, W. T., Boshoff, H. I. M., Dorrestein, P. C., and Barry, C. E. (2009) Proteasomal protein degradation in Mycobacteria is dependent upon a prokaryotic ubiquitin-like protein, J. Biol. Chem. 284, 3069-3075.

27. Zuhl, F., Seemuller, E., Golbik, R., and Baumeister, W. (1997) Dissecting the assembly pathway of the 20S proteasome, FEBS Lett. 418, 189-194.

28. Festa, R. A., McAllister, F., Pearce, M. J., Mintseris, J., Burns, K. E., Gygi, S. P., and Darwin, K. H. (2010) Prokayrotic ubiquitin-like protein (Pup) proteome of *Mycobacterium tuberculosis*, Plos One 5, e8589.

29. Watrous, J., Burns, K., Liu, W. T., Patel, A., Hook, V., Bafna, V., Barry, C. E., Bark, S., and Dorrestein, P. C. (2010) Expansion of the mycobacterial "PUPylome", Mol. Biosyst. 6, 376-385.

30. Poulsen, C., Akhter, Y., Jeon, A. H.-W., Schmitt-Ulms, G., Meyer, H. E., Stefanski, A., Stuhler, K., Wilmanns, M., and Song, Y.-H. (2010) Proteome-wide identification of mycobacterial pupylation targets, Mol Syst Biol 6, 386.